Static and Dynamic Analysis of Rectangular Sandwich Plates

THESIS SUBMITTED
TO THE SCHOOL OF GRADUATE STUDIES
AS PARTIAL FULFILLMENT FOR THE REQUIREMENTS OF THE
DEGREE OF MASTERS OF APPLIED SCIENCE

By
Narendra Mallakunta

at the
DEPARTMENT OF MECHANICAL ENGINEERING
UNIVERSITY OF OTTAWA

NOTICE

The quality of this microform is heavily dependent upon the quality of the original thesis submitted for microfilming. Every effort has been made to ensure the highest quality of reproduction possible.

If pages are missing, contact the university which granted the degree.

Some pages may have indistinct print especially if the original pages were typed with a poor typewriter ribbon or if the university sent us an inferior photocopy.

Reproduction in full or in part of this microform is governed by the Canadian Copyright Act, R.S.C. 1970, c. C-30, and subsequent amendments.

AVIS

La qualité de cette microforme dépend grandement de la qualité de la thèse soumise au microfilmage. Nous avons tout fait pour assurer une qualité supérieure de reproduction.

S'il manque des pages, veuillez communiquer avec l'université qui a conféré le grade.

La qualité d'impression de certaines pages peut laisser à désirer, surtout si les pages originales ont été dactylographiées à l'aide d'un ruban usé ou si l'université nous a fait parvenir une photocopie de qualité inférieure.

La reproduction, même partielle, de cette microforme est soumise à la Loi canadienne sur le droit d'auteur, SRC 1970, c. C-30, et ses amendements subséquents.

ISBN 0-315-60570-7

UNIVERSITÉ D'OTTAWA
UNIVERSITY OF OTTAWA

to my father

Prof. M. Raghupathi

Acknowledgements

I would like to express my sincere gratitude to my supervisor Prof. S. Mirza for his continuous encouragement and advice during the course of this work.

I wish to thank the Natural Sciences and Engineering Research Council of Canada for the financial support provided. Sincere thanks are due to the Department of Mechanical Engineering for the various teaching assistanships provided.

I also wish to thank M/s Bharat Heavy Electricals Limited, New Delhi, India, for granting study leave to pursue this work. My friends at the University of Ottawa are also acknowledged for their support.

Finally, I wish to thank my parents especially my father without whose continuous letters of advice and moral support, this work would not have been possible.

Abstract

The static and dynamic characteristics of homogeneous rectangular plates and rectangular sandwich plates are studied by the finite element method using a 8-node isoparametric rectangular element.

Various parametric studies are conducted in an attempt to establish the validity of the results. Convergence characteristics of the element used in the formulation has been highlighted. Wherever possible, results obtained from the present investigation are compared with those available in the technical literature.

A computer code utilizing the finite element method is developed to generate solutions for the static and dynamic analysis of homogeneous plates and sandwich plates for conditions of plane stress, plane strain, bending, and combined stress and bending for small deformation problems only. However, in this work, the scope is limited to bending problems only. Further, only the values for the center deflection are generated, in the static analysis, even though the code has the capability to generate the various stress components. In the dynamic analysis, the natural frequency and the associated mode shapes are determined. The boundary conditions are taken as free, simply supported, clamped edge constraints and their combinations. Uniformly distributed loads, concentrated loads or a combination of both can be applied. This study concentrates on free vibration problems in the case of the dynamic analysis.

The effect of considering non-uniform shear distribution in the core of the sandwich plate is studied for both the static and dynamic analysis. The impact of considering two different orders of numerical integration is also studied.

Solutions for the dynamic analysis are presented for various boundary conditions.

Results obtained from this numerical analysis are shown to be in good agreement with other precise analyses done by previous researchers. It is seen that the method outlined here, provides an effective and efficient means of analysing homogeneous rectangular plate and rectangular sandwich plate problems with various boundary conditions and loading conditions, to establish the static and dynamic characteristics.

Contents

List of Figures

List of Tables

Nomenclature

t	Face plate thickness
c	Core thickness
x,y,z	Rectangular coordinate system
a,b	Dimensions in the x and y directions
ξ, η	Natural coordinate system
u,v,w	Displacements in the x, y and z directions
M_x, M_y, M_{xy}	Moment resultants in rectangular coordinate system
N_x, N_y, N_{xy}	Force resultants in rectangular coordinate system
Q_x, Q_y	Transverse shear force resultants in rectangular coordinate system
σ_x, σ_y	Stresses in the x and y directions respectively.
τ_{xy}	Shearing stress in the xy plane
τ_{xz}, τ_{yz}	Transverse shear stresses in the xz and yz planes respectively
ϵ_x, ϵ_y	Extensional strains in the x and y directions respectively
γ_{xy}	Shear strain in the xy plane
γ_{xz}, γ_{yz}	Transverse shear strains in the xz and yz planes respectively
ϕ_x, ϕ_y	Transverse shear strains in the xz and yz planes respectively. These are similar to γ_{xz} and γ_{yz} and are used instead, in chapter 4.
θ_x, θ_y	Rotation made by the normal to midsurface of the plate about the y and x axis respectively
$\Gamma_x, \Gamma_y, \Gamma_{xy}$	Plate strain components in the x, y and xy planes respectively
Γ_{xz}, Γ_{yz}	Plate strain components in the xz and yz planes respectively
χ_x, χ_y	Bending deformation about the x and y axes respectively
χ_{xy}	Bending deformation in the xy plane

i	Nodal point
δ	Displacement field
ϕ	Shear deformation matrix
$\mathbf{N}$	Shape function matrix
$\mathbf{L}$	Displacement differential operator matrix
$\mathbf{B}$	Element strain matrix
$\mathbf{D}$	Matrix of elastic constants
χ	Bending deformation matrix
$\mathbf{J}$	Jacobian matrix
$\mathbf{I}$	Identity matrix
ρ_m	Matrix of density coefficients
$\mathbf{K}$	Stiffness matrix
$\mathbf{R}$	Load vector
$\mathbf{M}$	Mass matrix of the structure
$(\mathbf{K})$	Global stiffness matrix
$(\mathbf{M})$	Global mass matrix
E	Young's modulus
G	Shear modulus $= \frac{E}{2(1+\nu)}$
G'	Modified shear modulus $= G/\alpha$ (to account for the non-uniform shear strain displacement due to the transverse shear)
G_c	Shear modulus of the core that is isotropic with respect to the x and y axes in planes perpendicular to the xy plane
G_{xz}, G_{yz}	Shear modulus of the orthotropic core in the xz and yz planes respectively

$\mathcal{D}$	Plate rigidity for a homogeneous plate
	$= \frac{Et^3}{12(1-\nu^2)}$
$\mathcal{D}_{s_b}$	Plate rigidity due to bending for a homogeneous sandwich plate
	$= \frac{E_f t(c+t)^2}{2(1-\nu_f^2)}$
$\mathcal{D}_{s_s}$	Plate rigidity due to shear for a homogeneous sandwich plate
	$= \frac{G_c c}{\alpha}$
q	Distributed transverse load per unit area
ν	Poisson's ratio
ρ	Mass density unless specified as otherwise
α	Shear correction factor
	$= 6/5$
T	Time
V	Volume of the plate
A	Area of the plate
S	Surface of the plate
U	Strain energy stored in an elastic body
$\bar{U}$	Analogous strain energy stored in an elastic body
$\bar{U}_T$	Kinetic energy of the plate
$\bar{U}_P$	Potential energy of the plate
$\bar{U}_L$	Potential energy of the external loads
$\mathbf{f}^B$	Body forces
$\mathbf{f}^S$	Surface forces
$\mathbf{F}^i$	Concentrated forces
$\mathbf{F}$	Vector of all externally applied forces
$\mathbf{R}_B$	Element body forces
$\mathbf{R}_S$	Element surface forces

$\mathbf{R}_C$	Concentrated loads
$\mathbf{R}_I$	Nodal forces due to inertia
subscript f	Corresponds to face plates
subscript c	Corresponds to the core
subscript b	Corresponds to bending
subscript s	Corresponds to shear

Chapter 1

Introduction

1.1 Sandwich Plate

1.1.1 General

Sandwich plates used in this work are defined as a three layer type of construction, consisting of two thin sheets of high strength material between which a thick layer of low average strength and density is sandwiched. The two thin sheets are called the faces, and the intermediate layer is the core of the sandwich. The face sheets are usually made of aluminium alloys, reinforced plastic, titanium, heat resistant steel or other metals. A very popular type of core is the 'honeycomb' core, which consists of thin foils in the form of hexagonal cells perpendicular to the faces. Other types of cores are corrugated sheets, with corrugations running parallel to the faces, expanded materials, such as cellulose acetate, synthetic rubber etc., and

balsa wood. The material of honeycomb cores, corrugated cores, and the like can be similar to the material of the faces.

1.1.2 Advantages and applications

The main advantages of sandwich construction are

1. Weight savings of upto 30 percent over the conventional structures can be achieved in certain structures.
2. The good surface finish and the resistance to local deformations give rise to a high aerodynamic efficiency.
3. Outstanding rigidity is exhibited.
4. Fatigue properties are good especially with regard to acoustical fatigue.
5. Good thermal and acoustical insulation.
6. Ease of mass production.

Due to these advantages, sandwich construction has many applications in the aircraft and missile industry. Examples of applications are wings, fuselage and tailplane skins, pressure bulkheads, spar webs, ribs, flooring etc. Further, the building industry has used sandwich construction for partition walls, exterior curtain walls, roof cladding spanning between the primary structural framework and as shell type roofs for exhibition buildings such as the 1965 New York world fair and Expo 67 at Montreal.

1.1.3 Analytical methods

The theoretical and experimental investigation of sandwich construction has commanded a great deal of attention among researchers in the fields of elasticity and allied areas. Many theories have been proposed but in practice, a great deal of simplification is required before the design engineer is able to handle them effectively. Various methods have been employed by researchers including Fourier series, Lagrangian multiplier technique, Ritz energy method, Perturbation, Finite difference method, Finite strip method and the Finite element method.

1.2 Finite Element Analysis

1.2.1 General

The finite element analysis was first successfully utilized in the aerospace industry in response to the need for a procedure which could provide a refined solution for the problems resulting out of extremely complex airframe configurations. With the advent of high speed computers, the finite element analysis has become economically justified and has been successfully applied to industries such as nuclear, automotive, farm equipment, electronics, oil exploration and many others. This method has been and is being applied with success to many of the problems of elasticity which were previously solvable only with considerable computational difficulty.

The basic advantages of the finite element analysis is that irrespective of the

size of the structure, analysis can be done. Complex boundary conditions can be simulated with ease in the finite element analysis which cause considerable problems in other techniques. This analysis requires a lot less time than other methods of analyses. The relative merits and demerits between the finite element analysis and the modal analysis are listed in [69],[75].

Finite element analysis is an analytical technique in which a structure, which is theoretically a continuum mechanics problem, is approximated by an assembly of elements, called finite elements. A variety of finite elements have been developed which are very useful in solving practical problems. It is up to the user to include enough elements in his model such that the true stress distribution is adequately described by a series of linear segments. If only mode shapes and frequencies are desired, but accurate stress distributions are not required, experience has shown that fewer elements will suffice [75].

The solution of a model consisting of one element is trivial and could be solved in closed form. The power of the finite element method is that the stiffness of an assembly of elements is equal to the sum of the element stiffness matrices. For example, a table might be modeled by four beams for the legs and twenty shell elements for the top of the table. Mathematically,

$$(\mathbf{K}) = \sum_{i=1}^{n} \mathbf{K}_i$$

where n is the number of elements, $\mathbf{K}_i$ is the stiffness matrix of element i and $(\mathbf{K})$ is the stiffness matrix of the system.

Let $(\mathbf{X})$ be a vector of the displacement and rotational degrees of freedom of the system, and $(\mathbf{F})$ be a vector of the applied forces and moments, then:

$$(\mathbf{K})(\mathbf{X}) = (\mathbf{F})$$

For stress analysis, $(\mathbf{K})$ can be found by summing the element stiffness matrices and $(\mathbf{F})$ is the applied force. A significant amount of computer time is required to solve for $(\mathbf{X})$ and is dependent of the size of the stiffness matrix of the system. Stresses and strains can be computed from $(\mathbf{X})$. This method can be extended to the solution of dynamic problems. For free vibration problems with no damping,

$$(\mathbf{M})(\ddot{\mathbf{X}}) + (\mathbf{K})(\mathbf{X}) = 0$$

where $(\ddot{\mathbf{X}})$ is the acceleration and $(\mathbf{M})$ is the system mass matrix.

The above equations are dealt with in detail in Chapter 4.

1.2.2 Recent developments

Recent studies have been undertaken to further improve the conventional finite element method. Gupta [74] in 1976, explored the concept of dynamic elements involving higher order dynamic correction terms in the associated stiffness and mass matrix. Such matrices were then developed for a rectangular prestressed membrane element. In 1978, he developed an efficient free vibration analysis

procedure for two dimensional structures [35]. This analysis proved to give a more efficient and economical solution than the conventional finite element method.

In 1980, Soares et al [63] developed two mixed isoparametric elements for the dynamic analysis of plate structures.

Stavrindis et al [68] in 1989, presented a improved finite element formulation for dynamic analysis. Improvements are based on modifications of the finite element mass matrix. Frequency errors and stress errors are at least three times smaller than the corresponding consistent or lumped mass formulation error.

However, in the present work, the conventional finite element technique is followed.

1.3 Scope of Present Work

Finite element analysis for rectangular sandwich plates has been presented in several publications namely [71],[41],[40]. Various displacement fields were assumed by the authors for obtaining the center deflections and natural frequencies for flat sandwich plates.

The present work uses a 8-node isoparametric element for the analysis. Isoparametric elements have a distinct advantage over the subparametric elements in relation with the number of elements used to represent a relatively complex system and for modelling geometric boundary conditions. Isoparametric elements also facilitates the use of Gaussian numerical integration procedure which is the numerical

technique used in this work.

A versatile computer code is developed to include static and dynamic analysis of homogeneous thin plates, thick plates and sandwich plates for clamped, simply supported and free boundary conditions. Sandwich plates with orthotropic cores can also be analyzed provided the contribution of the core in resisting bending and torsional loads is negligible. The code developed is capable of handling conditions of plane stress , plane strain, bending and even combined plane stress and bending for small deformation problems only. However, in this work, scope has been limited to bending problems only. Further, only the values for the center deflection are generated, in the static analysis, even though the code has the capability to generate the various stress components. Comparisons are made with available analytical solutions.

The shear correction required for the non-uniform shear distribution in the core of the sandwich plate has been considered in this present analysis. Most of the previous work done for determining the static characteristics of sandwich plates has been with an uniform shear distribution in the core. In this work, a detailed analysis is presented regarding the difference in results obtained by neglecting or including this factor for the static analysis of sandwich plates with varying parameters. The shear correction has also been considered for the dynamic analysis of sandwich plates in this work.

Most of the solutions generated for the dynamic analysis of sandwich plates by previous researchers have been for clamped and simply supported boundary conditions only. A detailed parametric study is done in this work for four different boundary conditions including two with free edges.

Gaussian numerical integration has always been a very important aspect in finite element analysis. There is an enormous literature available on this, with regard to the most optimum and efficient order of Gaussian numerical integration required for various problems. A discussion and difference in convergence is brought out in the present work between two different orders of Gaussian numerical integration in Chapter 6.

In finite element analysis, depending upon the number of simultaneous equations to be solved, the usage of computer time dramatically increases. It is of utmost importance to predict the rapid convergence of the element and its related shape functions so as to optimize the number of elements used in the finite element analysis. In this work, convergence is shown for the static and dynamic cases with various boundary conditions and loadings for homogeneous plates and sandwich plates. This helps predict the mesh size required for satisfactory solution for any related structural problem. The above has not been highlighted in any previous paper.

The present study is motivated by the fact that sandwich plates have fairly wide spread applications as discussed earlier in section 1.1.2, and yet there are some shortcomings. Hence, the basic aim is to provide an efficient and accurate computer code to analyze the static and dynamic characteristics for various plates and provide results which the design engineer can use within the scope of the assumptions made. It is not the intent of this work to give an exhaustive record of results, but rather to present results which tend to instill confidence in the analysis method presented.

1.4 Thesis organization

Chapter 2 reviews the past work done in the static and dynamic analysis of sandwich plates. Some papers which are not entirely relevant to this work have also been included so as to provide a broader perspective on the work done on sandwich plates.

Chapter 3 contains the theoretical basis for the code developed for the analysis of sandwich plates. The fundamental differential equations are detailed out and boundary conditions considered are also discussed.

Chapter 4 discusses the isoparametric element used in the analysis and the development of the displacement based formulations used in the code.

Chapter 5 discusses the basic features of the computer code developed.

Chapter 6 presents a detailed analysis of the results obtained for the static and dynamic analysis of homogeneous plates and sandwich plates.

Conclusions and recommendations are presented in **Chapter 7**.

Three appendices are included at the end of this thesis. **Appendix A** contains all the relevant figures based on the results obtained in this work. **Appendix B** contains the general flow chart for the code developed and also a sample input and output of the code. **Appendix C** gives the recommended order of Gauss numerical integration for two dimensional isoparametric elements.

Chapter 2

Review of Literature

2.1 Review of previous work on static analysis of sandwich plates

The theories of sandwich plates were investigated by several authors. Hopkins et al [12] in 1944 described the experimental and theoretical work on the behavior of flat sandwich panels under uniform transverse loading. The theory developed applied to sandwiches composed of isotropic materials and was based on the assumptions that the edges are simply supported and that the panel deflections are less than the panel thickness. Further, the faces take bending only and, the core, only shear. Fair agreement was found between the experimental and theoretical work.

The basic differential equations for the finite deflections of sandwich plates were developed by Reissner [23] in 1948. In his work, the development of the

bending theory for sandwich plates was based upon several fundamental assumptions regarding the behavior of the faces and the core. These assumptions are as follows.

1. The thickness of the faces is very small compared to the thickness of the core and hence the stresses in the faces parallel to their planes are distributed uniformly over the thickness of the face layers.

2. The values of the elastic constants E_f, G_f for the face layers are large compared with the values of the elastic constants E_c, G_c for the core layer. Further, the products tE_f, tG_f are large compared with the values of cE_c and cG_c. On the basis of this assumption, the face parallel stresses in the core layer and their effect on the deformation of the composite plate is neglected.

Thus, Reissner treated the sandwich plate as a combination of two plates without bending stiffness (the face layers), and of a third plate (the core layer) offering resistance only to transverse shear stresses.

With these assumptions, a system of equations has been derived to describe the behaviour of sandwich plates under the bending loads. In this study, he found that the transverse normal stress in the core is negligibly small compared with the transverse shear stress and that the range of deflections for which the linear theory is adequate decreases as the core is made softer relative to the faces.

In 1950, Hoff [11] derived a set of differential equations by means of the principle of virtual displacements from the essential parts of the strain energy stored in the sandwich plate. The essential parts were the strain energy of bending in the faces and the strain energy of shear caused in the core. Boundary conditions

corresponding to simply supported, clamped and free edges were considered.

Eringen [6] in 1951 obtained four partial differential equations for the bending and buckling of rectangular, flat sandwich plates having homogeneous core and identical faces subjected to various types of loading and boundary conditions by use of the theorem of minimum total potential energy. Various effects previously omitted were incorporated into the analysis. The three-dimensional stress distribution in the core is taken into account and thus the bending rigidity and the flattening of the core are not neglected. Also, the face layers, which are customarily assumed to be thin, have bending rigidity. The theory developed inherently unifies overall bending and buckling and the bending and buckling with the flattening of the core.

In 1951, Yen et al [15] used a Fourier series to solve the governing differential equations proposed by Hoff and get numerical results for the maximum deflection of a simply supported rectangular sandwich plate for loading consisting of either a uniformly distributed transverse load or a concentrated load applied at the center of the plate. Both the upper bound and lower bound solutions were presented in this work. The calculated values of the maximum deflection compared favorably with the test results, although many of the results were of slightly smaller values than the test results. This behaviour is to be expected since the theoretical boundary conditions correspond to a greater degree of constraint along the edges than do the experimental boundary conditions.

Gerrard [22] in 1951, developed a system of equations describing the bending of thick sandwich plates. The thick plate system is required when the thickness relative to the characteristic length is not small, and hence includes deflections

due to shear. The need arose in connection with an investigation of the instability behaviour of thick sandwich plates for which wrinkling is the usual mode of instability.

Kroll et al [14] in 1953, investigated the effects of lateral and axial loads on sandwich construction. Experimental results were obtained for sandwich panels with simply supported edges and free edges. The maximum load and the mode of failure were observed and lateral deflection and the axial strains were also measured. Equilibrium equations for a sandwich column with simply supported ends under combined axial load and lateral pressure were derived and from them, the formulas for axial strain and lateral deflection.

Ikeda [7] in a paper published in 1955 developed a theory of bending of isotropic flat sandwich plates in which the individual stiffness of the facing or of the core is not neglected in comparison with the total bending stiffness of the sandwich plate as a whole.

Thurston [4] in 1957 applied the Lagrangian multiplier method to Hoff's energy expressions for sandwich plates to derive equations for finding the deflections and buckling loads of rectangular plates clamped on all four edges.

Harris et al [27] in 1960 presented buckling curves for the general instability of flat, simply supported, corrugated core, rectangular sandwich plates under longitudinal compression and bending, transverse compression and bending, and shear. The stability criterion is formulated by means of the Rayleigh-Ritz energy method.

Seide [28] in his comments on Harris et al's paper in 1961 pointed out that

their assumption that any line in the sandwich core that is initially straight and normal to the middle surface will remain straight after deformation of the plate but will deviate from the direction of the normal to the deformed middle surface by an amount that is proportional to the slope of the plate surface, this proportionality factor being constant, throughout the plate is misleading.

In 1962, Cheng [30] developed a system of differential equations for the small deflection of a sandwich plate by means of the variational theorem of complimentary energy in conjunction with Lagrangian multipliers. From these equations, a governing linear differential equation of sixth order for the deflection is derived and the solution of this resultant equation may be readily obtained thru the use of the techniques that have been developed in the classical theory of plates.

In 1962, Okamoto [8] extended Hoff's energy method to the case of the cylindrical coordinates with the view of applying to circular and sectorial plates.

Okamoto [33] in 1963, assumed the components of displacements in the form of double Fourier series and derived the equations of strain energies based on the principle of virtual displacements. In this method, the differential equations were not used and the problems are solved by the direct method for the calculus of variations.

Alwan [73] in 1964 derived the differential equations for large deflection of sandwich plates taking the core to be an orthotropic honeycomb-type structure instead of the isotropic core assumed by past researchers. He took the same assumptions as Reissner.

Habip [66] in 1965 also reviewed the developments in the analysis of structures

which covers the elastic behaviour of sandwich beams, plates and shells under various loadings, and problems of elastic stability and dynamic response, including geometrically non-linear effects.

In 1965, Lin et al [5] developed a method for calculating the deflections and bending moments of rectangular sandwich panels with clamped edges under combined biaxial compression and pressure.

Liaw et al [21] in a paper published in 1967, developed the governing equation for bending of multilayered sandwich plates by variational methods. The plate is considered to be composed of n membranes, having different thicknesses and possessing different isotropic elastic properties, and $(n-1)$ orthotropic cores. Equations developed by Reissner and Cheng can also be extended to include multilayer sandwich plates by redefining the physical constants of the plate.

In 1967, Alwan [73] presented a solution of Reissner's equation for the case of a simply supported rectangular sandwich plates subjected to uniform normal pressure.

2.2 Review of previous work on dynamic analysis of sandwich plates

In 1959, Yu [1] extended the new flexural theory developed by Mindlin [32] to include the effects of transverse shear deformation and rotatory inertia in both the core and faces of the sandwich. No limitation was imposed upon the magnitudes of the ratios between the thicknesses, material densities, and elastic constants of

the core and faces of the sandwich.

In the same year, Yu [2] investigated the simple thickness-shear modes of infinite sandwich plates on the basis of both the elasticity theory and the new sandwich plate theory developed by him in the earlier paper.

In 1960, Chang [13] investigated the flexural motion of a rectangular sandwich panel with an orthotropic viscoelastic core. Differential equations and boundary conditions were derived by taking into account the rotational inertia of the whole panel and the shearing deformation and viscoelastic damping of the core. The dynamic response of a simply supported rectangular panel to a unit step function is first obtained and the general transient and steady state response of the panel to an arbitrary input function is then expressed in terms of the unit response by means of the convolution integral.

Yu [3] in 1960, investigated the flexural vibrations of sandwich plates based on the new sandwich theory developed by him in a earlier paper [1] and the exact elasticity theory. Numerical results yielded by both the theories showed excellent agreement with each other, and the new sandwich plate theory is seen to be good for a very wide frequency range which is of practical interest. In a subsequent paper in the same year, Yu [9] simplified the vibration analysis for ordinary sandwich plates which have thin face layers and low frequency ranges.

Ueng [19] in 1966 used the Lagrangian multiplier method to develop a solution for calculation of the natural frequencies of free vibration of a rectangular sandwich panel clamped on all edges. Both the lower bounds and the upper bounds of the natural frequencies were obtained.

In 1967, Raville et al [20] presented the natural frequencies for free vibrations of a simply supported sandwich plates. Experimental results were in close agreement with the theoretical results obtained.

In 1972, Shahin [37] obtained the natural frequencies of a simply supported plate with isotropic facings and orthotropic cores in a closed form as a function of parameters depicting in-plane load, aspect ratio, and orthotropicity of the cores. Influence of these parameters on the natural frequencies were presented. For a double sandwich plate, the influence of the face thickness and Young's modulus on the fundamental frequency are studied and illustrated.

Bert [29] in 1979, surveyed the literature concerning dynamics of plate-type structural elements of either composite material or sandwich construction. Papers from 1976-1979 were reviewed and special attention is given to rectangularly orthotropic, cylindrically orthotropic, and anisotropic plates; laminated plates;thick and sandwich plates; and nonlinearities.

Ozguven [65] in 1982 did mathematical modelling for dynamic response analysis of partially coated or laminated plates by an energy approach.

Balendra [70] analyzed the free vibration of plated structures by the grillage method in 1985. Accuracy of the method was assessed by comparing with published results and the finite element method. Reasonably good results were obtained by the grillage method.

In 1988, Kanematsu [36] presented a linear analysis for bending and vibration of sandwich plates consisting of an orthotropic core and unbalanced laminated face plates. A solution method was proposed through the principle of minimum

total potential energy, and a double Fourier series approach was used for the displacement functions.

2.3 Finite Element Analysis of Sandwich Constructions

In the last 25 years, this method has been used widely to solve various structural problems. However, this method is not intended to replace the other numerical methods developed and used by other researchers but rather to supplement them. Finite element method has been used for complex structural problems such as stiffened plates, cellular structures and sandwich plates with great success.

One of the first finite element analysis of sandwich structures was done by Abel et al [24] in 1968. The finite element method was extended to the refined elastic analysis of sandwich beams and shells with no restriction placed upon the ratios of the layer thicknesses and properties. Element stiffnesses were developed based on polynomial displacement models. The theory adopted was based on the Yu's new sandwich theory. The element utilized was the doubly curved element which duplicates the position, slope, and curvature of the original structure at each nodal circle.

Monforton et al [71], also used the finite element method to predict displacements, stresses, and natural frequencies of sandwich plates and shells with unbalanced laminated faces. The assumed displacement field was represented by the sum of products of one dimensional Hermite Interpolation polynomials. Stiffness

and consistent mass matrices for small displacements were presented in terms of the element geometry, the stiffness of the faces and the transverse shear stiffness of the orthotropic core. As a result, eighty degrees of freedom per element was used in the analysis.

Ahmed [41] in 1971, analysed the static and dynamic characteristics of doubly curved sandwich plates, with or without the application of initial membrane static stresses. The element used was the rectangular element having five and seven degrees of freedom per node. Both constant and parabolic variation of strain in the honeycomb core were used. He also presented the comparison between the static and dynamic analysis of a clamped flat sandwich plate with the results obtained by well established methods. The rectangular element with seven degrees of freedom per node was found to give a better representation of shears in the core, and hence yielded reasonable estimates of natural frequency, mode shapes and static displacement.

In 1972, Chan et al [34] solved the problems of bending and vibration of multilayered sandwich plates by the finite strip method. This approach greatly reduces the number of variables as compared with the finite element analysis. The assumption of common shear angle for the cores is excluded from the analysis. He detailed out the values for the center deflection for a three-layer sandwich plate under uniform load with various boundary conditions. Natural frequencies for the three-layer simply supported sandwich plate were also obtained and compared favorably with the results obtained by other researchers.

Khatua et al [40] in 1973 presented a finite element analysis of multilayer sandwich beam and plates, each with n stiff layers and $n-1$ weak cores. Each

layer of the sandwich structure may have individual orthotropic properties of its own and the bending rigidities of the stiff layers are taken into account while direct stresses in cores are neglected in the analysis. The condition of common shear angle for all cores is not implied in the formulation. Bending and vibration problems for sandwich plates have been solved using lower order elements and examples shown amply demonstrate the accuracy and versatility of the finite element method.

Kasemset et al [64] in 1976, presented the study of axisymmetric vibration of multilayer sandwich plates and shells with n stiff layers and $n-1$ weak cores. A curved multilayer element is used in the analysis.

Ng et al [43] in 1985, presented a finite element displacement model for the dynamic and static analysis of clamped and simply supported skew sandwich plate.

Owen et al [67] presented a refined analysis of laminated plates by the finite element displacement methods for problems of vibration and stability.

Mallikarjuna et al [38] in 1988, presented a simple isoparametric finite element formulation based on higher-order displacement model for dynamic analysis of multilayer symmetric composite plates with an explicit time marching scheme. In 1989, the same authors [42] used a finite element formulation of the higher order theory to determine the natural frequency of isotropic, orthotropic and layered anisotropic composite and sandwich plates.

In 1989, Chan et al [34] described a correlation study to evaluate finite element models for vibration of composite material and structures.

Chapter 3

Theory of Plates

3.1 General

Various theories for flat sandwich plates were propounded by many authors as given in the previous chapter. Depending upon the various assumptions considered by different authors, the derived formulas differ greatly in complexity. In this research work, the differential equations for the sandwich plate are developed from the differential equations of a homogeneous plate. The equations account for the effects of transverse shear and the rotatory inertia. Assumptions considered are detailed out and the final equations developed are based on them.

The fundamental differential equations for the homogeneous plate have been derived by other researchers [10], [25], [53], [54], [55], [56]. Based on these, the equations which form the theoretical basis for the code developed for the analysis of sandwich plates are discussed in Section 3.3.

A typical sandwich plate may be shown as given in the Fig. 3.1. The middle plane of the plate of dimensions 'a' and 'b', lies in the x-y plane.

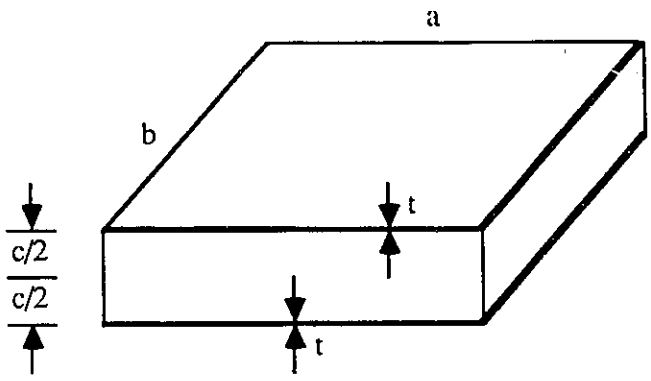

Figure 3.1: Dimensions of a sandwich plate

The faces are each of thickness 't' and the core is of thickness 'c'.

3.2 Assumptions

1. The displacement and strains are small and hence the equations of linear elasticity theory are valid.

2. A perfect bonding occurs between adjacent layers of the sandwich plate.

3. The faces and core are assumed to be homogeneous and isotropic. [1]

4. Faces are thin compared with the thickness of the core. Consequently local

[1]The computer code developed is capable of incorporating orthotropic core too provided that the contribution of the core in resisting bending and torsional loads is negligible

bending stiffness of the faces is neglected.

5. Transverse normal strains in the faces and the core is assumed to be negligible. This assumption implies that core must be rigid in a direction perpendicular to the faces to prevent crushing.

6. Direct stresses in the core in the plane of the plate are neglected.

7. Lines which are straight and normal to the middle surface before deformation remain straight during deformation, but do not necessarily remain normal to the middle surface.

3.3 Differential Equations

3.3.1 Plate-Stress Components

The bending and twisting moments and the transverse shearing forces, all per unit length, for a homogeneous plate of thickness t, are defined in the customary manner as given by Equations (3.1) and (3.2).

$$(M_x, M_y, M_{xy}) = \int_{-t/2}^{t/2} (\sigma_x, \sigma_y, \tau_{xy}) z dz \tag{3.1}$$

$$(Q_x, Q_y) = \int_{-t/2}^{t/2} (\tau_{xz}, \tau_{yz}) dz \tag{3.2}$$

The in-plane stress resultants are defined as given in Equations (3.3).

$$(N_x, N_y, N_{xy}) = \int_{-t/2}^{t/2} (\sigma_x, \sigma_y, \tau_{xy}) dz \tag{3.3}$$

3.3.2 Stress-Strain Relations

In case of an isotropic homogeneous plate, the plate stress components are expressed as,

$$M_x = \mathcal{D}(\Gamma_x + \nu\Gamma_y) \tag{3.4}$$

$$M_y = \mathcal{D}(\Gamma_y + \nu\Gamma_x) \tag{3.5}$$

$$M_{xy} = (1 - \nu)\mathcal{D}\Gamma_{xy}/2 \tag{3.6}$$

$$Q_x = G^{'} t\Gamma_{xz} \tag{3.7}$$

$$Q_y = G^{'} t\Gamma_{yz} \tag{3.8}$$

The Γ's in the Equations (3.4) to (3.8) are the plate-strain components defined by

$$(\Gamma_x, \Gamma_y, \Gamma_{xy}) = 12t^{-3} \int_{-t/2}^{t/2} (\epsilon_x, \epsilon_y, \gamma_{xy}) z dz \tag{3.9}$$

$$(\Gamma_{xz}, \Gamma_{yz}) = t^{-1} \int_{-t/2}^{t/2} (\gamma_{xz}, \gamma_{yz}) dz \tag{3.10}$$

As the non-uniform shear strain displacement due to the transverse shear, of the plate cross-section is also accounted for,

$$G' = G/\alpha \tag{3.11}$$

The coefficient α has been given various values by different authors. According to Timoshenko[60], $\alpha = 3/2$ while Reissner[25] assumes a value of $\alpha = 6/5$. Mindlin [10] has also suggested a formula for this constant, involving the Poisson's ratio and uses a value of $\alpha = 12/\pi^2$ which is close to that used by Reissner. In this work, Reissner's value of $\alpha = 6/5$ is taken.

Equations (3.1) to (3.10) are valid in the sandwich plate theory except for the plate rigidity $\mathcal{D}$ used for the homogeneous plate, which has to be modified to incorporate the properties of the sandwich plate. The plate rigidity $\mathcal{D}_s$ for a sandwich plate has contributions from bending as well as shear.

Consider an element of the sandwich plate as shown in Figure 3.2.

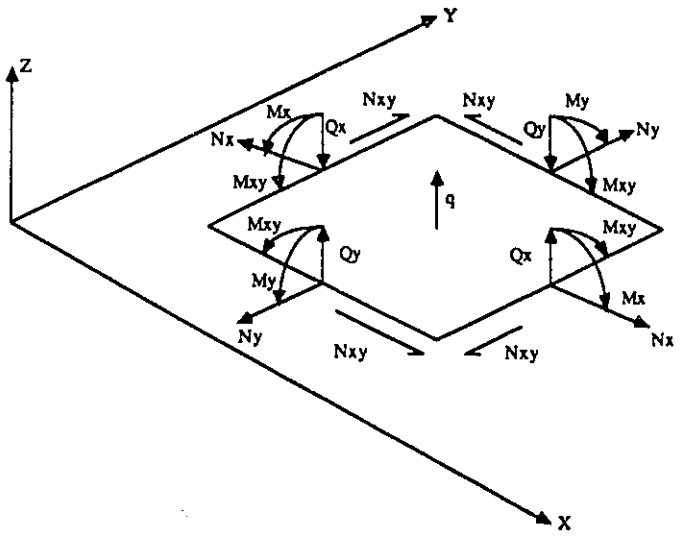

Figure 3.2: Sandwich Plate - Forces and Moments indicated are positive

The bending rigidity integrated over the thickness of the sandwich plate is written as,

$$\begin{aligned} \mathcal{D}_{s_b} &= \int_{-c/2}^{c/2} \frac{E_c z^2 dz}{(1-\nu_c^2)} + \int_{c/2}^{c/2+t} \frac{E_f z^2 dz}{(1-\nu_f^2)} \\ &\quad + \int_{-c/2-t}^{-c/2} \frac{E_f z^2 dz}{(1-\nu_f^2)} \end{aligned} \tag{3.12}$$

and the shear rigidity integrated over the thickness of the sandwich plate is written as,

$$\mathcal{D}_{s_s} = \int_{-c/2}^{c/2} G_c dz + \int_{c/2}^{c/2+t} G_f dz + \int_{-c/2-t}^{-c/2} G_f dz \tag{3.13}$$

where $G_c = \frac{E_c}{2(1+\nu_c)}$ and $G_f = \frac{E_f}{2(1+\nu_f)}$ are the shear modulus for the core and the faces respectively.

Based on the assumptions detailed out, we can define plate rigidities for the sandwich plate as,

$$\mathcal{D}_{s_b} = \frac{E_f t(c+t)^2}{2(1-\nu_f^2)} \tag{3.14}$$

$$\mathcal{D}_{s_s} = G_c c \tag{3.15}$$

Equation (3.15) is modified to account for the non-uniform shear strain displacement.

$$\mathcal{D}_{s_s} = \frac{G_c c}{\alpha} \tag{3.16}$$

By incorporating the plate rigidities of the sandwich plate, as given in the Equations (3.14) and (3.16), the plate stress components for an isotropic sandwich plate are

$$M_x = \mathcal{D}_{s_b}(\Gamma_x + \nu_f \Gamma_y) \tag{3.17}$$

$$M_y = \mathcal{D}_{s_b}(\Gamma_y + \nu_f \Gamma_x) \tag{3.18}$$

$$M_{xy} = (1-\nu_f)\mathcal{D}_{s_b}\Gamma_{xy}/2 \tag{3.19}$$

$$Q_x = \frac{G_c c \Gamma_{xz}}{\alpha} \tag{3.20}$$

$$Q_y = \frac{G_c c \Gamma_{yz}}{\alpha} \tag{3.21}$$

3.3.3 Plate-Displacement Components

For small displacements, the strain displacement relations for homogeneous plates can be written as,

$$\int_{-t/2}^{t/2} (\epsilon_x, \epsilon_y, \gamma_{xy}) z dz = \int_{-t/2}^{t/2} (\frac{\partial u}{\partial x}, \frac{\partial v}{\partial y}, \frac{\partial v}{\partial x} + \frac{\partial u}{\partial y}) z dz \tag{3.22}$$

$$\int_{-t/2}^{t/2} (\gamma_{xz}, \gamma_{yz}) dz = \int_{-t/2}^{t/2} (\frac{\partial u}{\partial z} + \frac{\partial w}{\partial x}, \frac{\partial v}{\partial z} + \frac{\partial w}{\partial y}) dz \tag{3.23}$$

The displacement of any point in the plate may be defined by the rotations θ_x, θ_y made by the normal to midsurface of the plate about the y and x axes respectively, and the lateral displacement w of the midsurface of the plate.

It is now assumed that u and v are proportional to z and w is independent of z [10].

$$u = -z\theta_x, \; v = -z\theta_y, \; w = w \tag{3.24}$$

From Equations (3.9),(3.10),(3.22),(3.23) and (3.24), we have the relations between the plate-strain components and the plate-displacement components θ_x, θ_y, w.

$$\Gamma_x = -\frac{\partial \theta_x}{\partial x},\ \Gamma_y = -\frac{\partial \theta_y}{\partial y},\ \Gamma_{xy} = -(\frac{\partial \theta_y}{\partial x} + \frac{\partial \theta_x}{\partial y}) \tag{3.25}$$

$$\Gamma_{xz} = \frac{\partial w}{\partial x} - \theta_x,\ \Gamma_{yz} = \frac{\partial w}{\partial y} - \theta_y, \tag{3.26}$$

The analogous equations for classical thin plate theory are obtained by setting $\Gamma_{xz} = \Gamma_{yz} = 0$. In the case of the sandwich plate, bending is taken by the faces and shear by the core.

3.3.4 Energy Functions

The strain-energy-function U in the three dimensional theory is given by

$$\begin{aligned} U &= \frac{1}{2}(\sigma_x \epsilon_x + \sigma_y \epsilon_y + \sigma_z \epsilon_z + \tau_{xy}\gamma_{xy} + \tau_{yz}\gamma_{yz} + \tau_{xz}\gamma_{xz}) \\ &= \frac{1}{2}(\sigma_x \frac{\partial u}{\partial x} + \sigma_y \frac{\partial v}{\partial y} + \sigma_z \frac{\partial w}{\partial z} + \tau_{xy}(\frac{\partial v}{\partial x} + \frac{\partial u}{\partial y}) \\ &\quad + \tau_{xz}(\frac{\partial u}{\partial z} + \frac{\partial w}{\partial x}) + \tau_{yz}(\frac{\partial v}{\partial z} + \frac{\partial w}{\partial y})) \end{aligned} \tag{3.27}$$

The analogous plate-strain-energy-function $\bar{U}$ is now obtained by substituting Equations (3.24), (3.25) and (3.26) into Equations (3.27) and integrating over the sandwich plate thickness, with the result

$$\bar{U} = \frac{1}{2}(M_x\Gamma_x + M_y\Gamma_y + M_{xy}\Gamma_{xy} + Q_x\Gamma_{xz} + Q_y\Gamma_{yz}) \tag{3.28}$$

Substituting from Equations (3.17) to (3.21) into Equation (3.28) we get,

$$\begin{aligned}\bar{U} &= \frac{1}{4}[\mathcal{D}_{s_b}(1+\nu_f)(\Gamma_x+\Gamma_y)^2 + \frac{2G_c c}{\alpha}(\Gamma_{xz}^2+\Gamma_{yz}^2) \\ &\quad + \mathcal{D}_{s_b}(1-\nu_f)((\Gamma_x-\Gamma_y)^2+\Gamma_{xy}^2)]\end{aligned} \tag{3.29}$$

Castigliano's theorem of least work is applied which states that, among all statically correct states of stresses, the state of stress which also satisfies the stress-strain relation and the displacement boundary conditions is characterized by the condition that the variation of $\bar{U}$ vanishes. Then, if $\bar{U} = 0$, all the plate strain components vanish and, through Equations (3.17) to (3.21), so do the plate-stress components.

From Equations (3.29) and Equations (3.17) to (3.21), we find

$$\frac{\partial \bar{U}}{\partial \Gamma_x} = M_x;\ \frac{\partial \bar{U}}{\partial \Gamma_y} = M_y;\ \frac{\partial \bar{U}}{\partial \Gamma_{xy}} = M_{xy} \tag{3.30}$$

$$\frac{\partial \bar{U}}{\partial \Gamma_{xz}} = Q_x;\ \frac{\partial \bar{U}}{\partial \Gamma_{yz}} = Q_y \tag{3.31}$$

The kinetic energy per unit volume, according to the general linear theory, is

$$\frac{\rho}{2}[(\frac{\partial u}{\partial T})^2 + (\frac{\partial v}{\partial T})^2 + (\frac{\partial w}{\partial T})^2] \tag{3.32}$$

Substituting for Equation (3.24) in Equation (3.32) and integrating over the sandwich plate thickness, we get

$$\frac{\rho_c c^3}{24}[(\frac{\partial\theta_x}{\partial T})^2+(\frac{\partial\theta_y}{\partial T})^2]+\frac{\rho_c c}{2}(\frac{\partial w}{\partial T})^2 + (\frac{\rho_f(2t+c)^3-\rho_f c^3}{24})[(\frac{\partial\theta_x}{\partial T})^2+(\frac{\partial\theta_y}{\partial T})^2]+\frac{\rho_f(2t)}{2}(\frac{\partial w}{\partial T})^2 \quad (3.33)$$

3.3.5 Total Energy and External Work

The kinetic energy in the plate is given by,

$$\bar{U}_T = \int_A [\frac{\rho_c c^3}{24}[(\frac{\partial\theta_x}{\partial T})^2+(\frac{\partial\theta_y}{\partial T})^2]+\frac{\rho_c c}{2}(\frac{\partial w}{\partial T})^2 + (\frac{\rho_f(2t+c)^3-\rho_f c^3}{24})[(\frac{\partial\theta_x}{\partial T})^2+(\frac{\partial\theta_y}{\partial T})^2]+\frac{\rho_f(2t)}{2}(\frac{\partial w}{\partial T})^2]dA \quad (3.34)$$

and the potential energy in the plate is given by

$$\bar{U}_P = \int_A \bar{U}\,dA \quad (3.35)$$

where the integrations are extended over the surface of the plate.

The potential of the external loads does not depend on the construction of the plate and is therefore given by the same expression as for ordinary plates. Referring for instance to Ref.[61], this is expressed as

$$\bar{U_L} = \frac{1}{2}\int_A [N_x(\frac{\partial w}{\partial x})^2 + N_y(\frac{\partial w}{\partial y})^2 + 2N_{xy}\frac{\partial w}{\partial x}\frac{\partial w}{\partial y} - 2qw]dA \qquad (3.36)$$

when the boundary reactions do no work.

The total energy is the sum of the kinetic energy and the total potential energy,

$$\begin{aligned}\bar{U_T} + \bar{U_P} + \bar{U_L} &= \int_A [\frac{\rho_c c^3}{24}[(\frac{\partial \theta_x}{\partial T})^2 + (\frac{\partial \theta_y}{\partial T})^2] + \frac{\rho_c c}{2}(\frac{\partial w}{\partial T})^2 \\ &+ (\frac{\rho_f(2t+c)^3 - \rho_f c^3}{24})[(\frac{\partial \theta_x}{\partial T})^2 + (\frac{\partial \theta_y}{\partial T})^2] + \frac{\rho_f(2t)}{2}(\frac{\partial w}{\partial T})^2]dA \\ &+ \int_A \bar{U}dA + \frac{1}{2}\int_A [N_x(\frac{\partial w}{\partial x})^2 + N_y(\frac{\partial w}{\partial y})^2 \\ &+ 2N_{xy}\frac{\partial w}{\partial x}\frac{\partial w}{\partial y} - 2qw]dA \qquad (3.37)\end{aligned}$$

Based on the above, variational formulation of the structural mechanics problem will be done in the next chapter.

3.4 Boundary Conditions

Appropriate boundary conditions for a system of differential equations are those which are sufficient to assure a unique solution. There are basically two classes of boundary conditions, which are referred to as geometric and force boundary conditions. The geometric boundary functions are of the translation or rotational displacement type and the force conditions correspond to the prescribed boundary forces. In the finite element analysis, the geometric boundary conditions are also

the interelement continuity conditions to be satisfied. On the other hand, the force boundary conditions correspond to actual boundary and surface forces. It is important to note that the finite element functions need only satisfy geometric functions, since the simpler the finite element functions we use in the analysis, the easier is the implementation [48].

As the geometric boundary conditions considered are the free, simply supported and the clamped conditions, we have

(a) Free edge.

At $x = 0$, there are no restraints.

At $y = 0$, there are no restraints.

(b) Simply supported edge.

At $x = 0$, w and θ_y are restrained i.e. $w = 0$; $\theta_y = 0$

At $y = 0$, w and θ_x are restrained i.e. $w = 0$; $\theta_x = 0$

(c) Clamped edge

At $x = 0$, w,θ_x and θ_y are all restrained. i.e. $w = 0$; $\theta_x = 0$; $\theta_y = 0$

At $y = 0$, w,θ_x and θ_y are all restrained. i.e. $w = 0$; $\theta_x = 0$; $\theta_y = 0$

Chapter 4

Solution Technique

4.1 General

4.1.1 Isoparametric Element

In the modern finite element methods, the use of numerically integrated isoparametric elements is becoming increasingly common. Use of isoparametric elements progressively decreases the number of elements representing a relatively complex form of the type which is liable to occur in real, rather than academic problems. These elements are more suitable than subparametric elements for modeling geometric boundary conditions as they are usually curved.

A finite element is said to be isoparametric if the same interpolation formulas define both the geometric and the displacement shape functions. In other words,

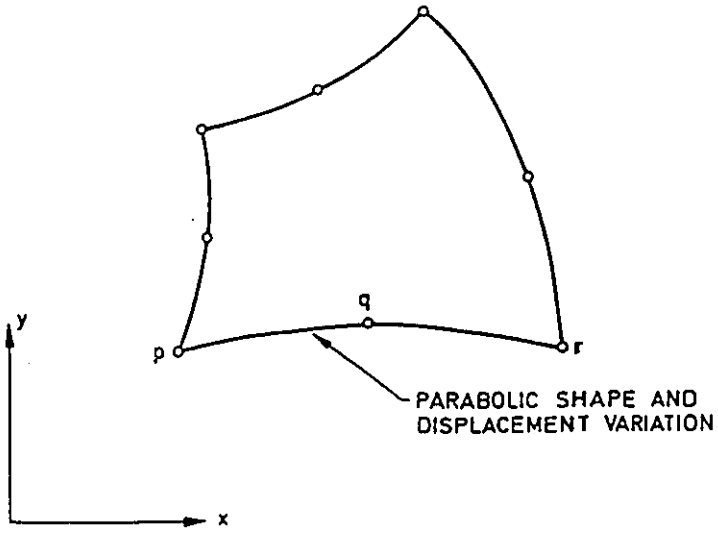

Figure 4.1: 8-Node Isoparametric Quadrilateral

the same (iso) local coordinate parametric equations (interpolation functions) used to define any quantity of interest within the elements are also utilized to define the global coordinates of any point within the element, in terms of the global spatial coordinates of the nodal points.

4.2 Formulation

4.2.1 8-Node Parabolic Isoparametric Quadrilateral

The finite element employed for the development of the computer code is a version of the two dimensional 8-node parabolic isoparametric quadrilateral (Fig.4.1).

The element is similar to the thick shell element first introduced by Ahmad

et.al[17] and later modified by Zienkiewicz et.al [18]. It is a highly versatile element and its application to problems involving thin, thick, cellular and sandwich plates and bridge decks have been discussed in Ref.[31].

4.2.2 Displacement Method

The problem is formulated here using the displacement method in which case the displacements are taken to be the prime unknowns. The natural (or dimensionless) coordinate system is used in place of the cartesian coordinates as the former allows to use elements with curvilinear shapes. This also helps to simplify the derivatives and integrals required in the development of stiffness and consistent mass matrices as the coordinates are consistent with the local geometry. The natural coordinates ξ and η are dimensionless and range from -1 to 1. This is directly compatible with the definition of abscissa utilized in numerical integration by Gaussian Quadrature which is the numerical technique used in the code.

As the displacement method is used, in cases of Plane stress and strain, the nodal displacement fields $u(\xi,\eta)$ and $v(\xi,\eta)$ throughout the element are defined using two displacement degrees of freedom u_i and v_i at each of the eight nodes and a quadratic interpolation scheme.

$$\delta = \begin{pmatrix} u \\ v \end{pmatrix} \tag{4.1}$$

In case of plate flexure, the displacement field can be uniquely specified by an independent variation of the lateral displacement w and the rotations θ_x and θ_y

which are chosen independently of w and are not related to it by differentiation. The variables θ_x and θ_y are the rotations and a correction factor is also included to allow for non-uniform shear distribution. The angles ϕ_x and ϕ_y denote the shear deformations.

$$\delta = \begin{pmatrix} w \\ \theta_x \\ \theta_y \end{pmatrix} = \begin{pmatrix} w \\ \frac{\partial w}{\partial x} + \phi_x \\ \frac{\partial w}{\partial y} + \phi_y \end{pmatrix} \tag{4.2}$$

and

$$\phi = \begin{pmatrix} -\phi_x \\ -\phi_y \end{pmatrix} \tag{4.3}$$

In the case of the combined stress and bending, we add the displacement fields of both plane stress and bending,

$$\delta = \begin{pmatrix} u \\ v \\ w \\ \theta_x \\ \theta_y \end{pmatrix} \tag{4.4}$$

4.2.3 Shape Functions

To derive the shape functions, the following second degree displacement functions are assumed [45],[47],[49].

$$u(\xi,\eta) = a_1 + b_2\xi + c_3\eta + d_4\xi^2 + e_5\xi\eta + f_6\eta^2 + g_7\xi^2\eta + h_8\xi\eta^2 \quad (4.5)$$

$$v(\xi,\eta) = a_9 + b_{10}\xi + c_{11}\eta + d_{12}\xi^2 + e_{13}\xi\eta + f_{14}\eta^2 + g_{14}\xi^2\eta + h_{16}\xi\eta^2 \quad (4.6)$$

$$w(\xi,\eta) = a_{17} + b_{18}\xi + c_{19}\eta + d_{20}\xi^2 + e_{21}\xi\eta + f_{22}\eta^2 + g_{23}\xi^2\eta + h_{24}\xi\eta^2 \quad (4.7)$$

$$\theta_x(\xi,\eta) = a_{25} + b_{26}\xi + c_{27}\eta + d_{28}\xi^2 + e_{29}\xi\eta + f_{30}\eta^2 + g_{31}\xi^2\eta + h_{32}\xi\eta^2 \quad (4.8)$$

$$\theta_y(\xi,\eta) = a_{33} + b_{34}\xi + c_{35}\eta + d_{36}\xi^2 + e_{37}\xi\eta + f_{38}\eta^2 + g_{39}\xi^2\eta + h_{40}\xi\eta^2 \quad (4.9)$$

Based on the assumed displacement functions, the two dimensional quadratic shape functions are

$$N_1(\xi,\eta) = -\frac{1}{4}(1-\xi)(1-\eta)(1+\xi+\eta) \quad (4.10)$$

$$N_2(\xi,\eta) = \frac{1}{2}(1-\xi^2)(1-\eta) \quad (4.11)$$

$$N_3(\xi,\eta) = \frac{1}{4}(1+\xi)(1-\eta)(-1+\xi-\eta) \quad (4.12)$$

$$N_4(\xi,\eta) = \frac{1}{2}(1+\xi)(1-\eta^2) \quad (4.13)$$

$$N_5(\xi,\eta) = \frac{1}{4}(1+\xi)(1+\eta)(-1+\xi+\eta) \quad (4.14)$$

$$N_6(\xi,\eta) = \frac{1}{2}(1-\xi^2)(1+\eta) \quad (4.15)$$

$$N_7(\xi,\eta) = \frac{1}{4}(1-\xi)(1+\eta)(-1-\xi+\eta) \quad (4.16)$$

$$N_8(\xi,\eta) = \frac{1}{2}(1-\xi)(1-\eta^2) \quad (4.17)$$

Each of these shape functions have a value of unity at the node to which they are related and zero at all other nodes . For example, N_1 is the shape function at node 1 and has the value of unity at node 1 and zero elsewhere. Further, they also have the property that their sum at any point within an element results in no element straining. The efficiency of any particular element type used will depend upon how well the shape functions are capable of representing the true displacement field. Shape functions must guarantee continuity between elements also known as the continuity condition. In the limit as the element size is reduced to infinitesimal dimensions, the shape function must be able to reproduce a constant strain condition through the element. The unknown function must be able to take up in the limit, any linear form throughout the element (known as the constant strain condition).

The displacement at a point within the element can be expressed as

$$\delta = \sum_{i=1}^{8} \mathbf{N}_i \delta_i \tag{4.18}$$

where

$$\mathbf{N} = [\mathbf{N_1}, \mathbf{N_2}, ..., \mathbf{N_8}] \tag{4.19}$$

and $\mathbf{N}_i = N_i\mathbf{I}$ where $\mathbf{I}$ is a $r \times r$ matrix with r being the degree of freedom per node.

The diplacement fields for various cases can thus be written as,

a) Plane stress and strain

$$\begin{pmatrix} u \\ v \end{pmatrix} = \sum_{i=1}^{8} \mathbf{N}_i \delta_i \tag{4.20}$$

where $\delta_i = (u_i, v_i)^T$ is the vector of displacement at node i.

b) Plate flexure

$$\begin{pmatrix} w \\ \theta_x \\ \theta_y \end{pmatrix} = \sum_{i=1}^{8} \mathbf{N}_i \delta_i \tag{4.21}$$

where $\delta_i = (w_i, \theta_{xi}, \theta_{yi})^T$ is the vector of displacements at node i.

c) Combined stress and bending

$$\begin{pmatrix} u \\ v \\ w \\ \theta_x \\ \theta_y \end{pmatrix} = \sum_{i=1}^{8} \mathbf{N}_i \delta_i \tag{4.22}$$

where $\delta_i = (u_i, v_i, w_i, \theta_{xi}, \theta_{yi})^T$ is the vector of displacements at node i.

4.2.4 Element Topology

The orientation of the local coordinate directions ξ and η is important as the shape function defined earlier are dependent on the orientation of ξ and η. The variable ξ and η are curvilinear coordinates and as such their direction will vary with position. However, their general direction are always known relative to the element sides. The shape functions described earlier are based upon the following dependence between the ordering of the element nodal connection numbers and the local coordinate axes ξ,η.

In this research work, as static and dynamic analysis of rectangular plates is envisaged, the 8-node rectangular isoparametric element is used. Depending upon the generation of the finite element mesh , either curvilinear or colinear coordinates can be chosen.

The nodes of an element are read in an anticlockwise sequence starting from any corner node.

The positive ξ axis is then in the direction defined by moving along an element edge from the 1st element nodal connection, through the 2nd to the 3rd.

The positive η axis is in the direction of the element edge from the 3rd nodal connection number, through the 4th to the 5th number.

The element topology is defined in the sequence indicated by nodal numbers 1 to 8, the direction of ξ and η are as shown in Figure 4.2.

As the isoparametric family is a group of elements in which the shape functions

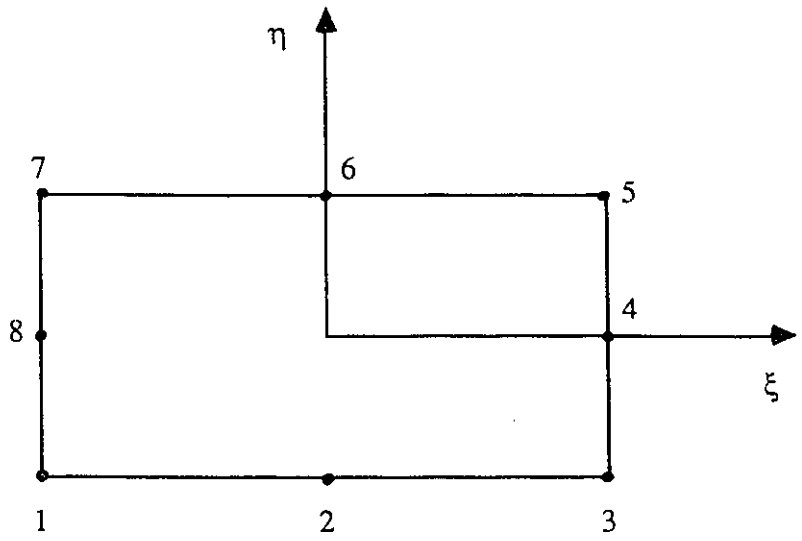

Figure 4.2: Element Topology

are used to define the geometry as well as the displacement field, we can define the geometry as

$$x = \sum_{i=1}^{8} \mathrm{N}_i x_i \tag{4.23}$$

$$y = \sum_{i=1}^{8} \mathrm{N}_i y_i \tag{4.24}$$

where (x_i, y_i) are coordinates of node i.

4.3 Element Strain Matrix

After establishing the displacements at all points within the element, the strain-displacement relationship can be expressed as

$$\epsilon = \mathbf{L}\delta \tag{4.25}$$

where ϵ is the strain vector, δ is the displacement vector and $\mathbf{L}$ is the matrix of displacement differential operators. The displacement vector at any point within the element can be written as,

$$\delta = \mathbf{N}\delta^e \tag{4.26}$$

where $\mathbf{N}$ is the matrix of the shape functions as given in Equation (4.19) and δ^e represents a listing of nodal displacements for a particular element.

$$\epsilon = \mathbf{L}\mathbf{N}\delta^e = \mathbf{B}\delta^e = \sum_{i=1}^{8} \mathbf{B}_i\delta_i \tag{4.27}$$

where $\mathbf{B} = (\mathbf{B_1}, \mathbf{B_2}, ...\mathbf{B_8})$ and is known as the element strain matrix, generally composed of derivatives of the shape functions.

In case of plane stress/strain situations, the strain/displacement relationship may be written as,

$$\begin{pmatrix} \frac{\partial u}{\partial x} \\ \frac{\partial v}{\partial y} \\ \frac{\partial u}{\partial y} + \frac{\partial v}{\partial x} \end{pmatrix} = \begin{pmatrix} \frac{\partial}{\partial x} & 0 \\ 0 & \frac{\partial}{\partial y} \\ \frac{\partial}{\partial y} & \frac{\partial}{\partial x} \end{pmatrix} \begin{pmatrix} u \\ v \end{pmatrix} \tag{4.28}$$

Using finite element idealisation, we can write,

$$\epsilon = \sum_{i=1}^{8} \begin{pmatrix} \frac{\partial N_i}{\partial x} & 0 \\ 0 & \frac{\partial N_i}{\partial y} \\ \frac{\partial N_i}{\partial y} & \frac{\partial N_i}{\partial x} \end{pmatrix} \begin{pmatrix} u_i \\ v_i \end{pmatrix} = \sum_{i=1}^{8} \mathbf{B}_i \delta_i \tag{4.29}$$

In case of plate flexure, the generalized strain/displacement relationship may be written as

$$\epsilon = \sum_{i=1}^{8} \mathbf{B}_i \delta_i \tag{4.30}$$

where $(\epsilon)^T = ((\chi)^T, (\phi)^T)$

and

$$\mathbf{B}_i = \begin{pmatrix} \mathbf{B}_{bi} \\ -- \\ \mathbf{B}_{si} \end{pmatrix} = \begin{pmatrix} 0 & -\frac{\partial N_i}{\partial x} & 0 \\ 0 & 0 & -\frac{\partial N_i}{\partial y} \\ 0 & -\frac{\partial N_i}{\partial y} & -\frac{\partial N_i}{\partial x} \\ --- & --- & --- \\ \frac{\partial N_i}{\partial x} & -N_i & 0 \\ \frac{\partial N_i}{\partial y} & 0 & -N_i \end{pmatrix} \tag{4.31}$$

where $\mathbf{B}_{bi}$ is the strain matrix associated with bending deformation χ and $\mathbf{B}_{si}$ is the strain matrix associated with shear deformation ϕ.

$$\chi = \begin{pmatrix} \chi_x \\ \chi_y \\ \chi_{xy} \end{pmatrix} = \begin{pmatrix} -\frac{\partial \theta_x}{\partial x} \\ -\frac{\partial \theta_y}{\partial y} \\ -(\frac{\partial \theta_x}{\partial y} + \frac{\partial \theta_y}{\partial x}) \end{pmatrix} \tag{4.32}$$

and the measures of shear deformation are as given in Equation (4.3).

In the combined stress and bending case, the strain/displacement relationships for the plane stress/strain and plate flexure are simply added together.

$$\mathbf{B}_i = \begin{pmatrix} \frac{\partial N_i}{\partial x} & 0 & 0 & 0 & 0 \\ 0 & \frac{\partial N_i}{\partial y} & 0 & 0 & 0 \\ \frac{\partial N_i}{\partial y} & \frac{\partial N_i}{\partial x} & 0 & 0 & 0 \\ 0 & 0 & 0 & -\frac{\partial N_i}{\partial x} & 0 \\ 0 & 0 & 0 & 0 & -\frac{\partial N_i}{\partial y} \\ 0 & 0 & 0 & -\frac{\partial N_i}{\partial y} & -\frac{\partial N_i}{\partial x} \\ 0 & 0 & \frac{\partial N_i}{\partial x} & -N_i & 0 \\ 0 & 0 & \frac{\partial N_i}{\partial y} & 0 & -N_i \end{pmatrix} \tag{4.33}$$

As the shape functions are expressed in terms of the (ξ, η) coordinate system, the chain rule must be used to calculate the components of the strain matrix.

$$\frac{\partial N}{\partial x} = \frac{\partial N}{\partial \xi}\frac{\partial \xi}{\partial x} + \frac{\partial N}{\partial \eta}\frac{\partial \eta}{\partial x}$$

$$\frac{\partial N}{\partial y} = \frac{\partial N}{\partial \xi}\frac{\partial \xi}{\partial y} + \frac{\partial N}{\partial \eta}\frac{\partial \eta}{\partial y}$$

The derivation of the shape functions $\frac{\partial N}{\partial \xi}$ and $\frac{\partial N}{\partial \eta}$ are directly obtained, however $\frac{\partial \xi}{\partial x}, \frac{\partial \xi}{\partial y}, \frac{\partial \eta}{\partial x}$ and $\frac{\partial \eta}{\partial y}$ must be evaluated from the inverse of the jacobian matrix. As an isoparametric formulation has been adopted in which the element geometry and displacement field are both defined by the same shape function, the jacobian matrix $\mathbf{J}(\xi, \eta)$ may be calculated from,

$$\mathbf{J} = \begin{pmatrix} \frac{\partial x}{\partial \xi} & \frac{\partial y}{\partial \xi} \\ \frac{\partial x}{\partial \eta} & \frac{\partial y}{\partial \eta} \end{pmatrix} = \sum_{i=1}^{8} \begin{pmatrix} \frac{\partial N_i}{\partial \xi} & \frac{\partial N_i}{\partial \xi} \\ \frac{\partial N_i}{\partial \eta} & \frac{\partial N_i}{\partial \eta} \end{pmatrix} \begin{pmatrix} x_i & 0 \\ 0 & y_i \end{pmatrix} \tag{4.34}$$

in which x_i and y_i are the x and y coordinates of the node i.

Thus the inverse of the jacobian can be readily obtained.

$$\mathbf{J}^{-1} = \begin{pmatrix} \frac{\partial \xi}{\partial x} & \frac{\partial \eta}{\partial x} \\ \frac{\partial \xi}{\partial y} & \frac{\partial \eta}{\partial y} \end{pmatrix} \tag{4.35}$$

It is also useful to note here that an element of area $dxdy$ may be calculated by the expression

$$dxdy = |\mathbf{J}| d\xi d\eta \tag{4.36}$$

where $|\mathbf{J}|$ is the determinant of $\mathbf{J}$.

4.4 Development of the Elasticity Matrix

The stress/strain relationships for an elastic material in the absence of initial stresses and strains, may be written in the form,

$$\sigma = \mathbf{D}\epsilon \tag{4.37}$$

where $\mathbf{D}$ is the matrix of elastic constants.

For plane stress case and for isotropic materials,

$$\mathbf{D} = \frac{E}{1-\nu^2}\begin{pmatrix} 1 & \nu & 0 \\ \nu & 1 & 0 \\ 0 & 0 & \frac{1-\nu}{2} \end{pmatrix} \tag{4.38}$$

whereas for plane strain case (isotropic case), the $\mathbf{D}$ matrix is of the form,

$$\mathbf{D} = \frac{E(1-\nu)}{(1+\nu)(1-2\nu)}\begin{pmatrix} 1 & \frac{\nu}{1-\nu} & 0 \\ \frac{\nu}{1-\nu} & 1 & 0 \\ 0 & 0 & \frac{1-2\nu}{2(1-\nu)} \end{pmatrix} \tag{4.39}$$

In the case of plate flexure, the stress-strain relationships may be written in the following form

$$M = \mathbf{D}_b\chi;\ Q = \mathbf{D}_s\phi_s \tag{4.40}$$

where M and Q are the bending moments and shear forces respectively and χ and ϕ_s are the measures of bending deformation and shear deformation.

For an isotropic homogeneous material,

$$\mathbf{D}_f = \frac{Et^3}{12(1-\nu^2)} \begin{pmatrix} 1 & \nu & 0 \\ \nu & 1 & 0 \\ 0 & 0 & \frac{1-\nu}{2} \end{pmatrix} \tag{4.41}$$

and

$$\mathbf{D}_s = \frac{Et}{2(1+\nu)\alpha} \begin{pmatrix} 1 & 0 \\ 0 & 1 \end{pmatrix} \tag{4.42}$$

The **D**-matrix in case of plate bending for isotropic materials is

$$\mathbf{D} = \frac{Et^3}{12(1-\nu^2)} \begin{pmatrix} 1 & \nu & 0 & 0 & 0 \\ \nu & 1 & 0 & 0 & 0 \\ 0 & 0 & \frac{1-\nu}{2} & 0 & 0 \\ 0 & 0 & 0 & \frac{12(1-\nu)}{2.4t^2} & 0 \\ 0 & 0 & 0 & 0 & \frac{12(1-\nu)}{2.4t^2} \end{pmatrix} \tag{4.43}$$

For combined stress and bending (Isotropic case), the **D**-matrix is the addition of the **D**-matrices for plane stress and bending cases.

$$\mathbf{D} = \frac{Et^3}{12(1-\nu^2)} \begin{pmatrix} \frac{12}{t^3} & \frac{12\nu}{t^3} & 0 & 0 & 0 & 0 & 0 & 0 \\ \frac{12\nu}{t^3} & \frac{12}{t^3} & 0 & 0 & 0 & 0 & 0 & 0 \\ 0 & 0 & \frac{1-\nu}{2}\left(\frac{12}{t^3}\right) & 0 & 0 & 0 & 0 & 0 \\ 0 & 0 & 0 & 1 & \nu & 0 & 0 & 0 \\ 0 & 0 & 0 & \nu & 1 & 0 & 0 & 0 \\ 0 & 0 & 0 & 0 & 0 & \frac{1-\nu}{2} & 0 & 0 \\ 0 & 0 & 0 & 0 & 0 & 0 & \frac{12(1-\nu)}{2.4t^2} & 0 \\ 0 & 0 & 0 & 0 & 0 & 0 & 0 & \frac{12(1-\nu)}{2.4t^2} \end{pmatrix} \tag{4.44}$$

4.5 Modification of Elastic Rigidities

For sandwich plate analysis, the terms developed earlier hold good except the elastic rigidities.

As mentioned earlier, the thickness and the elastic properties of the two face plates in this development has been taken to be the same.

The elastic rigidities for sandwich plates of isotropic material in flexure in both faces and cores may be calculated as follows.

The rigidities for a sandwich plate can be expressed as,

$$\mathbf{D} = \begin{pmatrix} \mathbf{D}_{11} & \mathbf{D}_{12} & \mathbf{D}_{13} & \mathbf{D}_{14} & \mathbf{D}_{15} \\ \mathbf{D}_{21} & \mathbf{D}_{22} & \mathbf{D}_{23} & \mathbf{D}_{24} & \mathbf{D}_{25} \\ \mathbf{D}_{31} & \mathbf{D}_{32} & \mathbf{D}_{33} & \mathbf{D}_{34} & \mathbf{D}_{35} \\ \mathbf{D}_{41} & \mathbf{D}_{42} & \mathbf{D}_{43} & \mathbf{D}_{44} & \mathbf{D}_{45} \\ \mathbf{D}_{51} & \mathbf{D}_{52} & \mathbf{D}_{53} & \mathbf{D}_{54} & \mathbf{D}_{55} \end{pmatrix} \tag{4.45}$$

Each rigidity has a contribution from the faces of the sandwich plate and also from the core.

a) Flexural rigidity : $\mathbf{D}_{11} = \mathbf{D}_{22} = (\mathbf{D}_{11})_c + (\mathbf{D}_{11})_f$

b) Coupling rigidity : $\mathbf{D}_{12} = \mathbf{D}_{21} = \nu_c(\mathbf{D}_{11})_c + \nu_f(\mathbf{D}_{11})_f$

c) Torsional rigidity : $\mathbf{D}_{33} = (1-\nu_c)(\mathbf{D}_{11})_c/2 + (1-\nu_f)(\mathbf{D}_{11})_f/2$

d) Shear rigidity : $\mathbf{D}_{44} = \mathbf{D}_{55} = (\mathbf{D}_{44})_c + (\mathbf{D}_{44})_f$

All the other terms of Equation (4.45) are equal to zero.

The expressions for the plate rigidities for sandwich plates have been given in Equations (3.14) and (3.16). Based on the assumptions made earlier, we can write

$$\mathbf{D}_{11} = \mathbf{D}_{22} = \frac{E_f t(c+t)^2}{2(1-\nu_f^2)} \tag{4.46}$$

$$\mathbf{D}_{12} = \mathbf{D}_{21} = \nu_f \mathbf{D}_{11} \tag{4.47}$$

$$\mathbf{D}_{33} = (\frac{1-\nu_f}{2})\mathbf{D}_{11} \tag{4.48}$$

$$\mathbf{D}_{44} = \mathbf{D}_{55} = \frac{E_c}{2(1+\nu_c)}\frac{c}{1.2} = \frac{G_c c}{1.2} \tag{4.49}$$

where 1.2 is the shear correction factor.

For an orthotropic core,

$$\mathbf{D}_{44} = \frac{G_{xz} c}{1.2} \tag{4.50}$$

$$\mathbf{D}_{55} = \frac{G_{yz} c}{1.2} \tag{4.51}$$

4.6 Static Equilibrium Equations

Using the principle of virtual work we generate the equilibrium equations needed for the solution of the nodal point displacements.

If the plate is subjected to body forces $\mathbf{f}^B$, surface forces $\mathbf{f}^S$, concentrated forces $\mathbf{F}^i$, the equilibrium of the body requires that for any compatible, small virtual displacements imposed onto the plate, the total internal virtual work done is equal to the total external virtual work [48]. Identifying virtual quantities by placing a bar over the quantity, we have

$$\int_V \bar{\epsilon}^T \sigma dV = \int_V \bar{\delta}^T \mathbf{f}^B dV + \int_S \bar{\delta}^{S^T} \mathbf{f}^S dS + \sum_i \bar{\delta}^{i^T} \mathbf{F}^i \tag{4.52}$$

where the integrations are performed over the volume V and surface S of the plate, respectively and the summation sign $\sum_i$ includes all points where concentrated forces $\mathbf{F}^i$ are applied. The above is a statement of the equilibrium of the plate. The plate is approximated as an assemblage of discrete finite elements in this analysis with the elements being interconnected at nodal points on the element boundaries. We also assume that the plate has been idealized in such a way that all concentrated forces are applied at the nodal points. The displacements and hence the strain measured within each element are assumed to be a function of the displacements at the all the finite element nodal points.

We can now derive equilibrium equations that correspond to the nodal point displacements of the assemblage of finite elements.

The above equation can be written as a sum of integrations over the volume and areas of all finite elements i.e.

$$\begin{aligned} \sum_n \int_{V^{(n)}} \bar{\epsilon}^{(n)^T} \sigma^{(n)} dV^{(n)} &= \sum_n \int_{V^{(n)}} \bar{\delta}^{(n)^T} \mathbf{f}^{B(n)} dV^{(n)} + \sum_n \int_{S^{(n)}} \bar{\delta}^{S(n)^T} \mathbf{f}^{S(n)} dS^{(n)} \\ &\quad + \sum_i \bar{\delta}^{iT} \mathbf{F}^i \end{aligned} \tag{4.53}$$

where n varies from 1 to the total number of elements.

Substituting in the Equation (4.53) for element displacements, strains and stresses expressed in Equations (4.26),(4.27) and (4.37), we have for the element assemblage,

$$
\begin{aligned}
(\bar{\delta})^T[\sum_n \int_{V^{(n)}} \mathbf{B}^{(n)^T}\mathbf{D}^{(n)}\mathbf{B}^{(n)}dV^{(n)}](\delta) = \\
(\bar{\delta})^T[\sum_n \int_{V^{(n)}} \mathbf{N}^{(n)^T}\mathbf{f}^{B(n)}dV^{(n)}] + \\
(\bar{\delta})^T[\sum_n \int_{S^{(n)}} \mathbf{N}^{S(n)^T}\mathbf{f}^{S(n)}dS^{(n)}] + (\bar{\delta})^T\mathbf{F}
\end{aligned}
\tag{4.54}
$$

where $\mathbf{F}$ is the vector of all the externally applied forces to the nodes of the element assemblage and (δ) is the vector of the global nodal displacements.

To obtain the equilibrium equations that we want to use for the solution of the nodal point displacements, we invoke the virtual displacement theorem, by imposing unit virtual displacements in turn at all displacement components. Thus the equilibrium equation of the element assemblage corresponding to the nodal point displacements are,

$$
(\mathbf{K})(\delta) = \mathbf{R} \tag{4.55}
$$

where $\mathbf{R}=\mathbf{R}_B + \mathbf{R}_S + \mathbf{R}_C$.

The matrix $(\mathbf{K})$ is the stiffness matrix of the element assemblage .

$$(\mathbf{K}) = \sum_n \int_{V^{(n)}} \mathbf{B}^{(n)^T} \mathbf{D}^{(n)} \mathbf{B}^{(n)} dV^{(n)} \tag{4.56}$$

and the element stiffness matrix $\mathbf{K}$ is

$$\mathbf{K} = \int_V \mathbf{B}^T \mathbf{D} \mathbf{B} dV \tag{4.57}$$

The load vector $\mathbf{R}$ includes the effect of the element body forces

$$\mathbf{R}_B = \sum_n \int_{V^{(n)}} \mathbf{N}^{(n)^T} \mathbf{f}^{B(n)} dV^{(n)} \tag{4.58}$$

the effect of the element surface forces

$$\mathbf{R}_S = \sum_n \int_{S^{(n)}} \mathbf{N}^{S(n)^T} \mathbf{f}^{S(n)} dS^{(n)} \tag{4.59}$$

and the concentrated loads

$$\mathbf{R}_C = \mathbf{F} \tag{4.60}$$

4.7 Dynamic Equilibrium Equations

Equation (4.55) is a statement of the static equilibrium of the element assemblage. It should be realized , though, the applied forces may vary with time, in which case the displacements also vary with time and (4.55) is a statement of equilibrium for any specific point in time. However, in most cases when the loads are time dependent, inertia forces need to be considered; i.e., a truly dynamic problem needs to be solved.

Using d'Alemberts principle, we can simply include the element inertia forces as part of the body forces. If the superscript dot denotes the differentiation with respect to time , then the nodal acceleration for node i may be written in the form [16]

$$(\ddot{\delta}_i)^T = (\ddot{u}_i, \ddot{v}_i, \ddot{w}_i, \ddot{\theta}_{xi}, \ddot{\theta}_{yi}) \tag{4.61}$$

In the case of plate flexure, the transverse and rotatory accelerations produce lateral inertia forces $-\rho(\frac{\partial^2 w}{\partial T^2})$ and rotatory inertia couples $\frac{-\rho t^2}{12}\frac{\partial^2 \theta_x}{\partial T^2}$ and $\frac{-\rho t^2}{12}\frac{\partial^2 \theta_y}{\partial T^2}$

The nodal forces due to these inertia forces may be expressed using the principle of virtual work as,

$$\mathbf{R}_I = -\sum_n \int_{V(n)} \mathbf{N}^{(n)^T} \begin{pmatrix} \rho\ddot{w} \\ \frac{\rho t^2}{12}\ddot{\theta}_x \\ \frac{\rho t^2}{12}\ddot{\theta}_y \end{pmatrix} dV^n \tag{4.62}$$

where $\mathbf{R_I}$ is the vector of element nodal inertia forces, ρ is the mass density per unit area of the plate, t is the plate thickness and $\mathbf{N}$ is the element shape function matrix.

Since the shape function used to describe the variation of acceleration over the element are identical to those used to describe the displacement field over the element, we can therefore write,

$$\mathbf{R}_I = -\sum_n \int_{V^{(n)}} \mathbf{N}^{(n)^T} \begin{pmatrix} \rho & 0 & 0 \\ 0 & \frac{\rho t^2}{12} & 0 \\ 0 & 0 & \frac{\rho t^2}{12} \end{pmatrix} \mathbf{N}^{(n)} dV^{(n)}(\ddot{\delta}) \tag{4.63}$$

Hence we can, now, say that the contribution from the total body forces to the load vector $\mathbf{R}$ is,

$$\mathbf{R}_B = \sum_n \int_{V^{(n)}} \mathbf{N}^{(n)^T} (\mathbf{f}^{B(n)} - \rho_m^{(n)} \mathbf{N}^{(n)} \ddot{\delta}) dV^{(n)}) \tag{4.64}$$

where $\mathbf{f}^{B(n)}$ no longer include inertia forces, $\ddot{\delta}$ lists the nodal point accelerations (i.e. the second time derivative of δ) and $\rho_m^{(n)}$ is the matrix of density coefficients for the translatory and rotatory inertia terms.

The equilibrium equation for the dynamic case is,

$$(\mathbf{M})\ddot{\delta} + (\mathbf{K})\delta = \mathbf{R} \tag{4.65}$$

The matrix (M) is the mass matrix of the structure and can be written as

$$(\mathrm{M}) = \sum_n \int_{V^{(n)}} \rho_m^{(n)} \mathbf{N}^{(n)^T} \mathbf{N}^{(n)} dV^{(n)} \tag{4.66}$$

and the mass matrix for an element is

$$\mathrm{M} = \int_V \rho_m \mathbf{N}^T \mathbf{N} dV \tag{4.67}$$

The mass matrix is also known as the consistent mass matrix as the same interpolation functions are employed in its evaluation as that in the calculation of the load vector and stiffness matrix.

4.8 Free Vibration Governing Equation

The matrix equation governing free vibrations may be expressed as

$$(\mathbf{K})(\delta) - \omega^2(\mathrm{M})(\delta) = 0 \tag{4.68}$$

where $(\mathbf{K})$ and (M) are global stiffness and mass matrix respectively obtained by the assembly of the corresponding element matrices. (δ) is the vector of global nodal displacements and ω is the natural frequency of the free vibration of the system.

Chapter 5

Discussion on the Computer Code

A computer code capable of handling static and dynamic analysis of homogeneous plates and sandwich plates with any uniform boundary conditions, with any aspect ratio, material properties and dimensions is developed.

The general flow chart for the program is given in Appendix B which shows a graphical representation of a specific sequence of steps performed by the program to produce the solutions of a given problem. A sample input and output is also appended in Appendix B.

Effort has been put to make the program highly versatile. Problems of plane stress, plane strain, bending and combined stress and bending can be handled. As discussed earlier in Chapter 4, the isoparametric element chosen is quite capable of handling multilayered plates and thick plates albeit with slightly different numerical integration procedures [18]. Static and Dynamic analysis can be performed for all of the above cases.

In the finite element method, we must evaluate certain integrals such as the stiffness integrals, consistent mass integrals and consistent load integrals. In this program, the Gauss-Legendre quadrature numerical integration procedure is used for its high accuracy [46],[39],[45] and the ease with which it can be implemented. It should be noted that an n-point rule integrates any polynomial of degree x^{2n-1} or less. In this procedure, both the positions of the sampling points and the weights have been optimized. For example, consider the following integral which is to be evaluated using a 3-point rule in both the ξ and η directions.

$$\begin{aligned} I_{3,3} &= \int_{-1}^{+1}\int_{-1}^{+1} f(\xi,\eta)d\xi d\eta = \int_{-1}^{+1}[\int_{-1}^{+1} f(\xi,\eta)d\xi]d\eta \\ &= \int_{-1}^{+1}(a_1 f(\xi_1,\eta) + a_{11}f(\xi_{11},\eta) + a_{111}f(\xi_{111},\eta))d\eta \\ &= a_1[a_1 f(\xi_1,\eta_1) + a_{11}f(\xi_1,\eta_{11}) + a_{111}f(\xi_1,\eta_{111})] \\ &\quad + a_{11}[a_1 f(\xi_{11},\eta_1) + a_{11}f(\xi_{11},\eta_{11}) + a_{111}f(\xi_{11},\eta_{111})] \\ &\quad + a_{111}[a_1 f(\xi_{111},\eta_1) + a_{11}f(\xi_{111},\eta_{11}) + a_{111}f(\xi_{111},\eta_{111})] \end{aligned}$$

where ξ_i is the ξ coordinate of the i^{th} Gauss point, η_i is the η coordinate of the i^{th} Gauss point and a_i is the weighting factor.

Subroutine GAUSSQ sets up the sampling point positions and weighting factors for numerical integration where 2-point,3-point and 4-point rules can be incorporated.

The choice of the order of numerical integration is important in practice, because, firstly, the cost of analysis increases when a higher-order integration is employed, and secondly, by using a different integration order, the results can be

affected by a very large amount. In general, the appropriate integration order depends on the matrix that is evaluated and the specific finite element considered. The stiffness of displacement elements is reduced as the order of numerical integration decreases and the convergence of a numerically integrated element is always guaranteed providing the integration order allows sufficient accuracy for an exact evaluation of the element volume in isoparametric formulation [18]. The recommended order of Gaussian numerical integration for two dimensional isoparametric elements is given in Appendix C [48].

In the analysis of structural engineering problems by the method of finite elements, solution of the large number of simultaneous equations is of prime importance. The size often exceeds the storage capacity of an average size computer. The number of equations depend upon the total number of degrees of freedom. As the accuracy of the solution generally increases with an increase of the number of elements taken into consideration i.e. increasing the grid fineness, the number of equations also increase. All this necessitates the economic use of the available computer memory. Fortunately, the structural engineering problems have some special characteristics like bandedness and symmetry which allows programming to effect an efficient and economic usage of the available storage space. Banded matrices, when handled properly, not only lead to saving of memory space in the computer, but also to a reduction in the time required for solving the many multiplications, additions and subtractions of zero quantities. In this work, semi-bandwidth of the upper portion of the assembled matrices are stored in a rectangular matrix. There is a further reduction possible by using the 'skyline technique' wherein the zeroes within the semi-bandwidth are avoided. This leads to further reduction of storage space. However, this has not been incorporated in this program.

Preparing input data is not a very cumbersome procedure for this program . The program is capable of taking variable dimensioning in the x and y directions respectively. As the stresses and strains are more pronounced near the boundaries, this facility gives us an option to a create a finer mesh near the boundaries than in the middle. Due to this, more precise analysis of the displacements can be performed without wasting much computer time.

Though in this work all elements have the same material, the program has the added facility of incorporating elements of different material properties too.

Boundary conditions are also incorporated in a very simple manner. '0' signifies free and '1' signifies fixed. The boundary condition for each and every degree of freedom for each boundary node is thus listed out as either 0 or 1. It should be noted here that as the shear deformation is being taken into account, it is not entirely true if the rotations are fully restrained i.e. equal to 1. For thin plates, these are fully restrained to match the theoretical values but in case of slightly thick plates, it is not entirely correct, as by restraining the rotations θ_x, θ_y, the existing shear is also restrained. However, it does not create any problem as only small thicknesses of the plate are considered in this present study.

The program separates out the fixed and free nodes which help in generating the number of modified equations. The number of modified equations to be solved is equal to the total number of degrees of freedom minus the number of imposed restraints. Some amount of computer time can be saved in this case. The load vector is also modified to account for these restraints. The program is capable of different types of loading at the nodes including uniformly distributed loads, concentrated loads or a combination of both.

Detailed discussion of the various solution methods used for calculating the unknown displacements or eigenvalue problems in finite element analysis can be found in Ref.[46],[47],[48],[49]. In this program, for static analysis, the Choleski method is employed. This method is quite suitable for matrices stored in the semi-bandwidth form [47].

For the calculation of the eigenvalues and the corresponding eigenvectors, two subroutines were used. The Subspace Iteration Method and the Jacobi Method. Both are well known eigensolvers but the former requires input to be in a banded form and the latter, in full form. As the code has the flexibility to generate both the banded and full form of matrices, results were checked and compared.Both the eigensolvers exhibited excellent comparison with each other. The Jacobi method is less tedious to use as compared to the subspace iteration because in the latter, trial eigenvectors have to be chosen [50] depending upon the number of total degrees of freedom everytime a different case has to be run. But the Jacobi method takes a much longer time to generate results as it calculates all the eigenvalues and eigenvectors unlike the Subspace method in which the number of modes to be calculated can be specified.

Chapter 6

Analysis and Discussion of Results

6.1 General

The aim of the numerical results presented herein is to provide information which may lead to a better understanding of static and dynamic behaviour of homogeneous rectangular plates and sandwich plates. The results presented are of limited number and any conclusions drawn therefrom are generally of qualitative nature.

Basis for the evaluation of a particular finite element is the consideration of all the factors that influence the results obtained with that element. Accuracy of the final answers and the amount of time and effort involved are the main aspects to be considered.

6.2 Errors in Finite Element Analysis

Errors in the results obtained using a finite element approximation may be broadly classified into the idealization or discretization error, illconditioning, truncation and rounding off errors [47]. To model a problem, the number, type and shape of elements and the grading of the mesh is decided. Elastic constants are chosen, loads are allocated to nodes and boundary conditions are selected. The model, which approximates a continuum having an infinite number of degrees of freedom, has only a finite number of degrees of freedom. Each of these factors may contribute to the misrepresentation of reality which is called the idealization or discretization error.

Equation $(\mathbf{K})(\mathbf{X}) = (\mathbf{R})$ is termed as illconditioned if small changes in $(\mathbf{K})$ or $(\mathbf{R})$ may lead to large changes of coefficients in the solution $(\mathbf{X})$. Illconditioning may reflect the physical reality of a structure. It may also arise even when the physical problem is stable, because of the way the computer manipulates numbers. Included in this manipulation errors are the truncation errors and the rounding off errors. The former is more important than the latter in finite element analysis as truncation leads to certain information being discarded whereas rounding off refers to the adjustment of the last bit during computation.

6.3 Comparision of Results

Comparisions are done to investigate the accuracy of the finite element used in this work when it is applied to rectangular homogeneous plates or sandwich plates

for static and dynamic analysis. The results presented herein are for bending problems only.

The convergence characteristics of the element used has been highlighted for various cases for both homogeneous plates and sandwich plates. The basic purpose to include many graphs exhibiting convergence, even at the risk of being redundant, is to instill confidence in the element used for the analysis.

Basically, three different types of edge conditions are considered in this work. For simplicity, following abbreviations have been used in this thesis.

C - Clamped
S - Simply Supported
F - Free

The boundary condition as shown in the Figure 6.1 will be specified as CCSF i.e. clamped-clamped-simple-free. They are defined as the edge conditions counted from the left side in an anticlockwise manner.

It should also be noted here that unless otherwise specified, all the mesh sizes are for the quarter plate.

6.3.1 Static analysis of rectangular homogeneous plates

Values are obtained for the center deflection for the rectangular homogeneous plate for simply supported and clamped boundary conditions. Both the uniformly

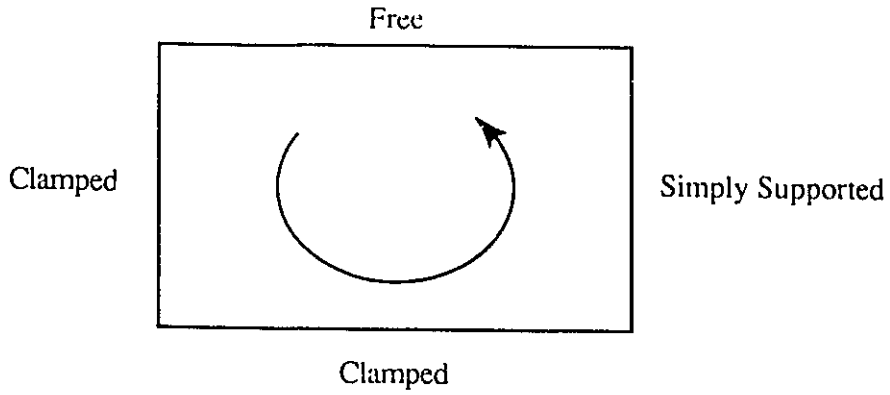

Figure 6.1: Specification of boundary conditions

distributed load and the concentrated load applied at the center of the plate are considered.

Figure A.1 shows the comparision and convergence of the center deflection for a simply supported plate with a concentrated load applied at its center. The results when compared with the classical solution of Timoshenko [61] show excellent agreement with a difference of 0.1%. It can be inferred from the figure that the convergence is achieved very rapidly as the values obtained by 3×3 mesh size and 4×4 mesh size have a difference of only 0.07%.

Figure A.2 similarly shows the comparision and convergence of the center deflection for a simply supported plate with an uniformly distributed load. Excellent agreement is shown here too with a difference of about 0.4% with the classical solution for a 4×4 mesh.

Figure A.3 and A.4 show the comparision and convergence of the center deflection for a clamped plate with a concentrated load applied at its center and an

uniformly distributed load respectively. The difference with the classical solution is about 0.21% for the former and 0.4% for the latter for a 4×4 mesh.

Figure A.5 exhibits an excellent comparision with previous finite element results generated for different mesh sizes for a fully clamped plate with a concentrated load applied at its center.

6.3.2 Dynamic analysis of rectangular homogeneous plates

Natural frequencies for various boundary conditions are presented in Figures A.6 to A.17 for a square rectangular homogeneous plate.

In figures A.6 to A.8, the comparision and convergence for a clamped plate is shown for the lowest three natural frequencies. Figures A.10 to A.12 show the comparision and convergence for a CCSS plate. The natural frequencies generated in the present work are generally lower than those by Leissa [59] as the latter neglected the rotatory inertia and shear deformation of the plate while calculating the frequencies. The maximum discrepancy does not exceed more than 3.2% between both the values. As the thickness of the plate is small compared to that of the sides, the effect is not quite predominant. The rotatory inertia and the shear deformation will have a much greater impact for higher modes and if the thickness of the plate increases. Hence, it can be stated that the formulations used by the present work produce more accurate solutions for various dimensions of the homogeneous rectangular plate.

Figure A.9 and A.13 show the comparision of the natural frequency for a clamped plate and a CCSS plate for various modes respectively.

Figures A.14 to A.17 similarly show the comparision of the natural frequencies for various cases with results generated by Leissa [59].

Excellent agreement is generally seen except for the difference due to the rotatory inertia and shear deformation.

Numerical integration techniques play an important part in the finite element analysis. Gaussian quadrature is the numerical integration method followed in this work. The order of the Gaussian quadrature chosen is very important. Hereafter, the order of the Gaussian quadrature will be referred to as

NGAUS = 2 (Lower order of Gaussian quadrature)

NGAUS = 3 (Higher order of Gaussian quadrature)

It was found in the course of generating results during this work that a lower order of Gaussian quadrature converges faster than a higher order of Gaussian quadrature.

However, in the case of the boundary conditions with adjacent free edges, it was seen that NGAUS=2 resulted in giving a diverging solution whereas NGAUS=3 gave a converging solution. The stiffness of the displacement elements is reduced as the order of numerical integration decreases [18]. It was inferred that as the plate with a completely free corner i.e. adjacent free edges, is already quite flexible and further reduction in the stiffness which generally is the case with a lower order of integration, leads to some sort of illconditioning in the matrix and hence the error with NGAUS=2. For all the other boundary conditions, results generated from NGAUS=2 converge far more rapidly than NGAUS=3.

Table 6.1: Natural frequencies for a homogeneous plate for the same mesh sizes

Boundary Condition	NGAUS=2 (4×4)	NGAUS=3 (4×4)	% Difference w.r.t. NGAUS=2
SSSS	51.41	52.2	1.5
CSSF	43.84	45.56	3.9
CFCF	57.67	62.64	8.6

All the results except for the boundary conditions with adjacent free edges have been generated by taking NGAUS=2.

Differences between the lowest natural frequencies calculated by considering NGAUS=2 and NGAUS=3 have been listed out in Table 6.1 and Table 6.2 for various boundary conditions. 4×4 mesh size for both the orders are considered in Table 6.1 and 4×4 mesh size for NGAUS=2 and 5×5 mesh size for NGAUS=3 are considered in Table 6.2. The mesh sizes are for a quarter plate.

It is inferred from Tables 6.1 and 6.2 that the difference between the two orders of integration reduces as a higher mesh size is considered for NGAUS=3. In other words, NGAUS=2 converges more rapidly than NGAUS=3.

Table 6.2: Natural frequencies for a homogeneous plate for different mesh sizes

Boundary Condition	NGAUS=2 (4×4)	NGAUS=3 (5×5)	% Difference w.r.t. NGAUS=2
SSSS	51.41	52.0	1.1
CSSF	43.84	44.0	0.36
CFCF	57.67	60.0	4.0

6.4 Static analysis of sandwich plates

The non-uniform shear strain displacement due to the transverse shear of the plate cross-section is accounted for, in the analysis of results. A shear correction factor $\alpha = 6/5$ is considered as proposed by Reissner [25] and is discussed in section 3.3.2 earlier. In the case of homogeneous plates it does not have much effect on the results as the thickness considered for the plates are small and hence the non-uniform shear effect is limited.

However, in case of the sandwich plates where thickness of the core is quite large, the non-uniform shear in the core plays an important role in the solutions generated. Most of the previous work done in the static analysis of sandwich plates, considered uniform shear distribution in the core. An attempt has been made in the static analysis of sandwich plates in this work to consider the effects of non-uniform shear distribution in the core and study the various parametric effects on the center deflection due to this.

Results have been presented for both the cases where the shear correction factor α is either considered or neglected. Figures A.18 to A.21 show the comparision and convergence of the center deflection of a sandwich plate with isotropic core for simply supported and clamped boundary conditions for both the uniformly distributed load and a concentrated load applied at the center of the plate.

It is observed from Figure A.20 that even without considering the shear correction, the values obtained by the present work are slightly higher than those of the previous works. As explained in section 4.5, the shear rigidity terms $\mathbf{D}_{44}$ and $\mathbf{D}_{55}$ are the terms which account for the transverse shear effects of the core for a sandwich plate. In the previous work [40], the terms $\mathbf{D}_{44}$ and $\mathbf{D}_{55}$ are,

$$\mathbf{D}_{44} = \mathbf{D}_{55} = G_c \frac{c}{(c/d)^2} \tag{6.1}$$

where $d = c + t$. In this case the denominator in the terms $\mathbf{D}_{44}$ and $\mathbf{D}_{55}$ is always less than one. In this work however,

$$\mathbf{D}_{44} = \mathbf{D}_{55} = G_c \frac{c}{1.0} \tag{6.2}$$

assuming that $t \ll c$. The shear correction factor has not been taken into account in Equation (6.2).

It is due to this reason that the value obtained by the present work even by neglecting the non-uniform shear in the core, is slightly higher than that obtained by previous works. However, in case of Figure A.18, the values are in excellent agreement with those in Ref. [15] as it also considers $t \ll c$. It is seen from

Table 6.3: Center deflections for sandwich plates by considering α. (udl=uniformly distributed load, conc. load=concentrated load applied at the center of the plate).

Boundary Condition/Load	Previous work	Present work (5×5) Mesh size with α (A)	% difference
SSSS/udl	1.486 [15]	1.587	6.8
SSSS/conc. load	0.0187 [15]	0.02406	28.6
CCCC/udl	0.000343 [40]	0.0004047	17.9
CCCC/udl	0.000349 [77]	0.0004047	15.9

the figures that the uniformly distributed load exhibits better results than the concentrated load as the former idealizes load conditions better than the latter.

The percentage difference between the values obtained by the present work by considering the shear correction factor α and the values obtained by previous researchers, for both cases are listed out in Table 6.3.

Table 6.4 lists out the difference in values of center deflection by either considering α or neglecting α for various boundary conditions and loading conditions.

During the course of the literature survey, results for a clamped sandwich plate with a concentrated load applied at its center were not found. Hence, these results could not be compared. However, the difference between the two center deflections by considering α and neglecting α is about 14.7%.

Table 6.4: Center deflections for sandwich plate by either considering or neglecting α. (udl=uniformly distributed load, conc. load=concentrated load applied at the center of the plate).

Boundary Condition/Load	Present work (5×5) Mesh size with α	Present work (5×5) Mesh size without α	% difference
SSSS/udl	1.587	1.487	6.8
SSSS/conc. load	0.02406	0.020	20.3
CCCC/udl	0.0004047	0.0003611	12.1

Figure A.22 to A.29 show the effect of the shear correction factor on the center deflection with the variation of the shear modulus G_c of the core and the variation of the aspect ratio for a simply supported plate and clamped plate, with an uniformly distributed load and a concentrated load applied at the center.

As evident from the figures, the difference is quite predominant for low values of G_c i.e. for soft cores, but as the core becomes more stiff, the difference reduces drastically. In case of Figure A.22, difference reduces from 8.2% for $G_c = 500$ to 0.49% for $G_c = 11000$.

As the aspect ratio increases, the effect of the shear correction factor reduces. For Figure A.23 difference reduces from 6.79% for $a/b = 1$ to around 2.0% for $a/b = 5.0$. Similar behaviour is exhibited for other conditions as shown in Figures A.24

to A.29. Inference can be drawn that as the core becomes stiffer and the aspect ratio incrcases, the effect of the shear correction factor on the center deflection decreases.

Depending upon the application and operating conditions of the sandwich plate, it is left upto the design engineer to consider or neglect the non-uniform shear strain displacement due to the transverse shear of the plate cross-section. However, as it has been stated before, this work is merely a qualitative analysis and more work is to be done if a more detailed analytical presentation is to be made.

6.5 Dynamic analysis of sandwich plates

Comparision and convergence of the lowest three natural frequencies for rectangular orthotropic sandwich plate with all simply supported or clamped edges are presented in Figures A.30 to A.32 and A.35 to A.37 respectively.

Convergence is achieved very rapidly in case of a simply supported plate as the difference between a 5×5 and a 4×4 mesh size for Mode 1, Mode 2 and Mode 3 are $0.04\%, 0.9\%$ and 0.8% respectively. Similarly in case of the clamped plate, the difference between the natural frequency for Mode 1, Mode 2 and Mode 3 for 5×5 and 4×4 mesh sizes are $1.3\%, 3.3\%$ and 2% respectively.

The natural frequencies generated take into account the non-uniform shear distribution in the core of the sandwich plate. The effect of the shear correction factor is minimal as shown in Table 6.5. This table compares the natural

Table 6.5: Natural frequencies for sandwich plate

Mode No.	Natural frequencies (with α)	Natural frequencies (without α)	% Difference
1	56.64	57.2	0.97
2	86.32	87.3	1.12
3	134.56	136.0	1.06
4	139.4	141.0	1.1
5	161.5	164.7	1.9
6	211.0	215.6	2.1
7	221.4	224.2	2.1
8	246.62	253.2	2.6
9	272.62	280.5	2.8
10	287.0	293.1	2.01

frequencies generated for a rectangular sandwich plate with all edges clamped.

As observed from the Table 6.5, even for the tenth mode, the difference in natural frequencies for both the cases is about 2%. The shear correction factor does not have a predominant role in the dynamic analysis as it has in the static analysis. The non uniform shear distribution was also considered by Ahmed [41] for the dynamic case only. The difference between the values generated by Ahmed by either considering or neglecting the shear correction factor varies from 0.8% for the first mode to about 3% for the tenth mode.

It can be thus inferred from the above cases that α does not have much impact in the dynamic analysis unlike the static cases for the present considered dimensions and elastic constants of the sandwich plate. This may be because unlike in static cases where the solution is inversely proportional to the stiffness matrix ($X = R/K$), the solution for the dynamic analysis is proportional to the square root of the stiffness matrix ($\omega = \sqrt{K/M}$). As the shear correction factor tends to reduce the stiffness, the solution for the static case will be affected more than the solution of the dynamic case.

Comparision curves have been presented in Figures A.33, A.34, A.38 and A.39 for both NGAUS=2 and NGAUS=3. Figures A.33 and A.34 show the comparision with results obtained by Khatua [40] and Raville [20] for a simply supported rectangular sandwich plate with an orthotropic core. Excellent comparision is exhibited as seen from the figures. The difference between the natural frequencies generated by the present work and [40] for the ninth mode is around 0.7% and the difference with the theoretical results [20] is around 1.6%.

For a higher order of Gaussian integration as shown in the Figure A.34, excellent comparision is exhibited. The differences are slightly more pronounced in cases of Mode 4, Mode 6 and Mode 7 where the difference between the two orders are about $5.1\%, 3.4\%$ and 7.5% respectively. It is also seen that convergence is more rapid in case of the lower order of Gaussian integration.

Similarly, for a fully clamped plate, results show excellent comparision with the results generated by Ahmed [41] and Ueng [19] for NGAUS=2 as shown in Figure A.38. For the same mesh size i.e. 5×5 for NGAUS=3, it seen from Figure A.39, the natural frequencies are higher for all modes except for the lowest three

natural frequencies. As a clamped plate is very stiff, a higher order of Gaussian integration will take a more dense mesh size than NGAUS=2 for converging to the solutions generated previously by other researchers. But as the lowest three natural frequencies are generally of prime importance, NGAUS=3 exhibits excellent comparision for these three frequencies as shown in Figure A.39.

6.5.1 Present work done in dynamic analysis

A mode shape is associated with each natural frequency of the structure. The mode shapes are functions of the two integer indices $i\&j$. Each of these indices may be associated with the number of flexural half waves in one of the two plate dimensions. For each $i\&j$ for which a vibration mode exists, there is a natural frequency and an associated mode shape. For free vibration such as in the present work, the total transverse deformation is the sum of the modal deformations. Mode shapes are important in the sense that it gives an idea as to the behaviour of the plate as it vibrates at different natural frequencies. Figures A.40 to A.45 show the mode shapes for the lowest three natural frequencies for a simply supported and clamped rectangular sandwich plate. The behaviour exhibited by the sandwich plate is as expected for the associated number of flexural half waves in $x\&y$ direction which are 1-1, 2-1 and 1-2 for the lowest three natural frequencies for the simply supported and clamped rectangular plate. As seen from Figures A.40 and A.43, symmetric mode shapes are associated with the lowest natural frequency. For Mode 2 and Mode 3, Figures A.41, A.42, A.44 and A.45 show that mode shapes are symmetrical about one center line and antisymmetrical about the other center line.

Most of the results generated for the dynamic analysis of sandwich plates by the previous researchers were either fully simply supported or clamped plates. An attempt has been made to fill that lacuna by presenting a parametric study of rectangular sandwich plate with four different boundary conditions including two with free edges. Natural frequencies for SCSF, CSCF, CCSS and CCCS sandwich plates have been presented with varying shear modulus of the core G_c and the core thickness (c) in Figures A.46 to A.53.

Figures A.46, A.48, A.50 and A.52 show the variation of the natural frequency with an increase of the shear modulus of the core. The shear modulus is varied from 500 psi to 100000 psi. In case of the SCSF sandwich plate, the increase in the lowest natural frequency with respect to an increase of 99500 psi is only about 1.9 Hz. The percentage increase in the natural frequency is only about 14.0% with a corresponding increase of 19900% of G_c. The increase of the lowest natural frequencies for the other boundary conditions are also quite insignificant when compared to the increase in the shear modulus. Compared to that, the increase in the natural frequency for Mode 3 and Mode 4 for the SCSF sandwich plate is of the order of 69.8%. The lowest natural frequency exhibits symmetric modes and hence the shearing effect is minimal but for higher modes, antisymmetric modes are exhibited and hence the shearing has a greater impact on the natural frequencies.

Inference can be drawn from the Figures A.46, A.48, A.50 and A.52 that the natural frequencies increase as the shear modulus increases and the effect is more pronounced for higher modes.

As shown in Figures A.47, A.49, A.51 and A.53, the natural frequencies in-

crease linearly as the core thickness increases. The effect is more pronounced for higher modes.

Chapter 7

Conclusions and Recommendations

A displacement based finite element method for static and dynamic analysis of homogeneous rectangular plates and rectangular sandwich plates is presented in this study. The results generated indicate that the method presented gives an excellent approximation for the displacements and natural frequencies of homogeneous plates and sandwich plates. A versatile computer code is developed for the above analysis.

Analysis can be applied to various homogeneous plates and sandwich plates with any aspect ratios, material properties and dimensions for free, simply supported and clamped boundary conditions. The code can handle uniformly distributed load, point loads and combinations of both.

Based on the work carried out, the following conclusions can be drawn.

(a) The 8-node isoparametric rectangular element is a highly versatile element as it can be applied to various homogeneous plates and sandwich plates. The element exhibits good convergence for both the static and dynamic analysis as a result of which the time and effort involved for the analysis is reduced.

(b) Based on the rapid convergence exhibited by the element used, the mesh size, adequate enough to provide an accurate solution for the static and dynamic analysis of homogeneous plates and sandwich plates is a 5×5 mesh size. The solutions are accurate even when the mesh size is for a full plate instead of a quarter plate, as revealed by the results generated for a fully clamped sandwich plate.

(c) A lower order of numerical integration converges faster than the higher order of numerical integration. It is also seen that for a plate with adjacent free edges, a lower order of integration does not give converging solutions.

(d) The shear deformation and rotatory inertia should be included in the formulation of the analysis technique so that a more accurate solution is generated for the dynamic analysis of homogeneous plates.

(e) The effect of the shear correction factor (α) on the center deflection decreases as the core becomes more stiff. The effect also decreases as the aspect ratio increases.

(f) The effect of the shear correction factor on the natural frequency is minimal. The maximum discrepancy by neglecting the shear correction factor does not exceed 3% for natural frequencies generated for the lowest ten modes.

(g) The mode shape associated with the lowest natural frequency of a sandwich

plate exhibits a symmetrical shape. Antisymmetrical mode shapes are exhibited for Modes 2 and 3.

(h) The lowest natural frequency exhibits a minimum variation even with a substantial increase of shear modulus for sandwich plates with various boundary conditions.

(i) Natural frequencies are presented for different boundary conditions for various modes which reveal that the natural frequency increases with an increase in the shear modulus of the core and the thickness of the core. The increase in the natural frequencies are more substantial for higher modes.

7.1 Recommendations for future work

The computer code can be extended to include laminated plates and voided plates too by modifying the plate rigidities. Structures with curvilinear boundaries can also be analyzed by modification of the mesh generation.

The effect of shear correction factor on the center deflection can be analysed by varying thickness and Young's modulus of the faces and poisson's ratio. The effect of unequal and orthotropic faces can also be investigated.

The effect of the inplane forces on the sandwich plate can also be studied after certain modifications to the code.

Bibliography

[1] Yu, Y., A New Theory of Elastic Sandwich Plates–One-Dimensional Case, Journal of Applied Mechanics, September 1959, pp 415-421.

[2] Yu, Y., Simple Thickness-Shear Modes of Vibration of Infinite Sandwich Plates, Journal of Applied Mechanics, September 1959, pp 679-681.

[3] Yu, Y., Flexural Vibrations of Elastic Sandwich Plates, Journal of Aeronautical Sciences, 27, 1960,pp 272-290.

[4] Thurston, G.A., Bending and Buckling of Clamped Sandwich Plates, Journal of Aeronautical Sciences, 24, 6, June 1957, pp 407-412.

[5] Lin, T.H., Yokota, L.T., Deflections and Bending Moments of Rectangular Sandwich Panels with Clamped Edges under Combined Biaxial Compressions and Pressure, AIAA Journal, 3, 1965, pp 1162-1164.

[6] Eringen, A.C., Bending and Buckling of Rectangular Sandwich Plates, Proceedings of the U.S. National Congress for Applied Mechanics, 1951, pp 381-390.

[7] Ikeda, K., Theory of Bending of Isotropic Flat Sandwich Plates and its Ap-

plications, Proceedings of the 5th Japan National Congress for Applied Mechanics, 1955, pp 103-106.

[8] Okamoto, M., Sekiya, T., Ikegawa, M., Numerical Analysis for Bending of Flat Sandwich Plates, Proceedings of the 12th Japan National Congress for Applied Mechanics, 1962, pp 103-108.

[9] Yu, Y., Simplified Vibration Analysis of Elastic Sandwich Plates, Journal of Aeronautical Sciences, 27, 1960, pp 894-900.

[10] Mindlin, R.D., Influence of Rotatory Inertia and Shear on Flexural Motions of Isotropic, Elastic Plates, Journal of Applied Mechanics, March 1951, pp 31-38.

[11] Hoff, N.J., Bending and Buckling of Rectangular Sandwich Plates, NACA 2225, 1950.

[12] Hopkins, H.G., Pearson, S., The Behaviour of Flat Sandwich Panels under Transverse Loading, Royal Aircraft Establishment, Farnborough, Report No. S.M.E. 3277, March 1944.

[13] Chang, C.C., Fang, B.T., Flexural Vibrations of a Rectangular Sandwich Panel, IAS Paper No. 60-21, January 1960.

[14] Kroll, W.D., Mordfin, L., Garland, W.A., Investigation of Sandwich Construction under Lateral and Axial Loads, NACA 3090, December 1953.

[15] Yen, K.T., Gunturken, S., Pohle, F.V., Deflections of a Simple Supported Rectangular Sandwich Plate subjected to Transverse Loads, NACA 2581, December 1951.

[16] Rock, T., Hinton, E., Free Vibration and Transient Response of Thick and Thin Plates using the Finite Element Method, Earthquake Engineering and Structural Dynamics, Vol. 3., 1974, pp 51-63.

[17] Ahmad, S., Irons, B.M., Zienkiewicz, O.C., Analysis of Thick and Thin Shell Structures by Curved Elements, International Journal for Numerical Methods in Engineering, 2, 1970, pp 419-451.

[18] Zienkiewicz, O.C., Taylor, R.L., Too, J., Reduced Integration Technique in General Analysis of Plates and Shells, International Journal for Numerical Methods in Engineering, 3, 1971, 275-290.

[19] Ueng, C.E.S., Natural Frequencies of Vibration of an All-Clamped Rectangular Sandwich Panel, Journal of Applied Mechanics, September 1966, pp 683-684.

[20] Raville, M.E., Ueng, C.E.S., Determination of Natural Frequencies of Vibration of a Sandwich Plate, Exp. Mech., 1967, 490-493.

[21] Liaw, B.D., Little, R.W., Theory of Bending of Multilayer Sandwich Plates, AIAA Journal, 5, N0.2, February 1967, pp 301-304.

[22] Gerrard, G., Note on Bending of Thick Sandwich Plates, Journal of Aeronautical Sciences, 18, 6, June 1951, pp 424-427.

[23] Reissner, E., Finite Deflections of Sandwich Plates, Journal of Aeronautical Sciences, July 1948, pp 435-440.

[24] Abel, J.F., Popov, E.P., Static and Dynamic Finite Element Analysis of Sandwich Structures, Proceedings of the 2nd Conference of Matrix Methods in Structural Mechanics, Wright-Patterson AFB, Ohio, 1968.

[25] Reissner, E., The Effect of Transverse Shear Deformation on the Bending of Elastic Plates, J. Appl. Mech., 12, 2, June 1945, pp A-69-77.

[26] Alwan, A.M., Bending of Sandwich Plates with Large Deflections, J. Engg. Mechanics Div., Proc. ASCE, EM 3, June 1967, pp 83-93.

[27] Harris, L.A., Auelmann, R.R., Stability of Flat, Simply Supported Corrugated-Core Sandwich Plates Under Combined Loads, J. Aero/Space Sci. , 27, 7, July 1960, pp 525-534.

[28] Seide, P., Comments on 'Stability of Flat, Simply Supported Corrugated- Core Sandwich Plates Under Combined Loads, J.Aero/space Sci., 28, 3, March 1961, p 248.

[29] Bert, C.W., Recent Research in Composite and Sandwich Plate Dynamics, Shock and Vibration Digest, 11, 10, Oct. 1979, pp 13-23.

[30] Cheng, S., On the Theory of Bending of Sandwich Plates, Proc. 4th U.S. National Congress of Applied Mechanics, V 1, 1962, pp 511-518.

[31] Hinton, E., Razzaque, A., Zienkiewicz, O.C., Davies, J.D., A Simple Finite Element Solution for Plates of Homogeneous, Sandwich and Cellular Construction, Proc. Instn. Civ. Engrs., Part 2, 59, 1975, pp 43-65.

[32] Mindlin, R.D., An Introduction to the Mathematical Theory of Vibration of Elastic Plates, A monograph prepared for U.S Army Signal Corps. Engineering Laboratories, 1955.

[33] Okamoto, M., Sekiya, T., Analysis of Rectangular Sandwich Plates Under Several Boundary Conditions by Double Fourier Series Method, Proc. 13th Japan Natl. Congress Appl. Mech., 1963, pp 67-75.

[34] Chan, H.C., Cheung, Y.K., Static and Dynamic Analysis of Multi-Layered Sandwich Plates, Int.J.Mech.Sci., 14, 1972, pp 399-406.

[35] Gupta, K.K., Development of a Finite Dynamic Element for Free Vibration Analysis of Two-Dimensional Structures, Int.J.Numerical Methods in Engg., 12, 1978, pp 1311-1327. 65 (1987) 864.

[36] Kanematsu, H.H., Hirano, Y., Bending and Vibration of CFRP-Faced Rectangular Sandwich Plates, Composite Structures, 10, n 2, 1988, pp 145-163.

[37] Shahin, R.M., Free Vibrations of Multilayer Sandwich Plates in the Presence of In-Plane Loads, The Journal of Astronautical Sciences, Vol. 19, No. 6, 1972, pp 433-447.

[38] Mallikarjuna, Kant, T., Free Vibration of Symmetrically Laminated Plates Using a Higher-Order Theory with Finite Element Technique, Intl.J.Numerical Methods in Engg., 28, 1989, pp 1875-1889.

[39] Hinton, E., A Note on Finite Element Method for the Free Vibrations of Laminated Plates, Int.J.Earthquake Engr. Struc. Dynam., 4(5), 1976, pp 515-516.

[40] Khatua, T.P., Cheung, Y.K., Bending and Vibration of Multilayer Sandwich Beams and Plates, Int.J.Numerical Methods in Engg., 6, pp 11-24.

[41] Ahmed, K.M., Static and Dynamic Analysis of Sandwich Structures by the Method of Finite Elements, Journal of Sound and Vibration, 18(1), 1971, pp 75-91.

[42] Mallikarjuna, Kant, T., Dynamics of Laminated Composite Plates with a Higher Order Theory and Finite Element Discretization, Journal of Sound

and Vibration, 126(3), 1988, pp 463-475.

[43] Ng, S.S.F., Lam, D.K.Y., Dynamic and Static Analysis of Skew Sandwich Plates, Journal of Sound and Vibration, 99(3), 1985, pp 393-401.

[44] Hinton, E., Owen, D.R.J., Finite Element Programming, Academic Press, 1977.

[45] Yang, T.Y., Finite Element Structural Analysis, Prentice Hall, 1986.

[46] Zienkiewicz, O.C., The Finite Element Method, 3rd Edition, McGraw Hill, 1977.

[47] Cook, R.D., Concepts and Applications of Finite Element Analysis, 2nd Edition, John Wiley and Sons, 1981.

[48] Bathe, K.J., Wilson, E.L., Numerical Methods in Finite Element Analysis , Prentice Hall Inc., 1976.

[49] Weaver, W., Johnston, P.R., Finite Elements for Structural Analysis, Prentice-Hall Inc., 1984.

[50] Rao, S.S., The Finite Element Method in Engineering, Pergamon Press, 1980.

[51] Plantema, F.G., Sandwich Construction, John Wiley and Sons, 1966.

[52] Allen, H.G., Analysis and Design of Structural Sandwich Panels, Pergamon Press, 1969.

[53] Ugural, A.C., Stresses in Plates and Shells, McGraw Hill, 1981.

[54] McFarland, D., Smith, B.L., Bernhart, W.D., Analysis of Plates, Spartan Books, 1972.

[55] Szilard, R., Theory and Analysis of Plates-Classical and Numerical Methods, Prentice-Hall Inc., 1974.

[56] Vinson, J.R., Structural Mechanics: The Behaviour of Plates and Shells, John Wiley and Sons, 1974.

[57] Roark, R.J., Young, W.C., Formulas for Stress and Strain, 5th Edition, McGraw Hill, 1975.

[58] Warburton, G.B., The Dynamical Behaviour of Structures, 2nd Edition, Pergamon Press, 1976.

[59] Leissa, A.W., The Free Vibration of Rectangular Plates, Journal of Sound and Vibration, 31, 1973, pp 257-293.

[60] Timoshenko, S., Young, D.H., Vibration Problems in Engineering, 3rd Edition, D.Van Nostrand Co., 1955.

[61] Timoshenko, S., Woinowsky-Krieger, S., Theory of Plates and Shells, 2nd Edition, McGraw Hill, 1959.

[62] Liou, W.J., Sun, C.T., Dynamic Response of Laminated Composite Plates Using a Three-Dimensional Hybrid-Stress Finite-Element Formulation, Shock and Vibration Symposium (58th), V1, Oct., 1987, pp 475-485.

[63] Soares,C.A.M , Campos, L.M.T., Gago, A.F.V., Dynamic Analysis of Plates by Mixed Elements, Recent Adv. in Struct. Dyn., Inst. of Sound and Vib. Res., 1980, pp 51-60.

[64] Kasemset, C., Cheung, Y.K., Axisymmetric Vibration of Multilayer Sandwich Plates and Shells, Proc. of the Intl. Conf. on Finite Elem. Meth. in Engg., 2nd, University of Adelaide, South Australia, Dec. 6-8, 1976, paper 25, pp 17.

[65] Ozguven, H.N., Mathematical Modelling for Dynamic Response of Partially Coated or Laminated Plates- An Energy Approach, Mechanique- Materiaux-Electricite, N 389-391, May-July 1982, pp 282-286.

[66] Habip, L.M., A survey of Modern Developments in the Analysis of Sandwich Structures, Applied Mechanics Review, Vol 18, No. 2, February 1965, pp 93-98.

[67] Owen, D.R.J., Li, Z.H., A Refined Analysis of Laminated Plates by Finite Element Displacement Methods - II. Vibration and Stability, Computers and Structures, Vol 26, No. 6, 1987, pp 915-923.

[68] Stavrindis, C., Clinckemaille, J., Dubois, J., New Concepts for Finite-Element Mass Matrix Formulations, AIAA Journal, Vol. 27, No. 9, September 1989, pp 1249-1255.

[69] Buhlmann, E.T., Welte, Y.P., Dynamic Behaviour of Structures with Finite Element Programs and Modal Analyses, Sulzer Tech. Rev., V 68, N 3, 1986, pp 33-36.

[70] Balendra, T., Shanmugam, N.E., Free Vibration of Plated Structures by Grillage Method, Journal of Sound and Vibration, 99(3), 1985, pp 333-350.

[71] Monforton, G.R., Schmit, L.A., Finite Element Analysis of Sandwich Plates and Cylinderical Shells with Laminated Faces, Proceedings of the Conference on Matrix Methods in Structural Mechanics, AFFDL-TR-68-150, 1968, pp 573-616.

[72] Chang, P.S.H., Wang, H.C., Zable, B., A Correlation of Finite Element Modeling for Vibrations of Composite Plates, Computers in Engineering, Proc. of the Intl. Computers in Engg., V 2, ASME, 1989, pp 399-405,

[73] Alwan, A.M., Large Deflection of Sandwich Plates with Orthotropic Cores, AIAA Journal, V 2, No. 10, 1964, pp 1820-1822.

[74] Gupta, K.K., On a Finite Dynamic Element Method for Free Vibration Analysis of Structures, Computer Methods in Applied Mechanics and Engineering, 9, 1976, pp 105-120.

[75] Rodamaker, M., The Use of Finite Elements in Dynamic Structural Evaluation, S V Sound and Vibration, V 17, N0. 8, August 1983, pp 12-13, 16-18.

[76] Srinivas, S., Rao, C.V.J., Rao, A.K., An Exact Analysis for Vibration of Simply Supported Homogeneous and Laminated Thick Rectangular Plate, Journal of Sound and Vibration, 12(2), 1970, pp 187-199.

[77] Lockwood, J., Taylor, Strength of Sandwich Panels, Proceedings of VII International Congress on Applied Mechanics, 1948, pp 187-199.

Appendix A

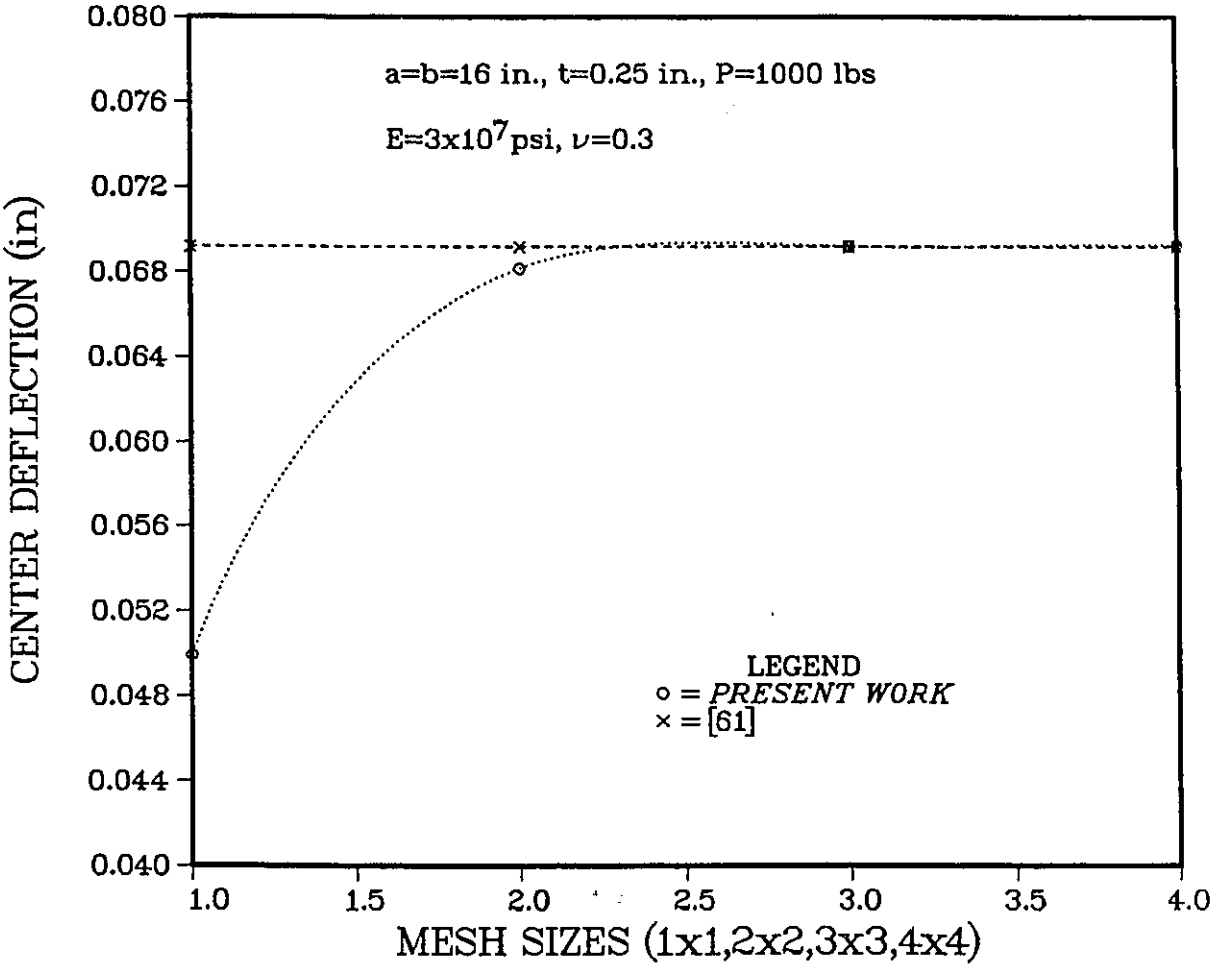

Figure A.1: Comparision and convergence of the center deflection of a homogeneous square plate simply supported on all sides with a concentrated load P applied at its center.

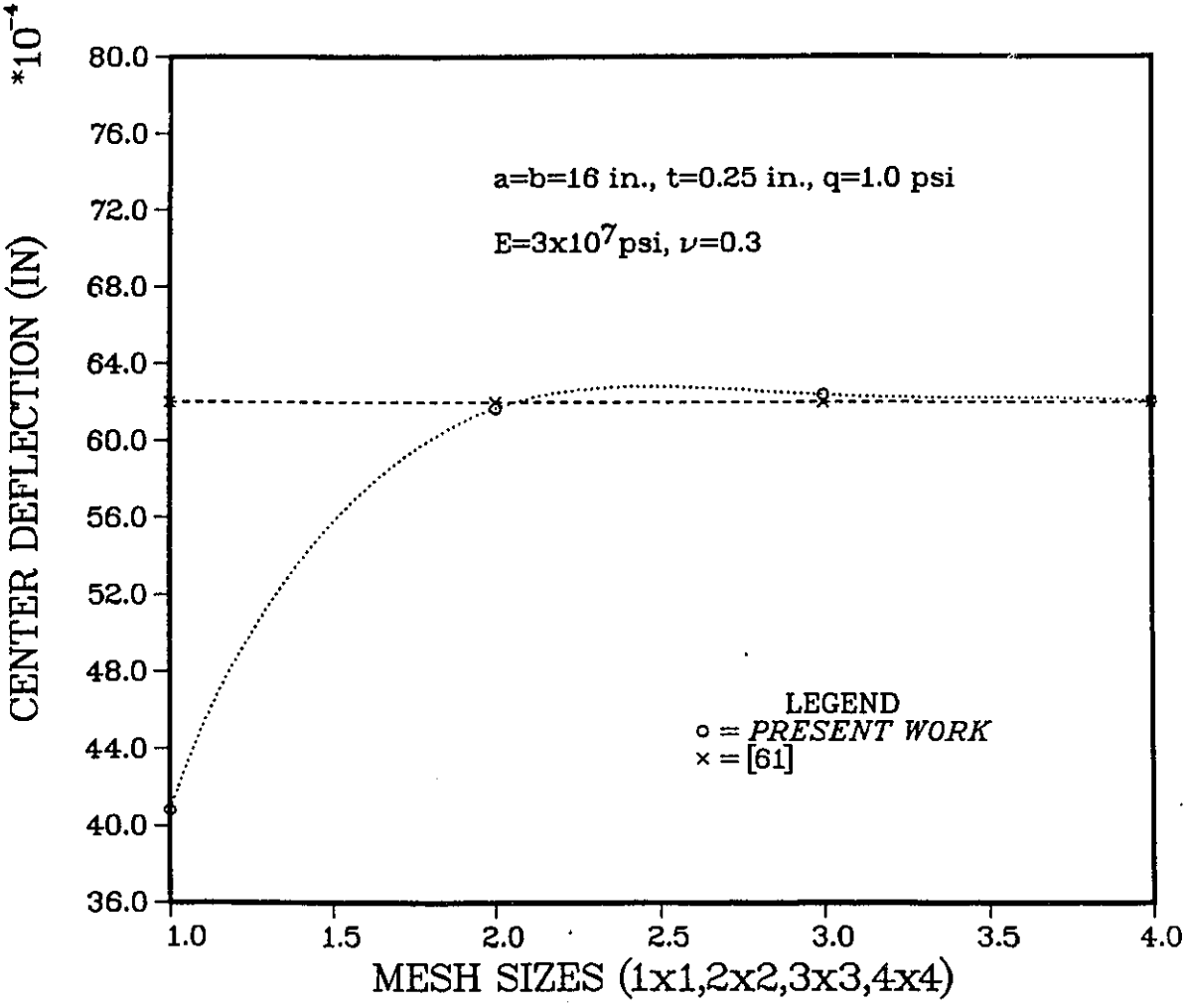

Figure A.2: Comparision and convergence of the center deflection of a homogeneous square plate simply supported on all sides with a uniformly distributed load.

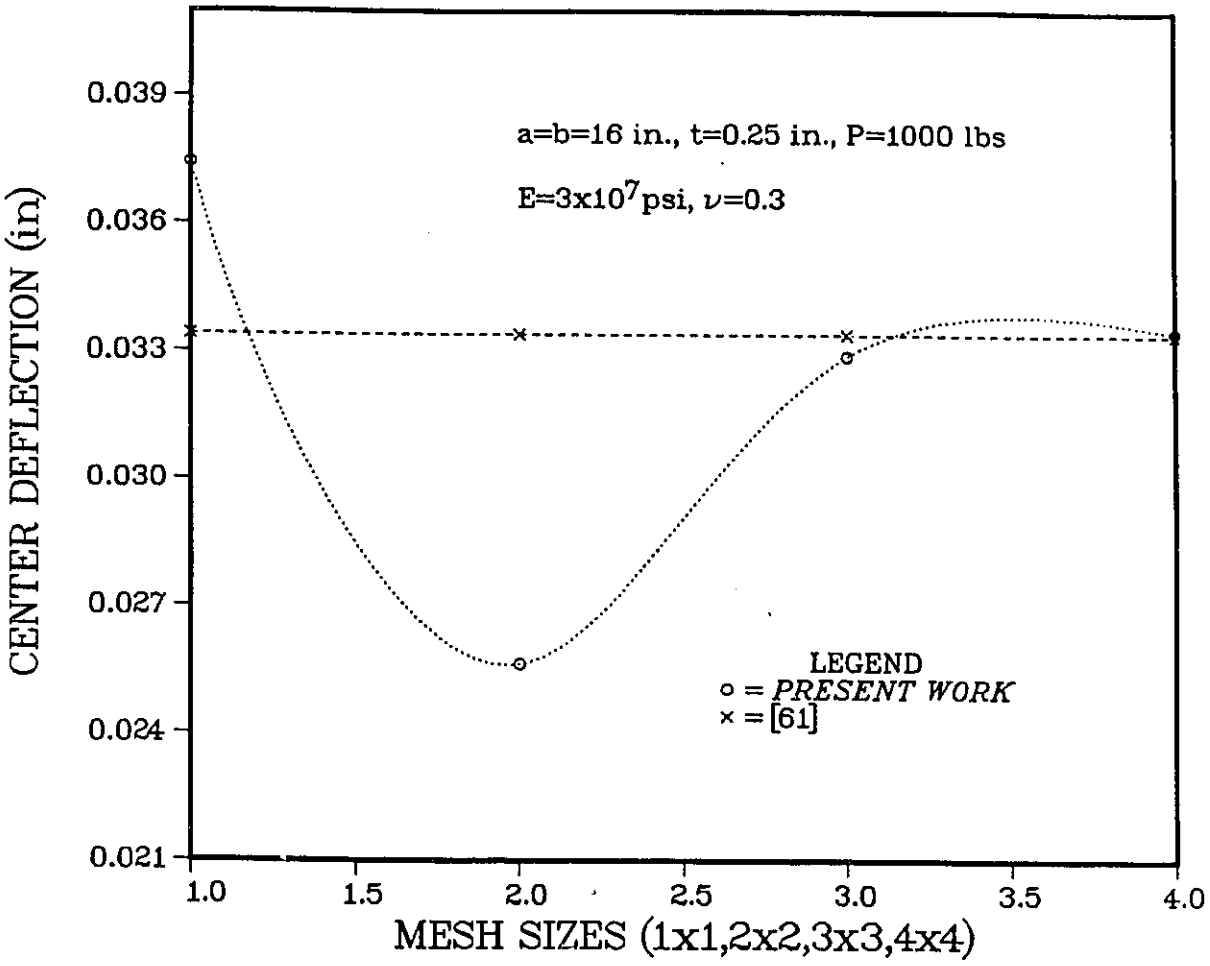

Figure A.3: Comparision and convergence of the center deflection of a homogeneous square plate clamped on all sides with a concentrated load P applied at its center.

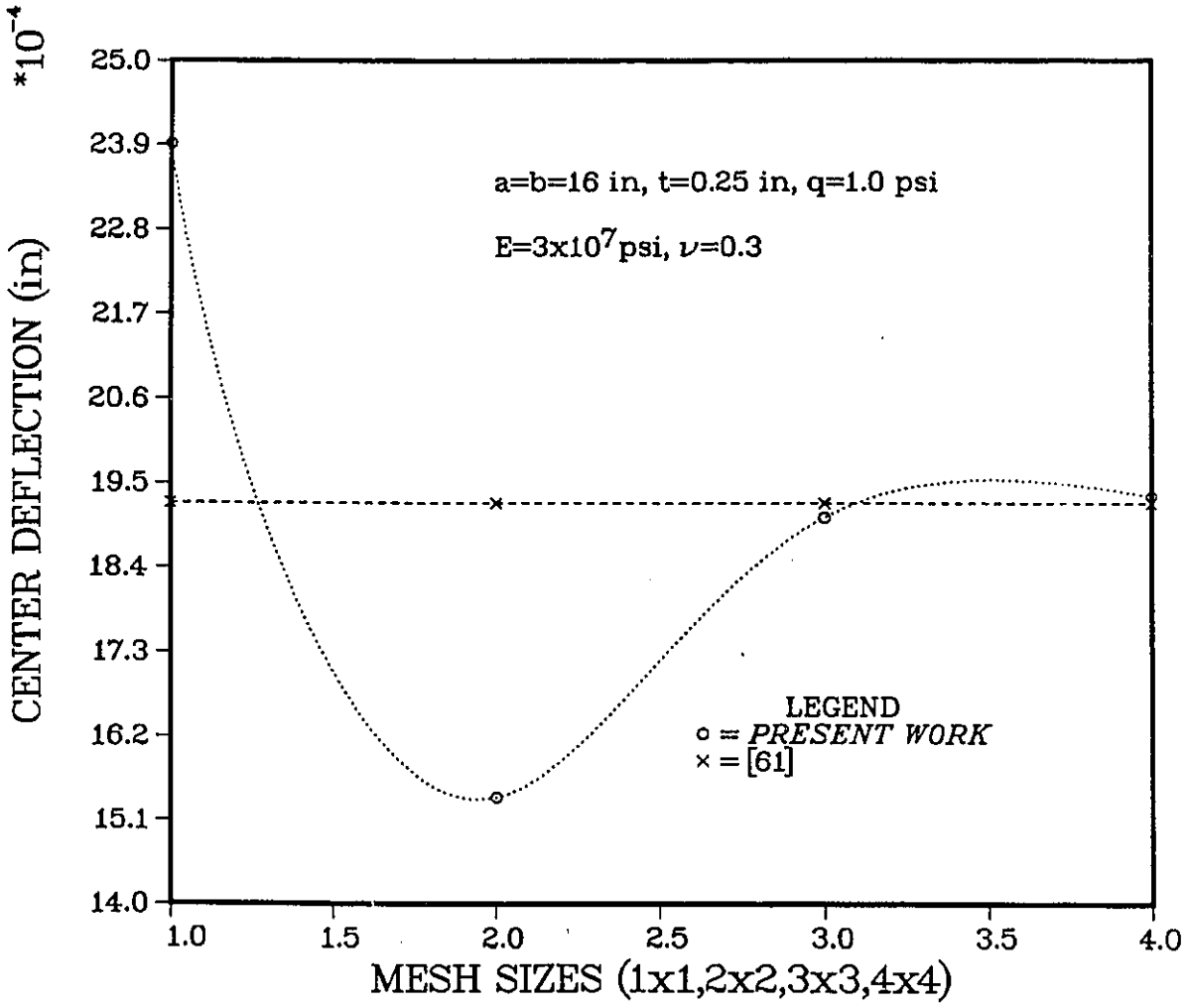

Figure A.4: Comparision and convergence of the center deflection of a homogeneous square plate clamped on all sides with a uniformly distributed load.

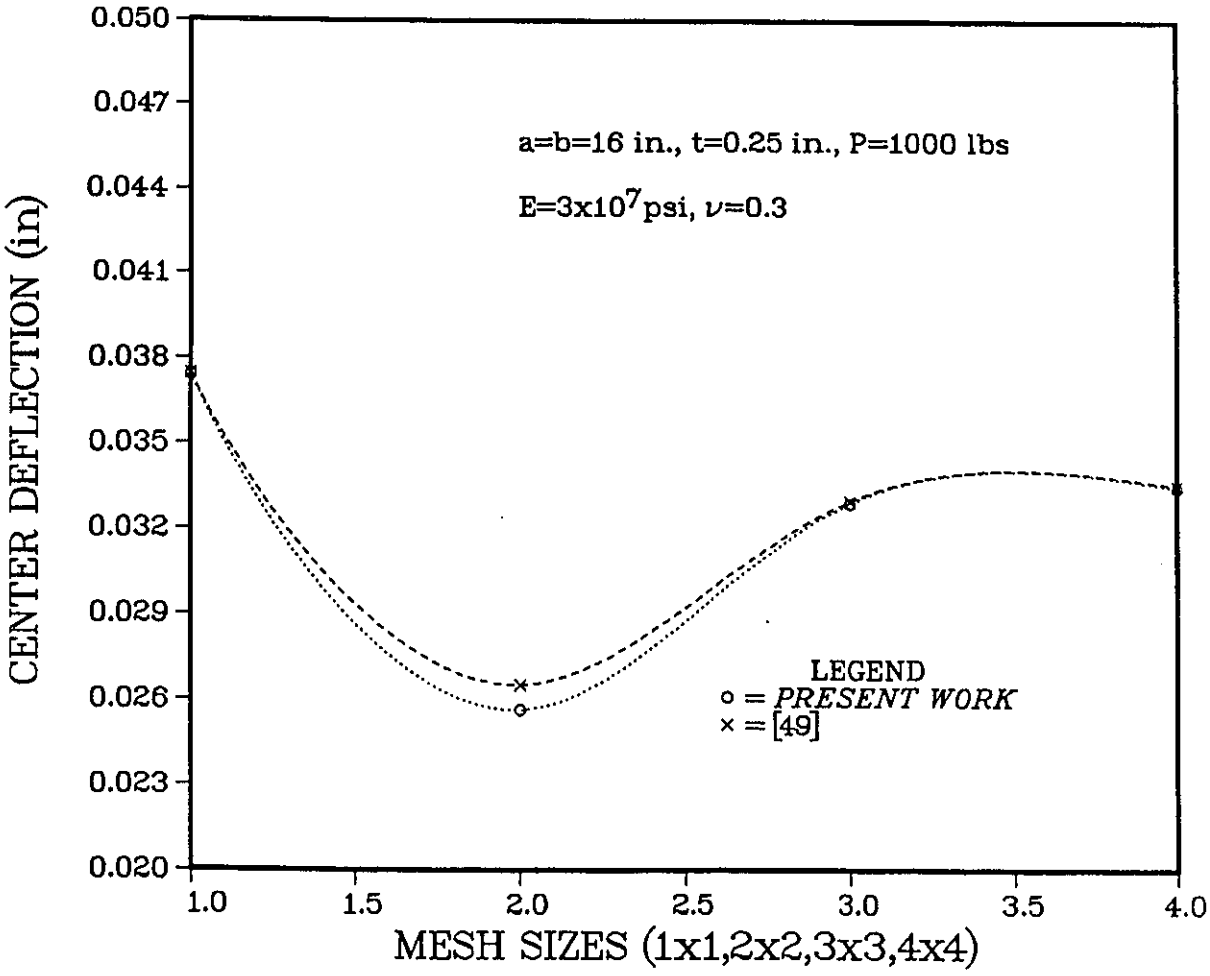

Figure A.5: Comparision of the center deflection of a homogeneous square plate clamped on all sides with a concentrated load P applied at its center.

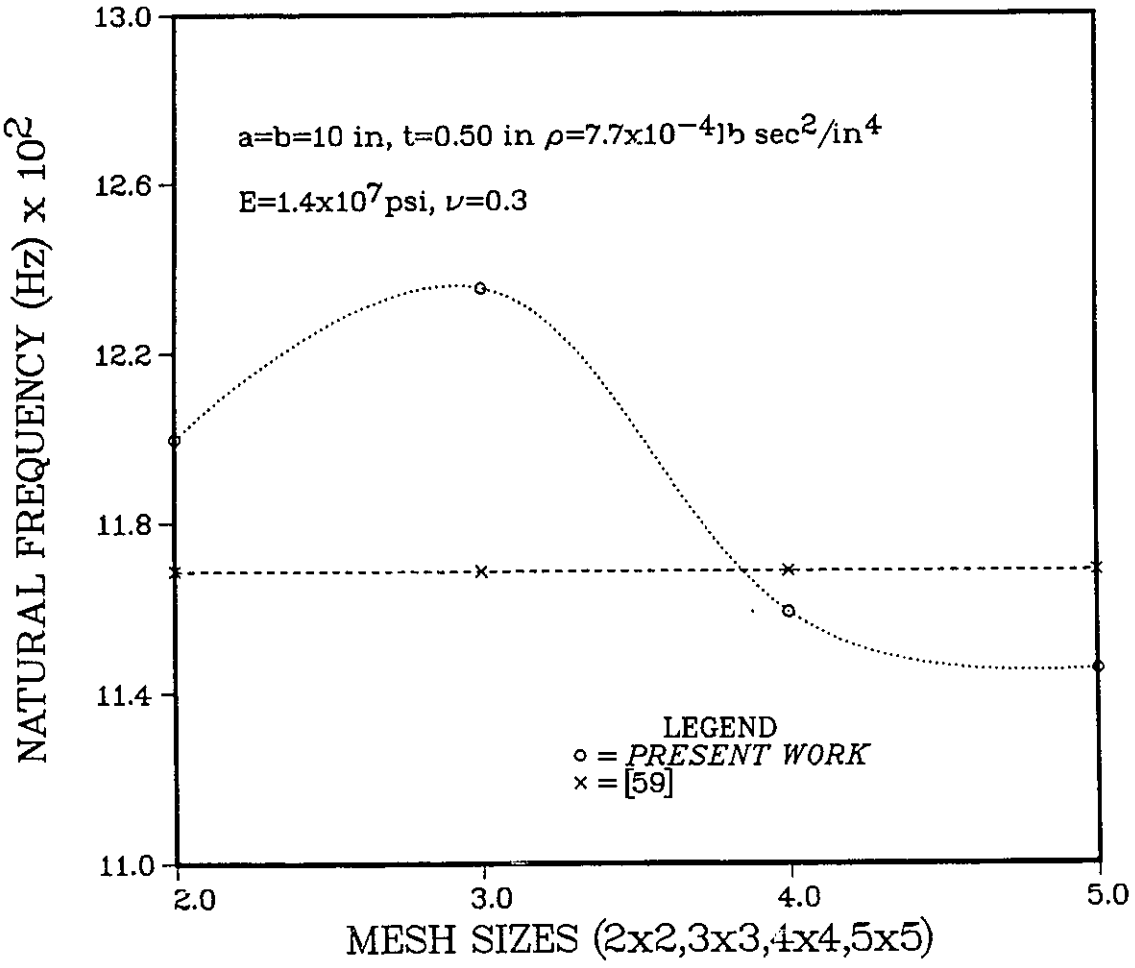

Figure A.6: Comparision and convergence of the natural frequency for a homogeneous square plate clamped on all sides (Mode 1).

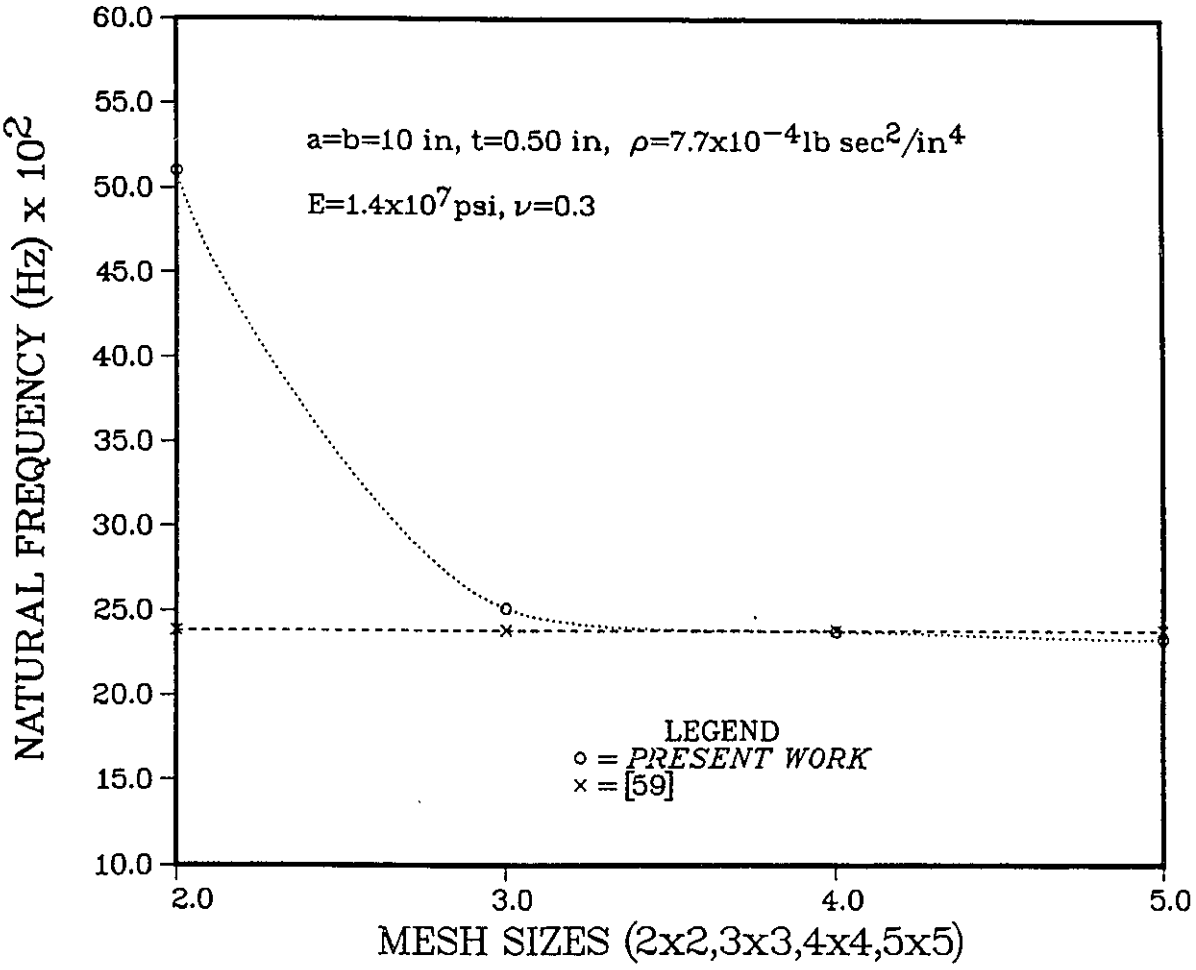

Figure A.7: Comparision and convergence of the natural frequency for a homogeneous square plate clamped on all sides (Mode 2).

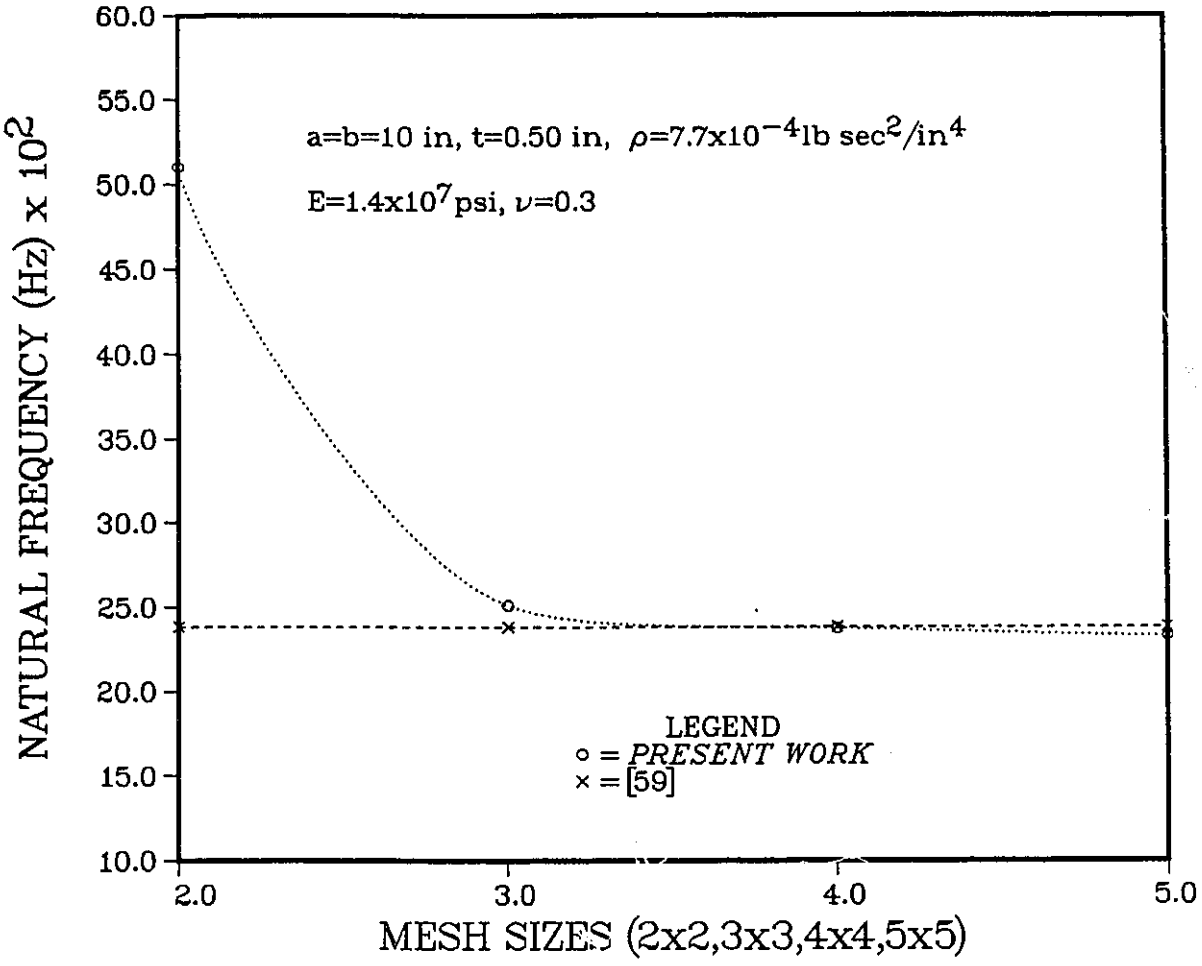

Figure A.8: Comparision and convergence of the natural frequency for a homogeneous square plate clamped on all sides (Mode 3).

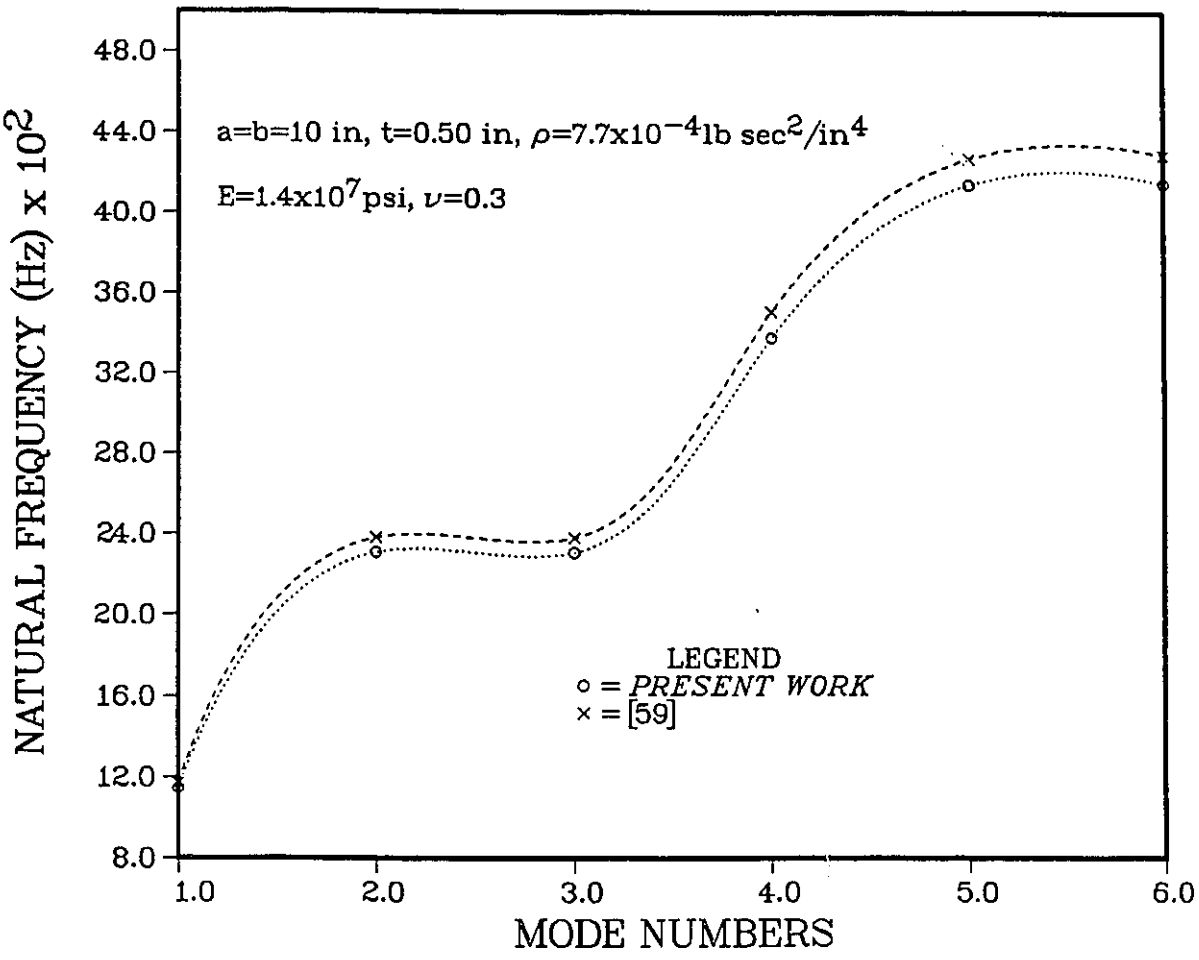

Figure A.9: Comparision of the natural frequencies for a homogeneous square plate clamped on all sides for various modes.

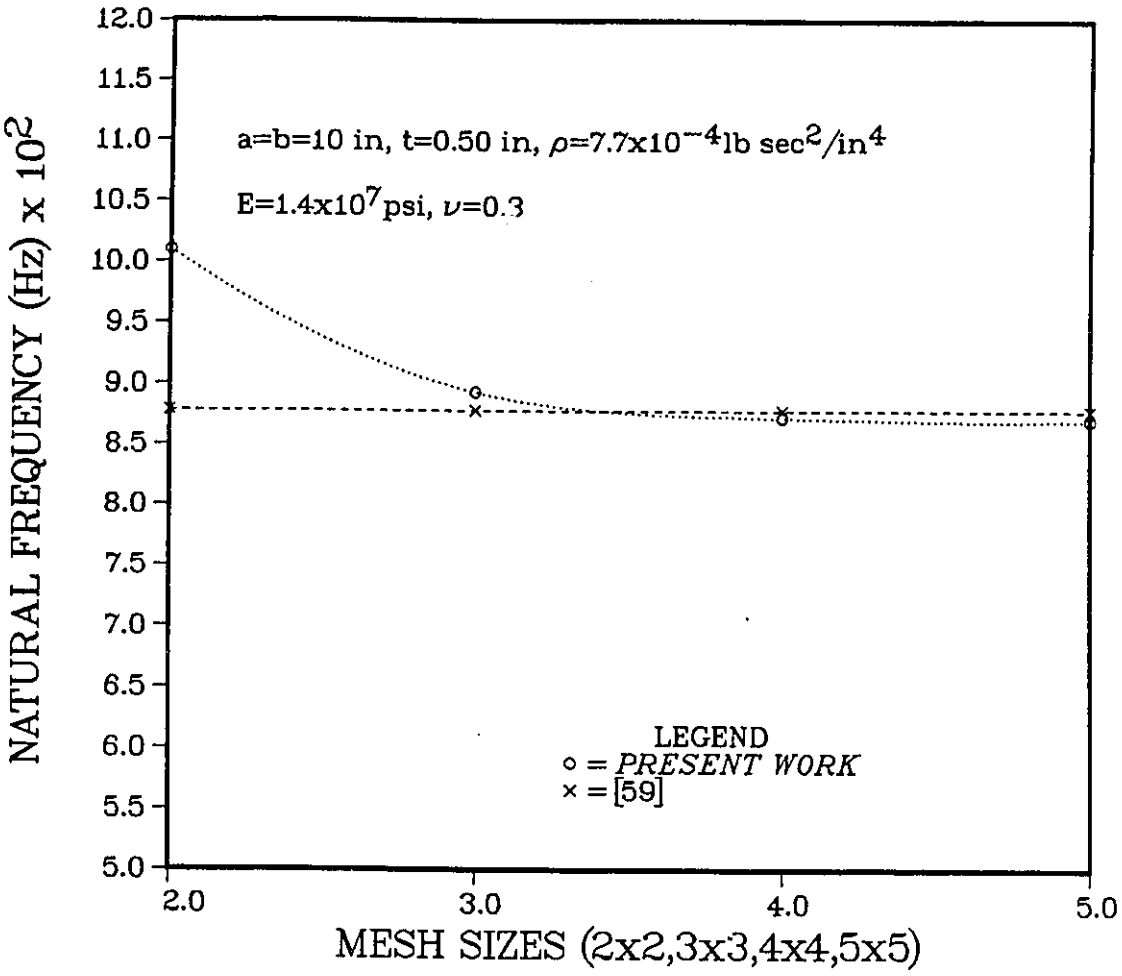

Figure A.10: Comparision and convergence of the natural frequency for a homogeneous square plate with CCSS boundary conditions (Mode 1).

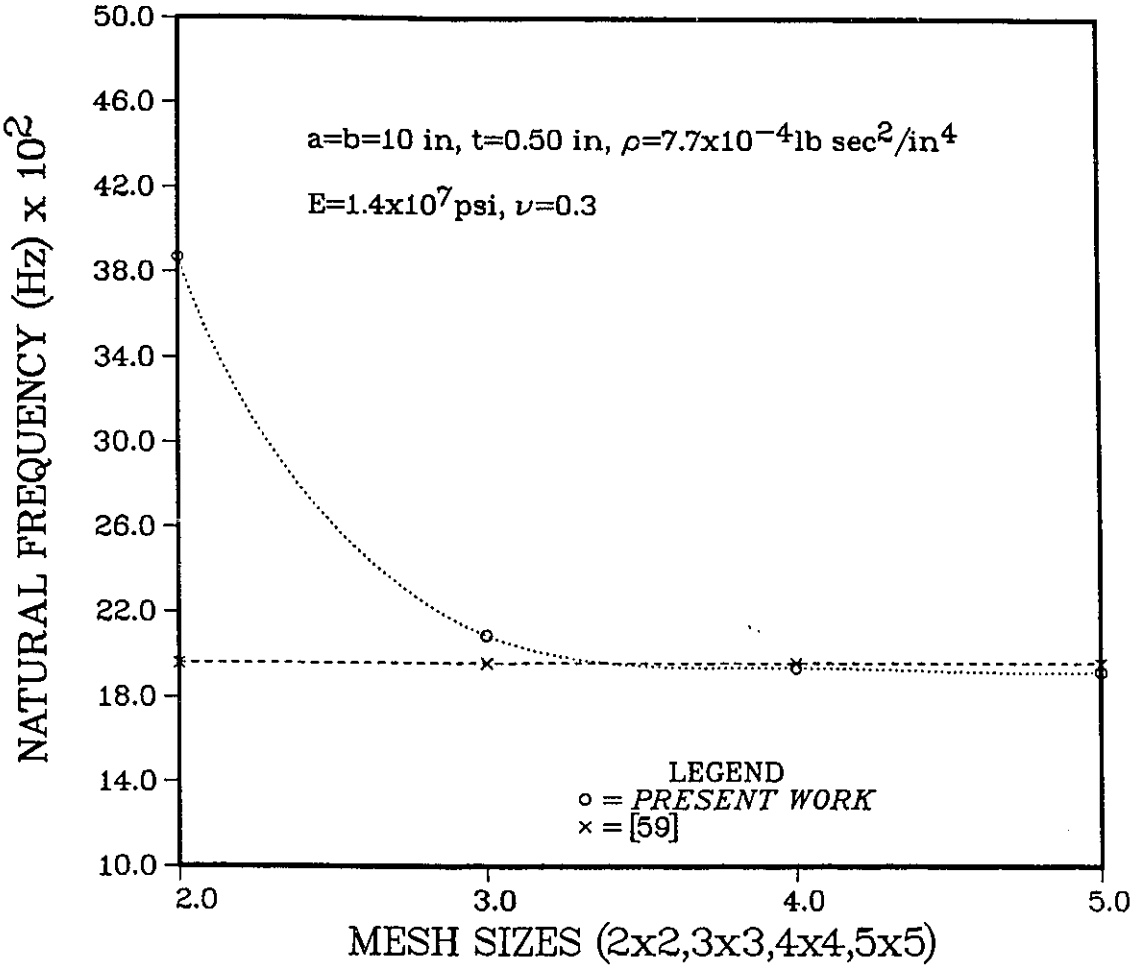

Figure A.11: Comparision and convergence of the natural frequency for a homogeneous square plate with CCSS boundary conditions (Mode 2).

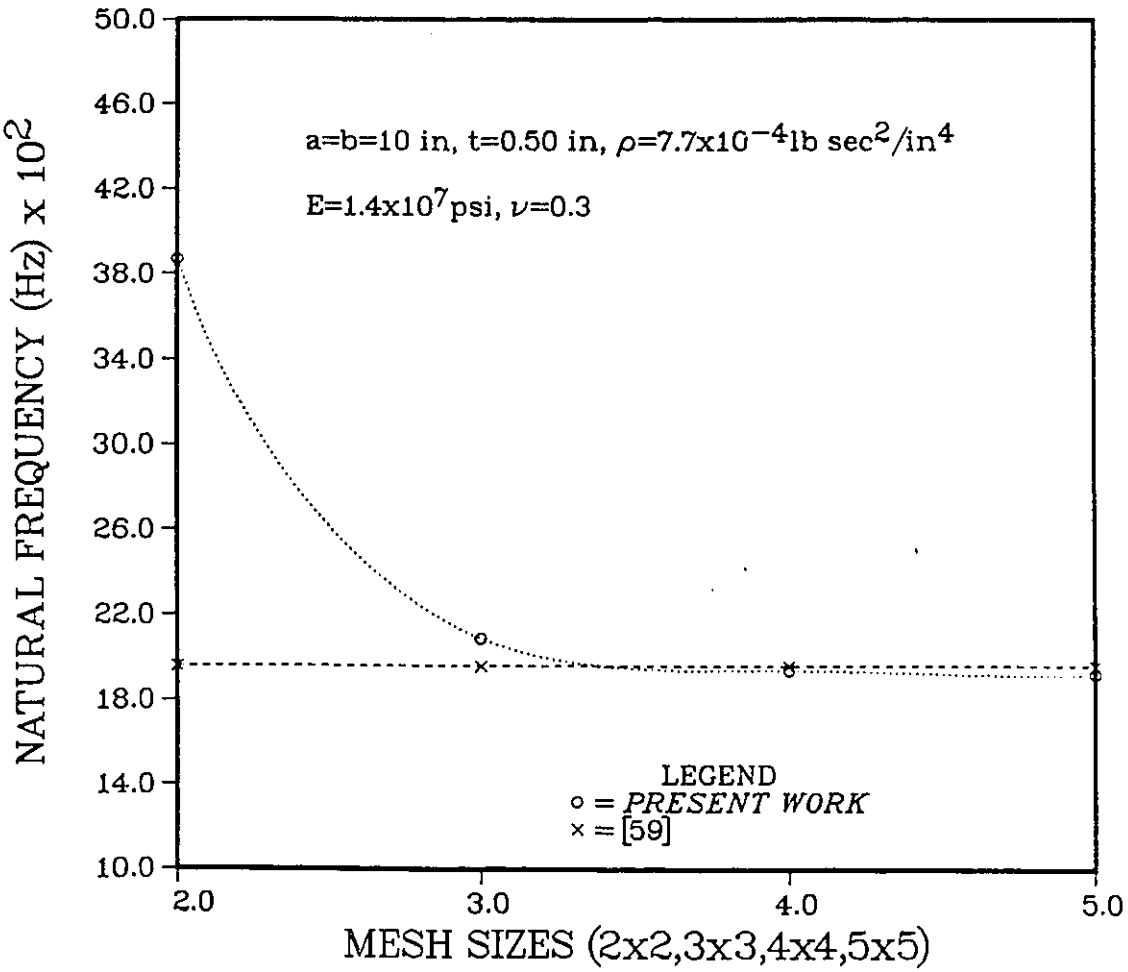

Figure A.12: Comparision and convergence of the natural frequency for a homogeneous square plate with CCSS boundary conditions (Mode 3).

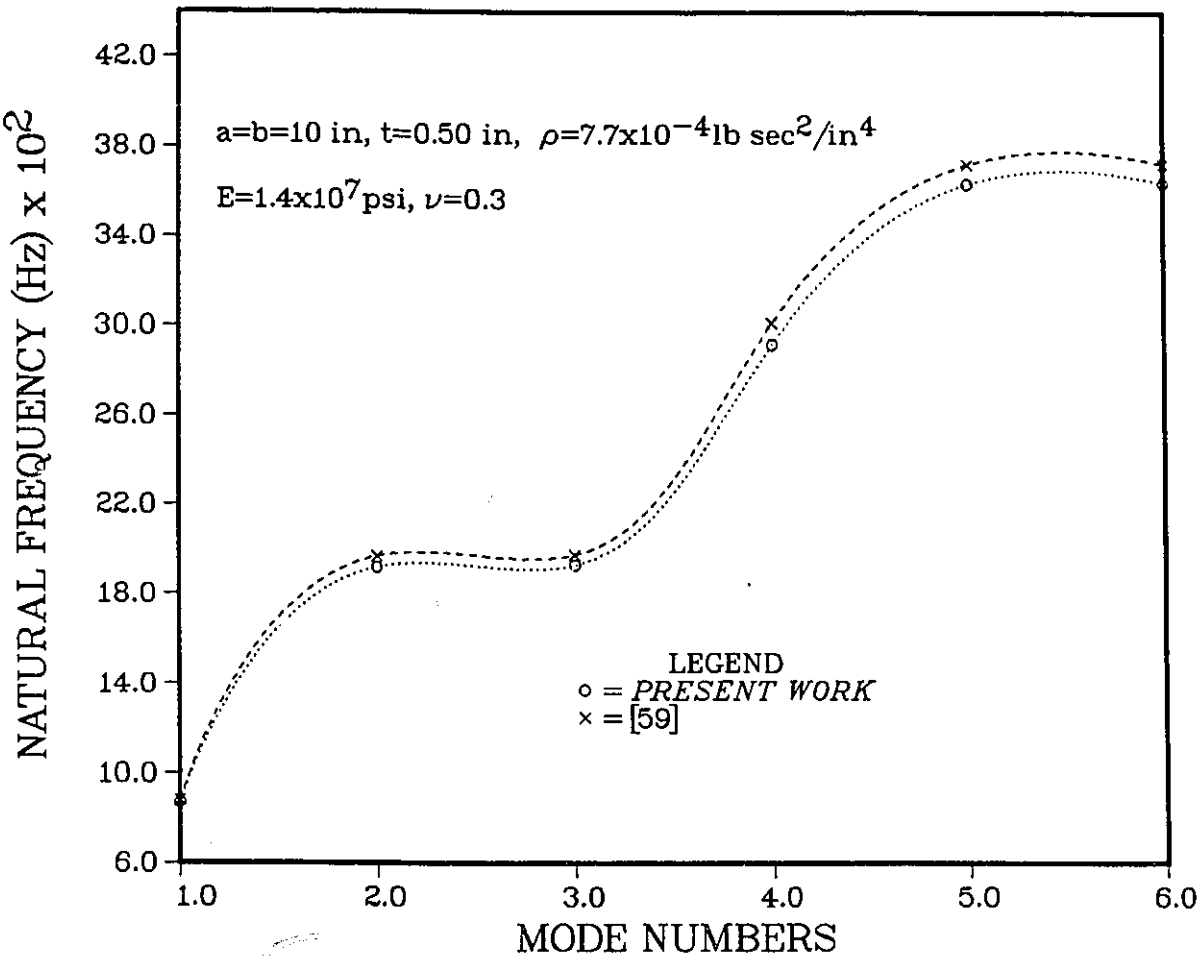

Figure A.13: Comparision of the natural frequencies for a homogeneous square plate with CCSS boundary conditions for various modes.

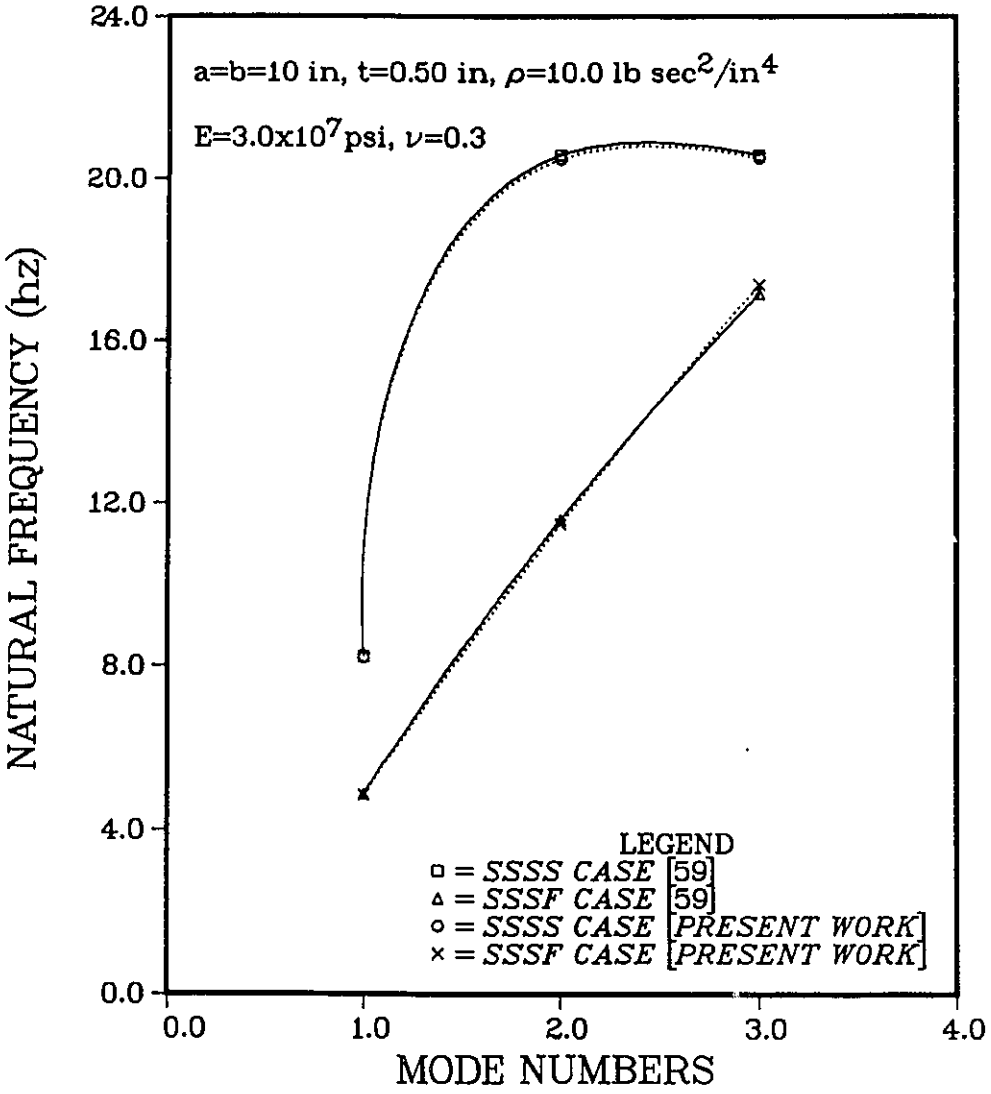

Figure A.14: Comparision of the natural frequencies for a homogeneous square plate with SSSS and SSSF boundary conditions for the lowest three natural frequencies.

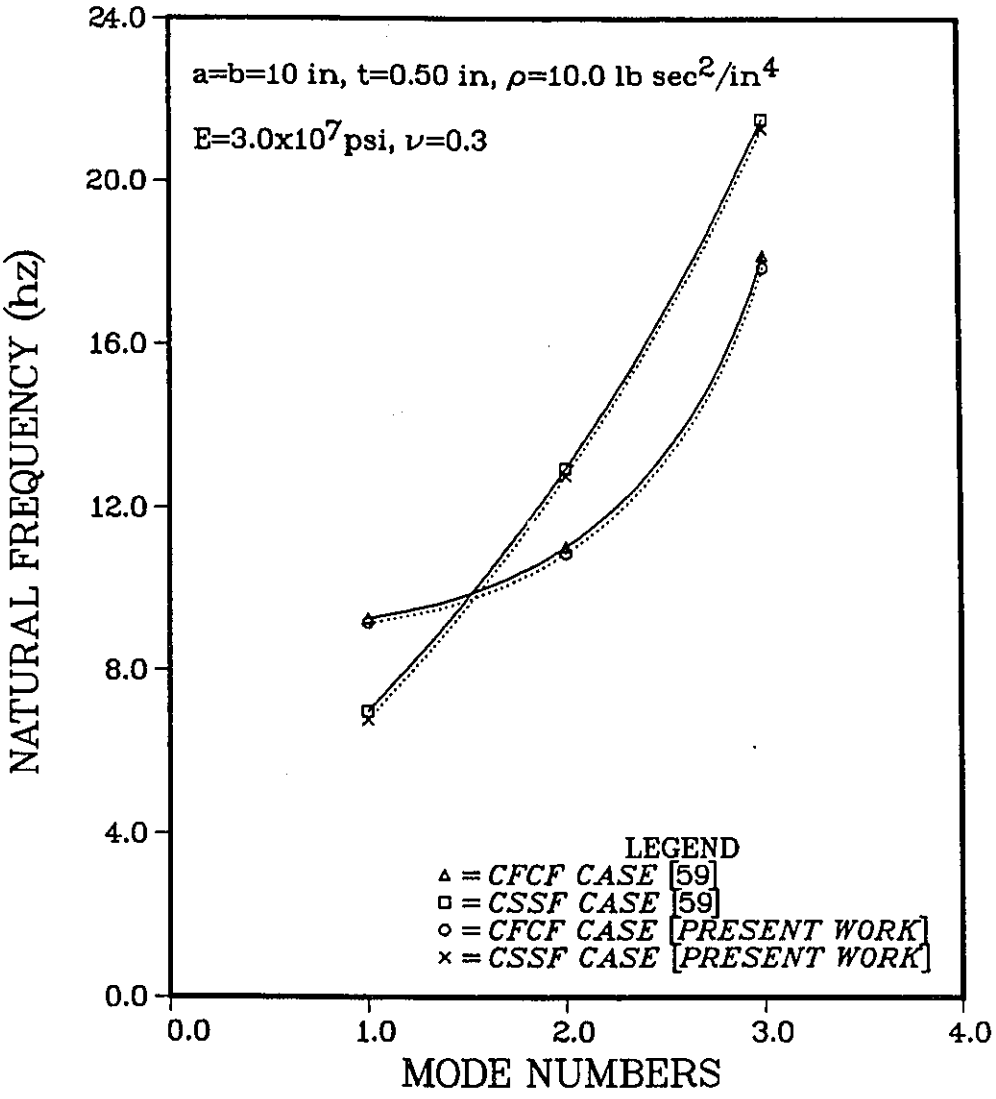

Figure A.15: Comparision of the natural frequencies for a homogeneous square plate with CFCF and CSSF boundary conditions for the lowest three natural frequencies.

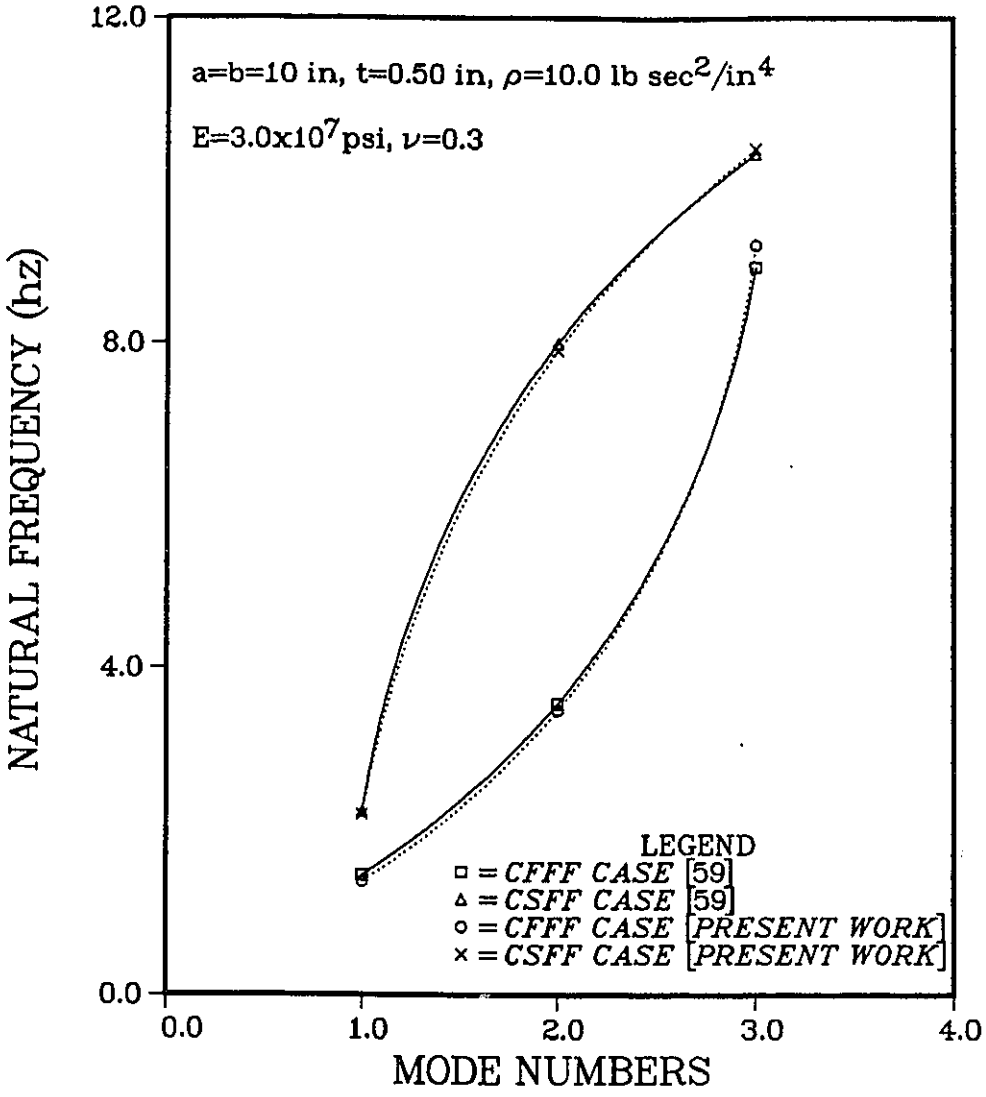

Figure A.16: Comparision of the natural frequencies for a homogeneous square plate with CFFF and CSFF boundary conditions for the lowest three natural frequencies.

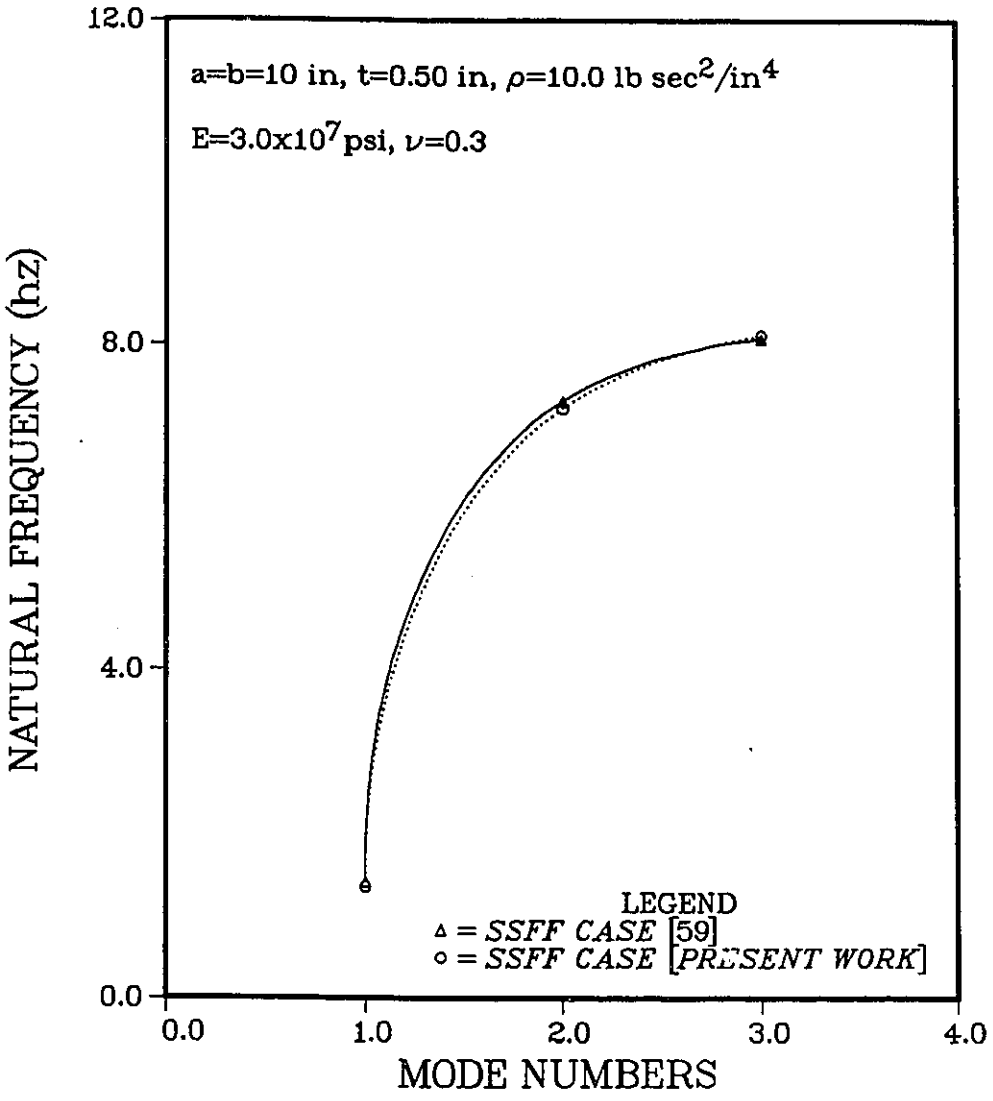

Figure A.17: Comparison of natural frequencies for a homogeneous square plate with SSFF boundary condition for the lowest of three natural frequencies.

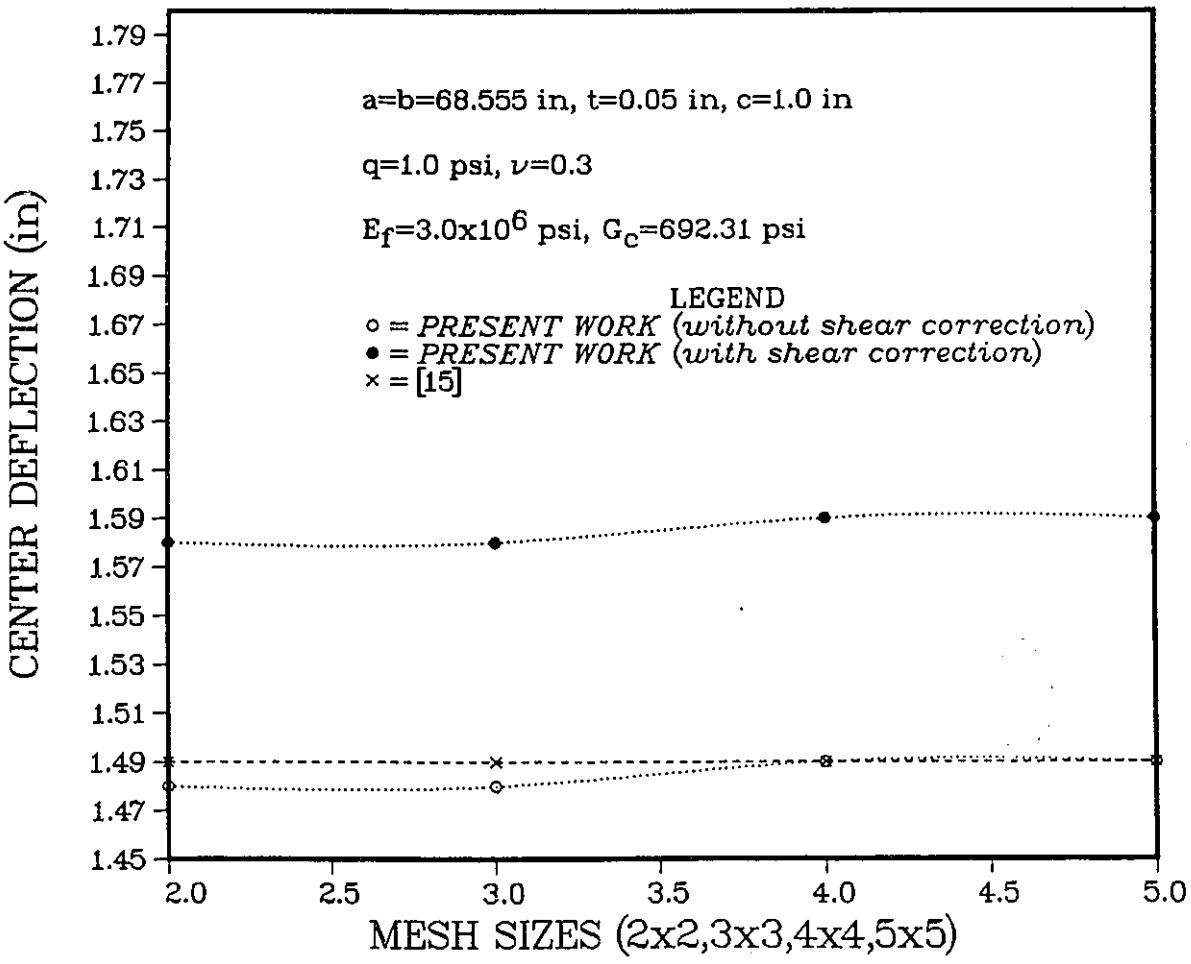

Figure A.18: Comparision and convergence of the center deflection of a rectangular sandwich plate with an isotropic core, simply supported on all sides with a uniformly distributed load.

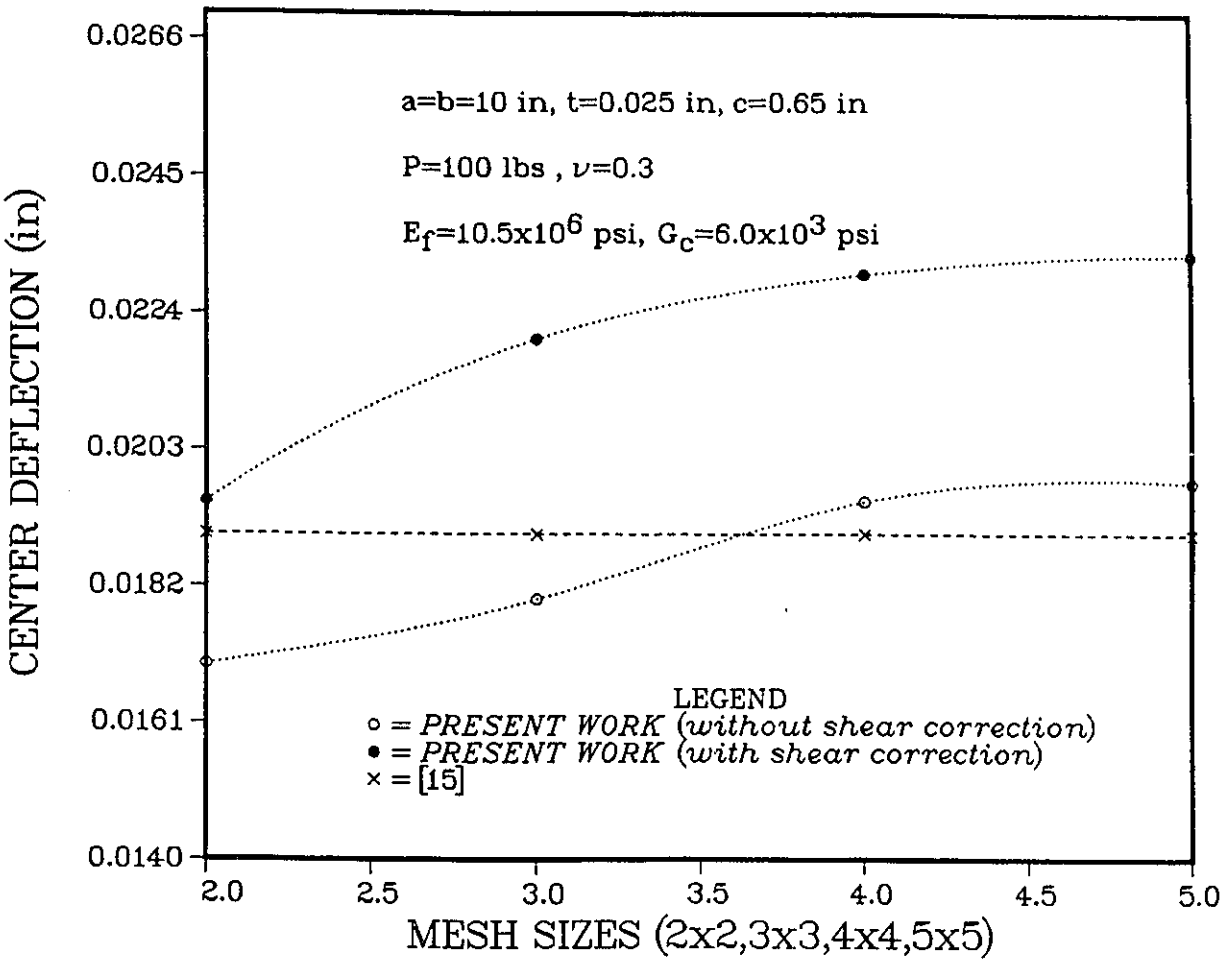

Figure A.19: Comparision and convergence of the center deflection of a rectangular sandwich plate with an isotropic core, simply supported on all sides with a concentrated load applied at its center.

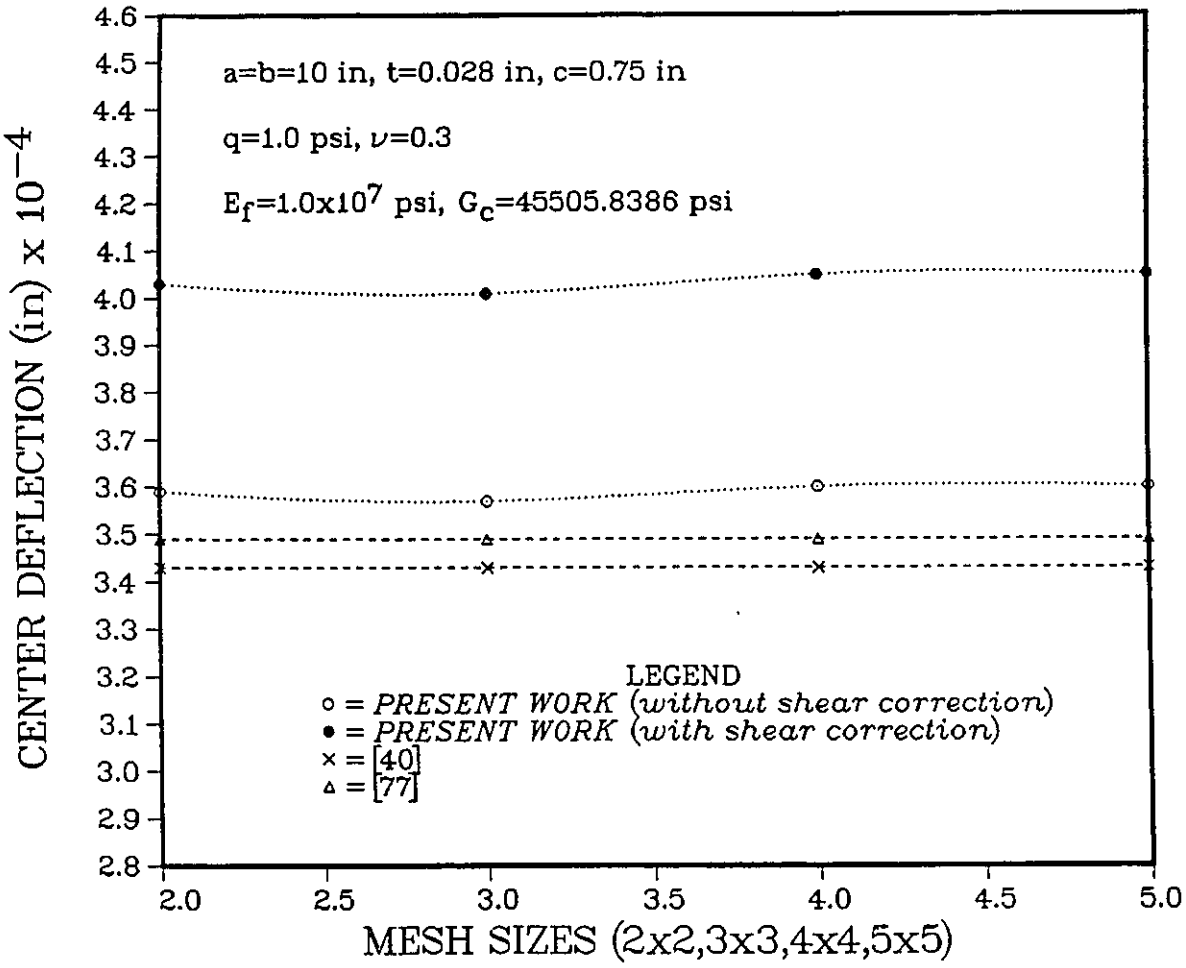

Figure A.20: Comparision and convergence of the center deflection of a rectangular sandwich plate with an isotropic core, clamped on all sides with a uniformly distributed load.

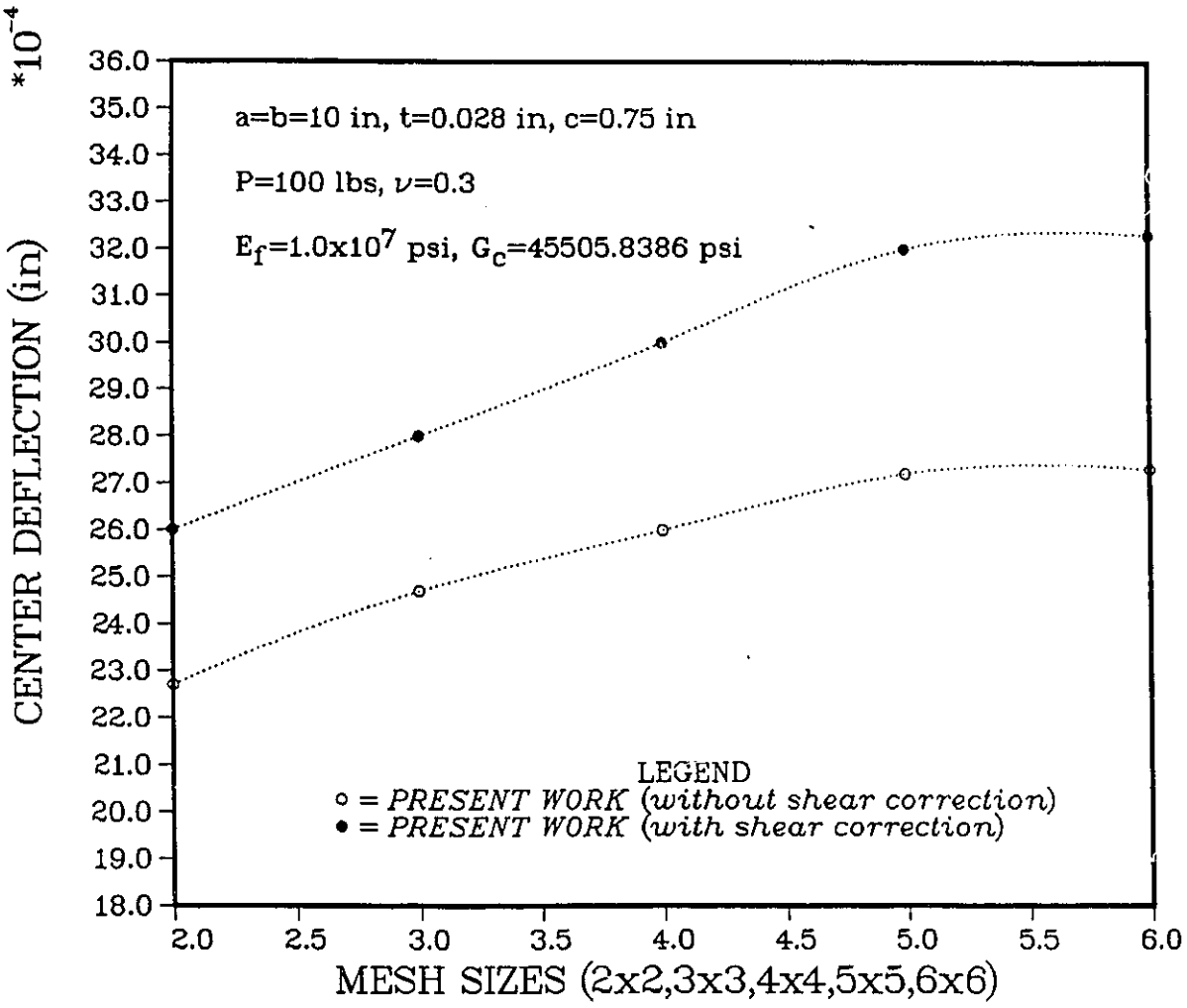

Figure A.21: Convergence of the center deflection of a rectangular sandwich plate with an isotropic core, clamped on all sides with a concentrated load applied at its center.

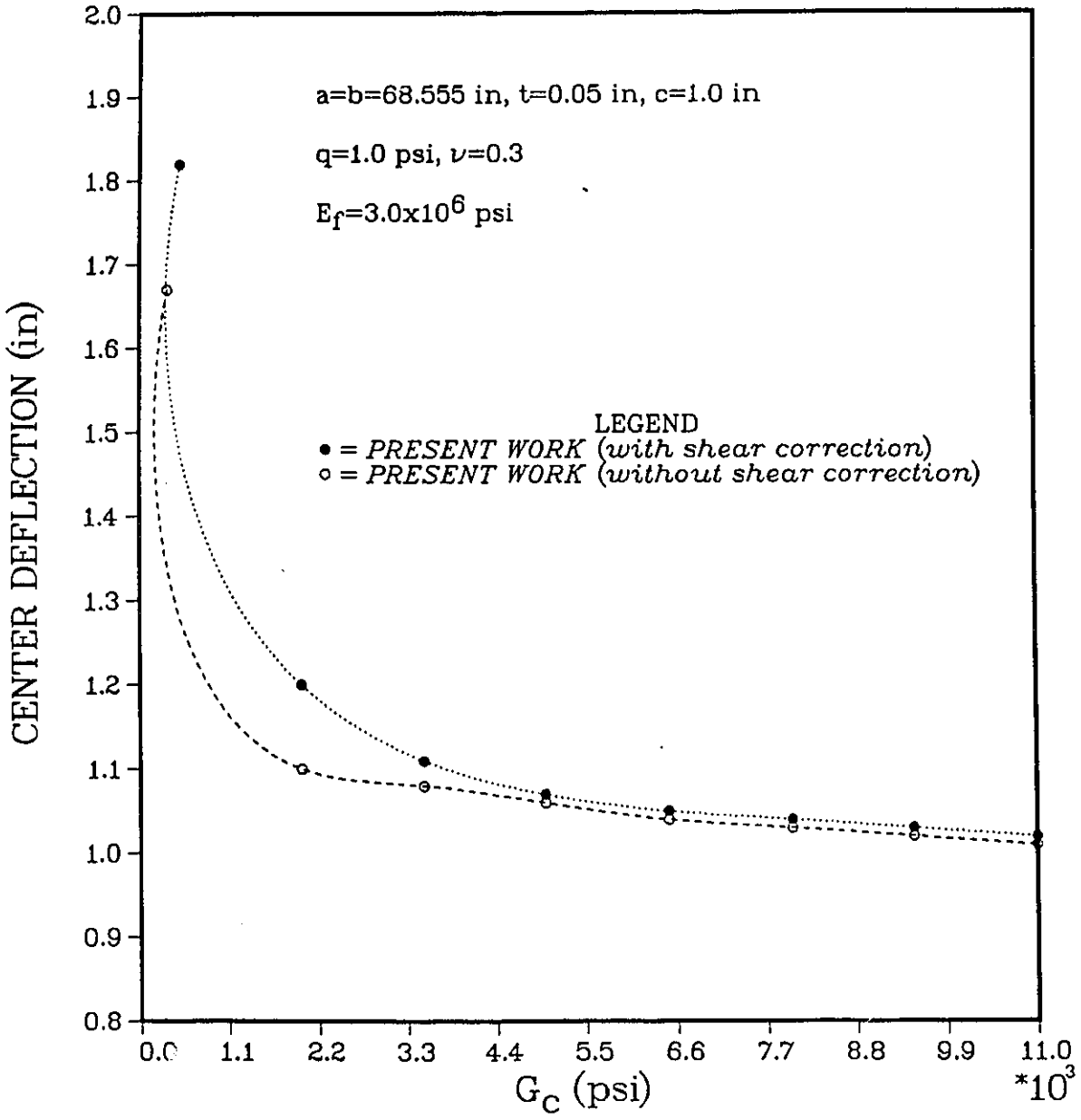

Figure A.22: Effect of the shear correction factor (α) with the variation of the shear modulus G_c of the core on the center deflection for a simply supported rectangular sandwich plate with an uniformly distributed load.

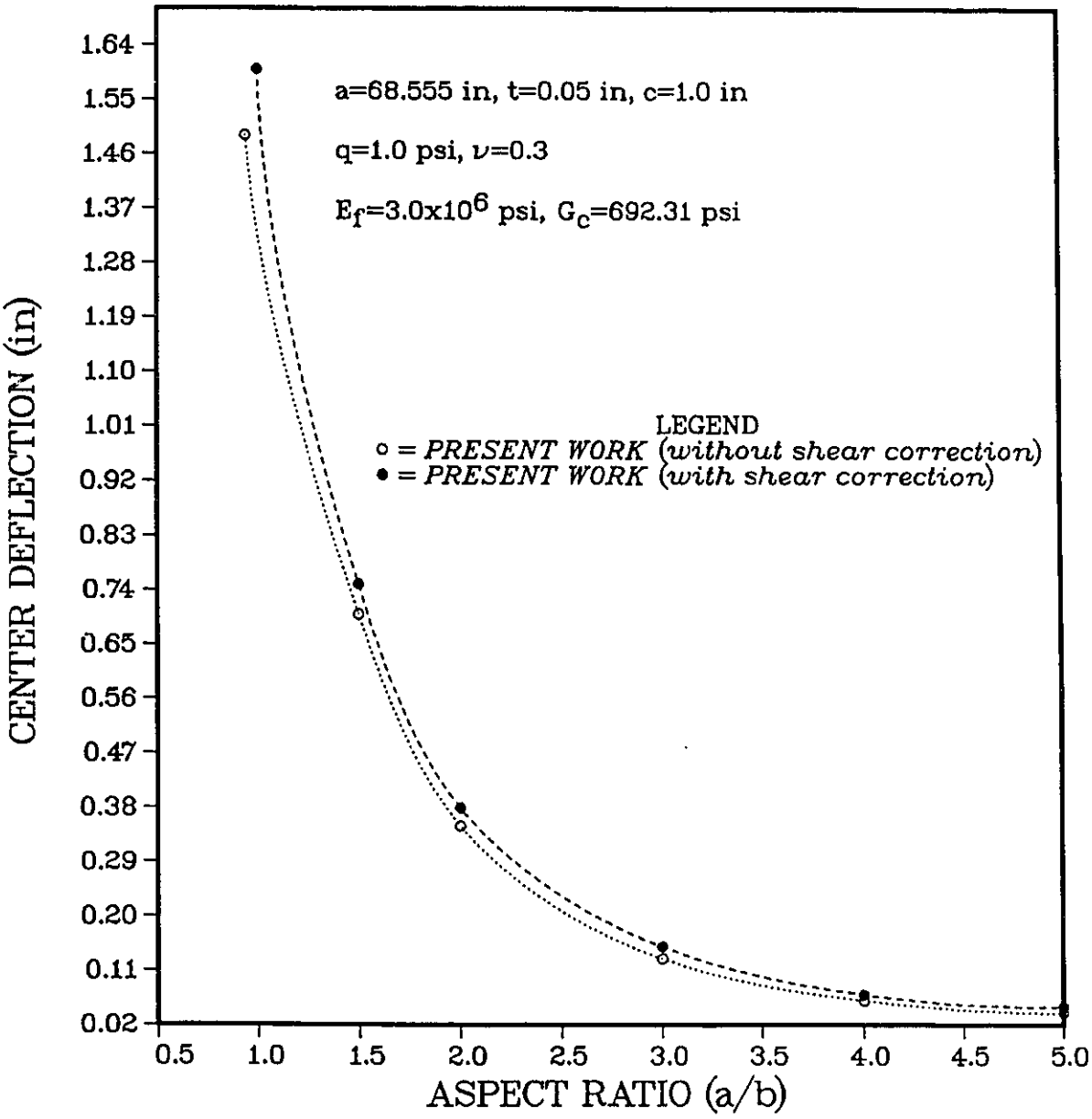

Figure A.23: Effect of the shear correction factor (α) with the variation of the aspect ratio (a/b) on the center deflection for a simply supported rectangular sandwich plate with an uniformly distributed load.

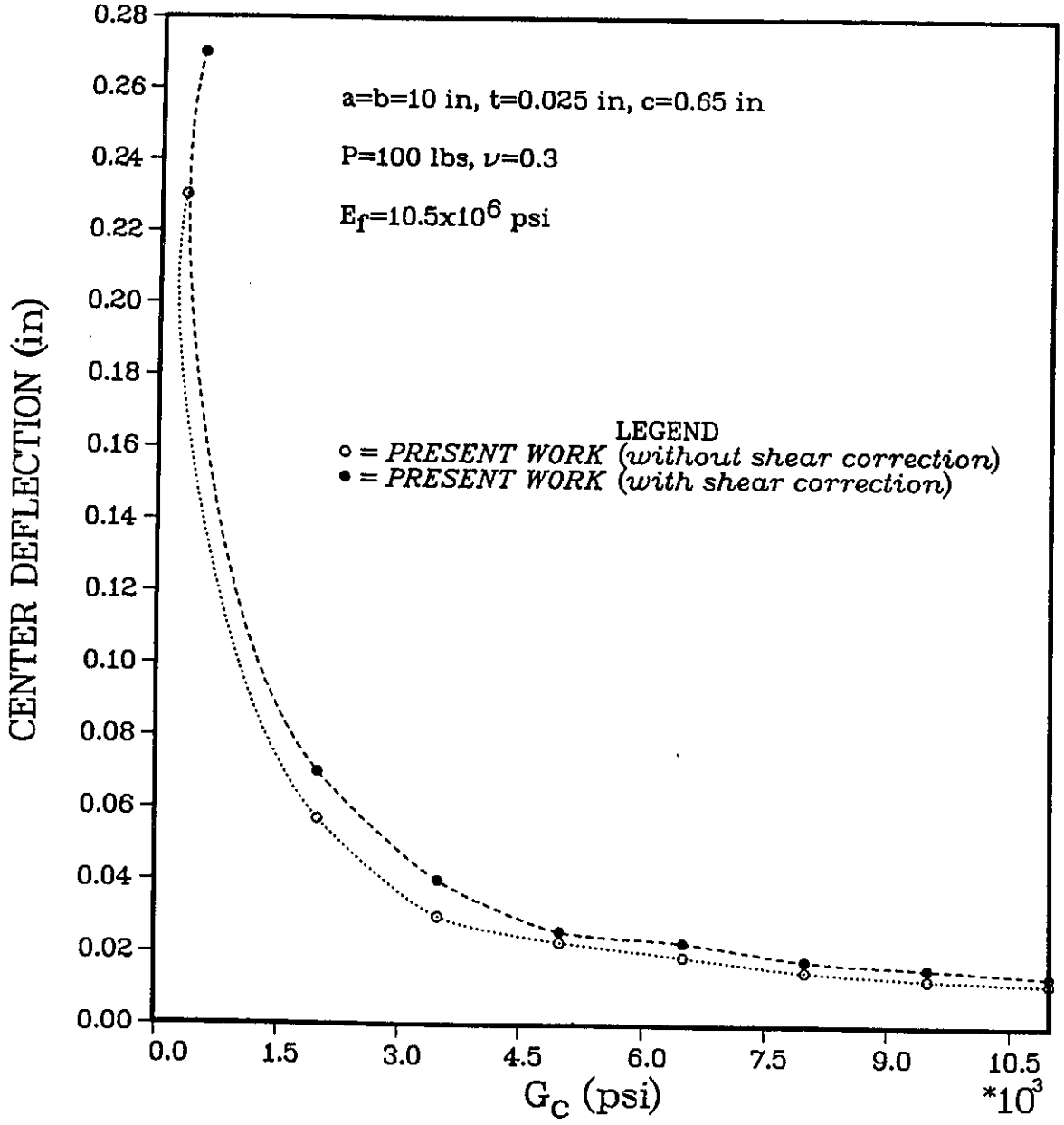

Figure A.24: Effect of the shear correction factor (α) with the variation of the shear modulus G_c of the core on the center deflection for a simply supported rectangular sandwich plate with a concentrated load applied at its center.

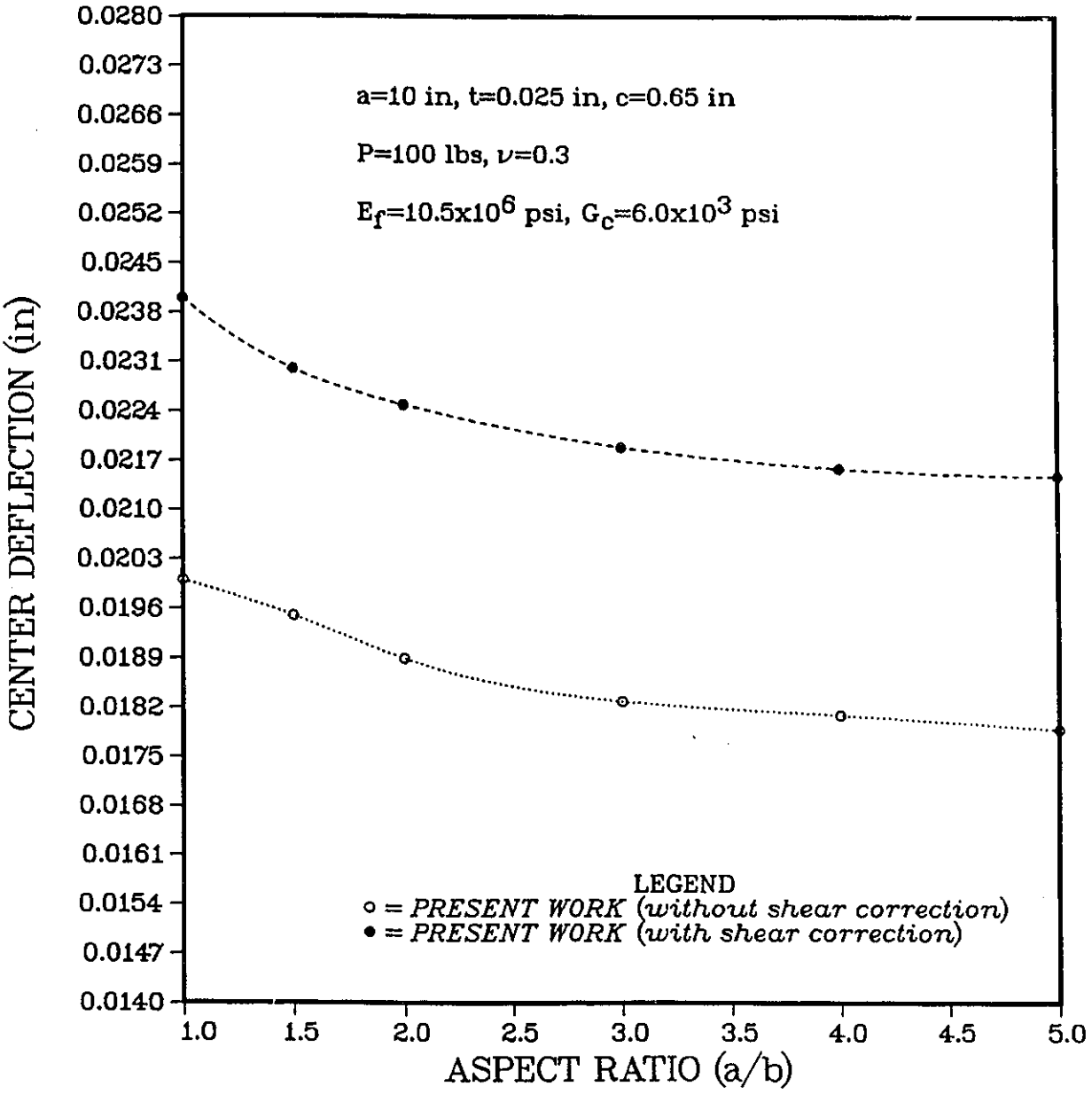

Figure A.25: Effect of the shear correction factor (α) with the variation of the aspect ratio (a/b) on the center deflection for a simply supported rectangular sandwich plate with a concentrated load applied at its center.

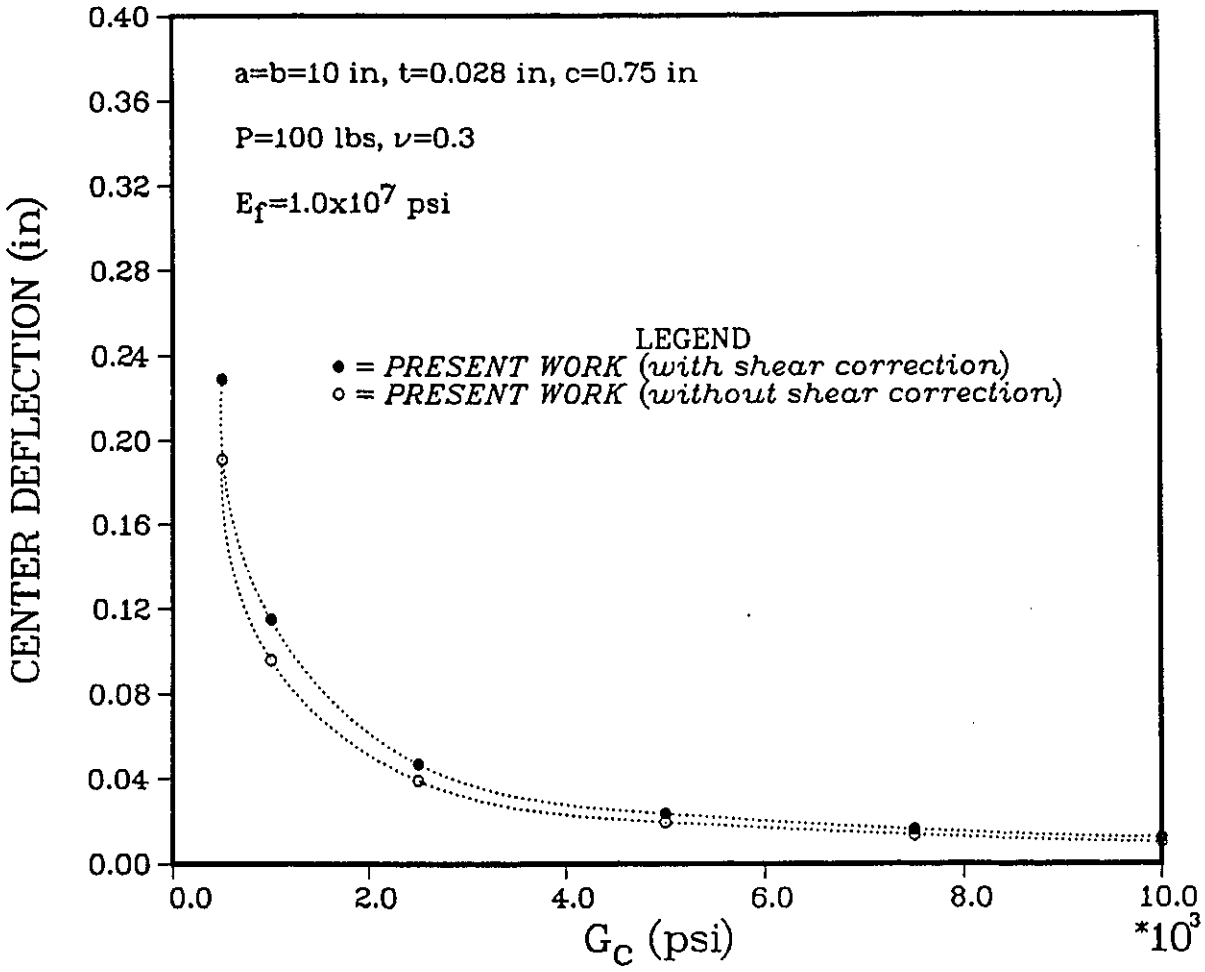

Figure A.26: Effect of the shear correction factor (α) with the variation of the shear modulus G_c of the core on the center deflection for a clamped rectangular sandwich plate with a concentrated load applied at its center.

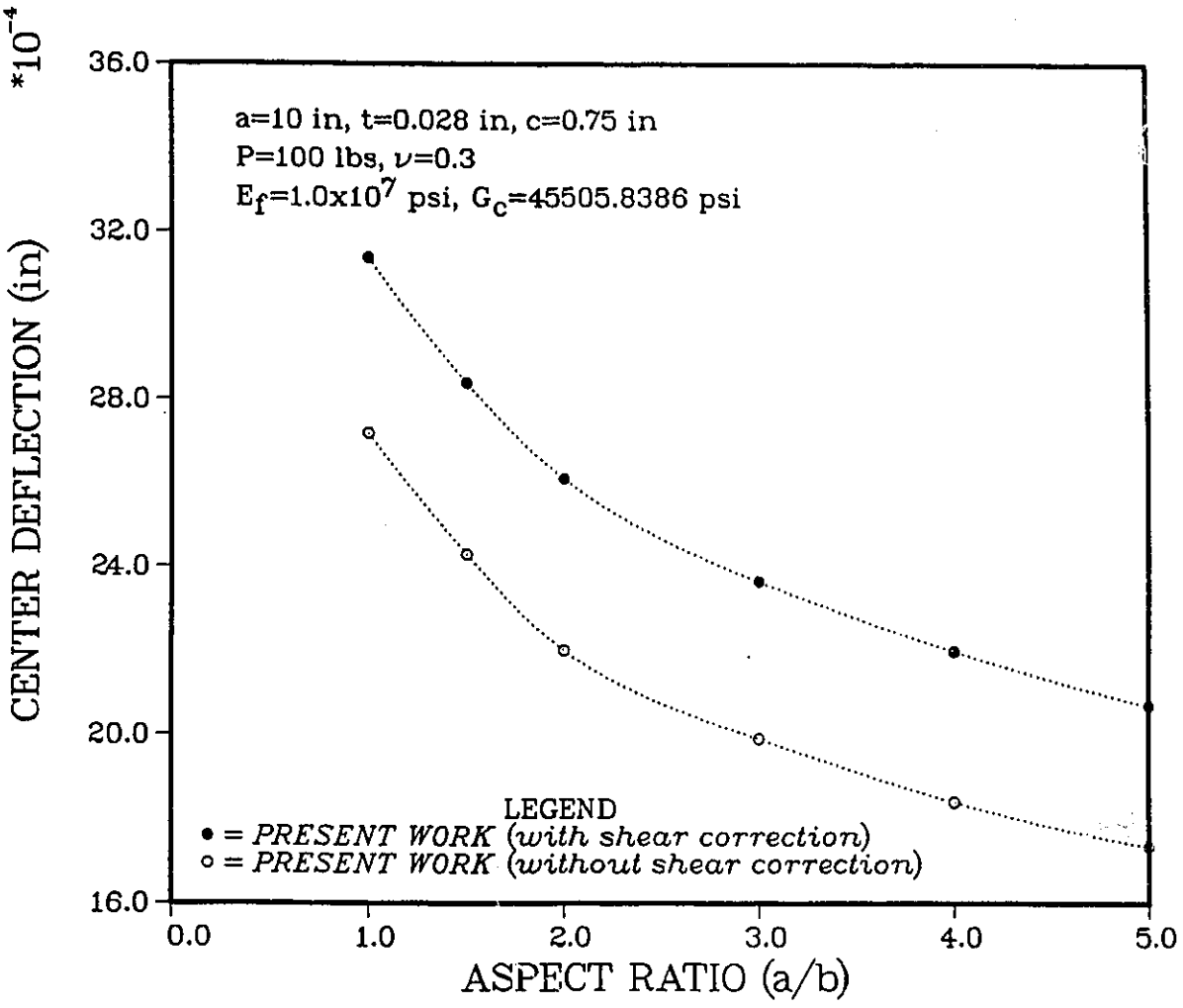

Figure A.27: Effect of the shear correction factor (α) with the variation of the aspect ratio (a/b) on the center deflection for a clamped rectangular sandwich plate with a concentrated load applied at its center.

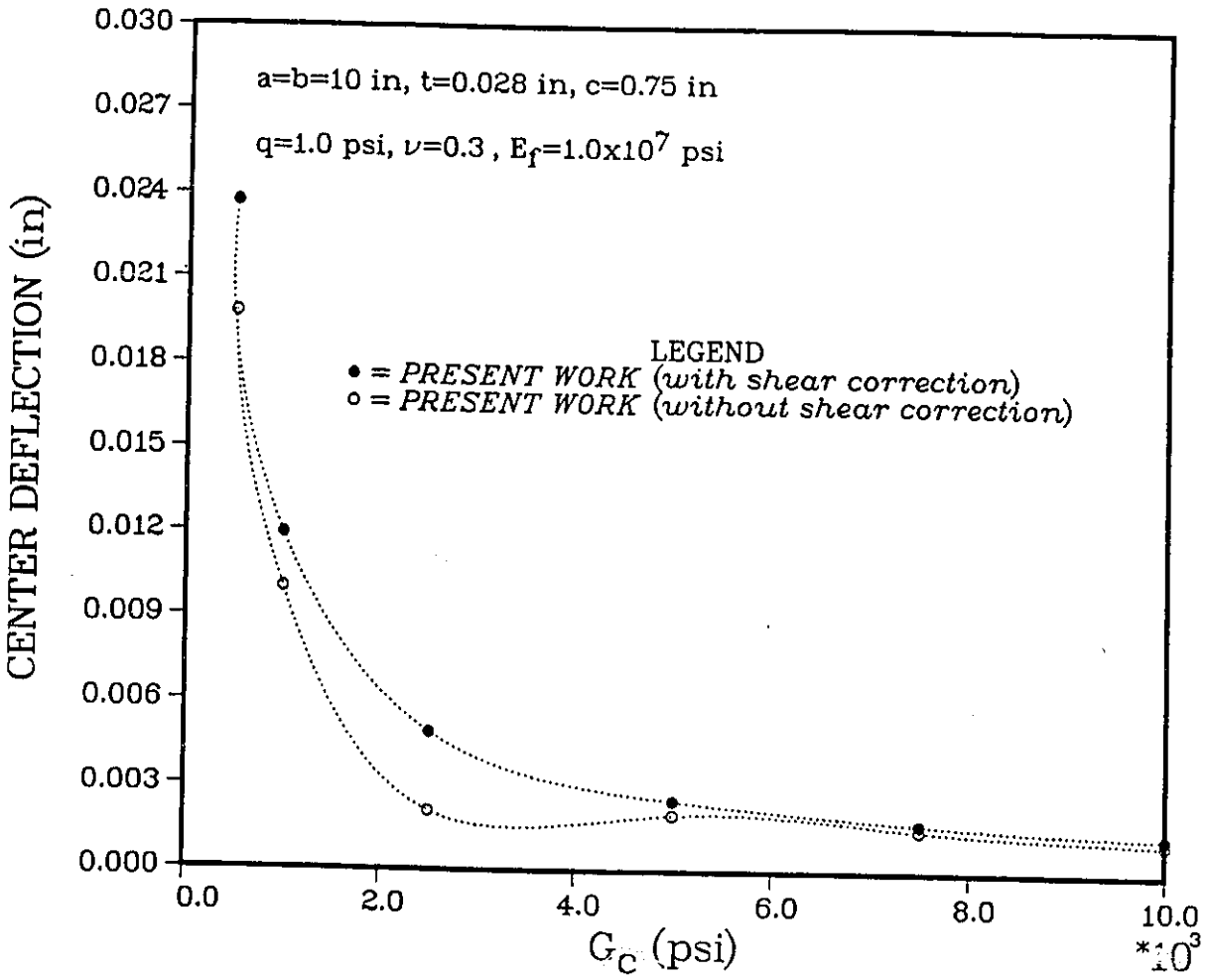

Figure A.28: Effect of the shear correction factor (α) with the variation of the shear modulus G_c of the core on the center deflection for a clamped rectangular sandwich plate with an uniformly distributed load.

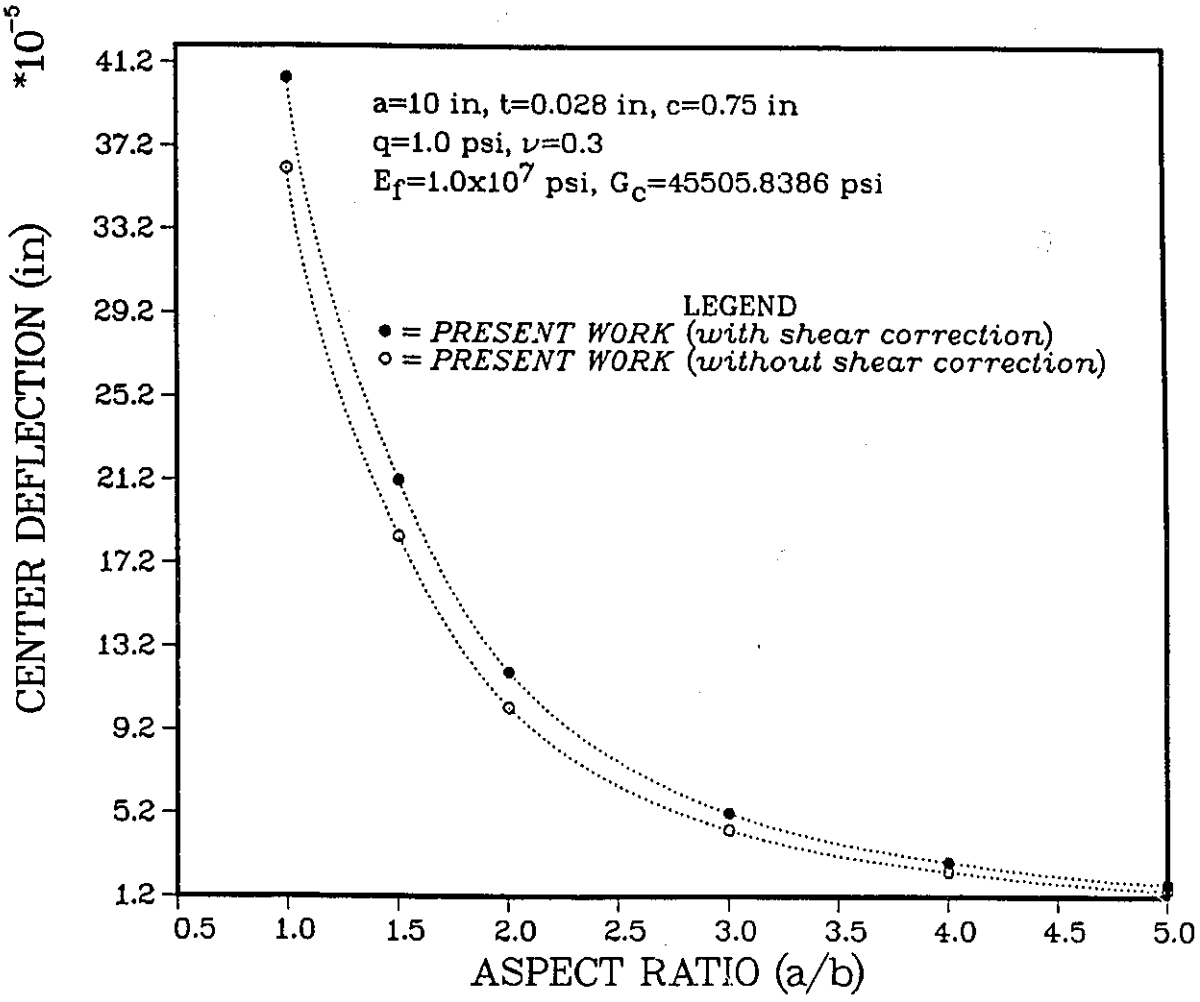

Figure A.29: Effect of the shear correction factor (α) with the variation of the aspect ratio (a/b) on the center deflection for a clamped rectangular sandwich plate with an uniformly distributed load.

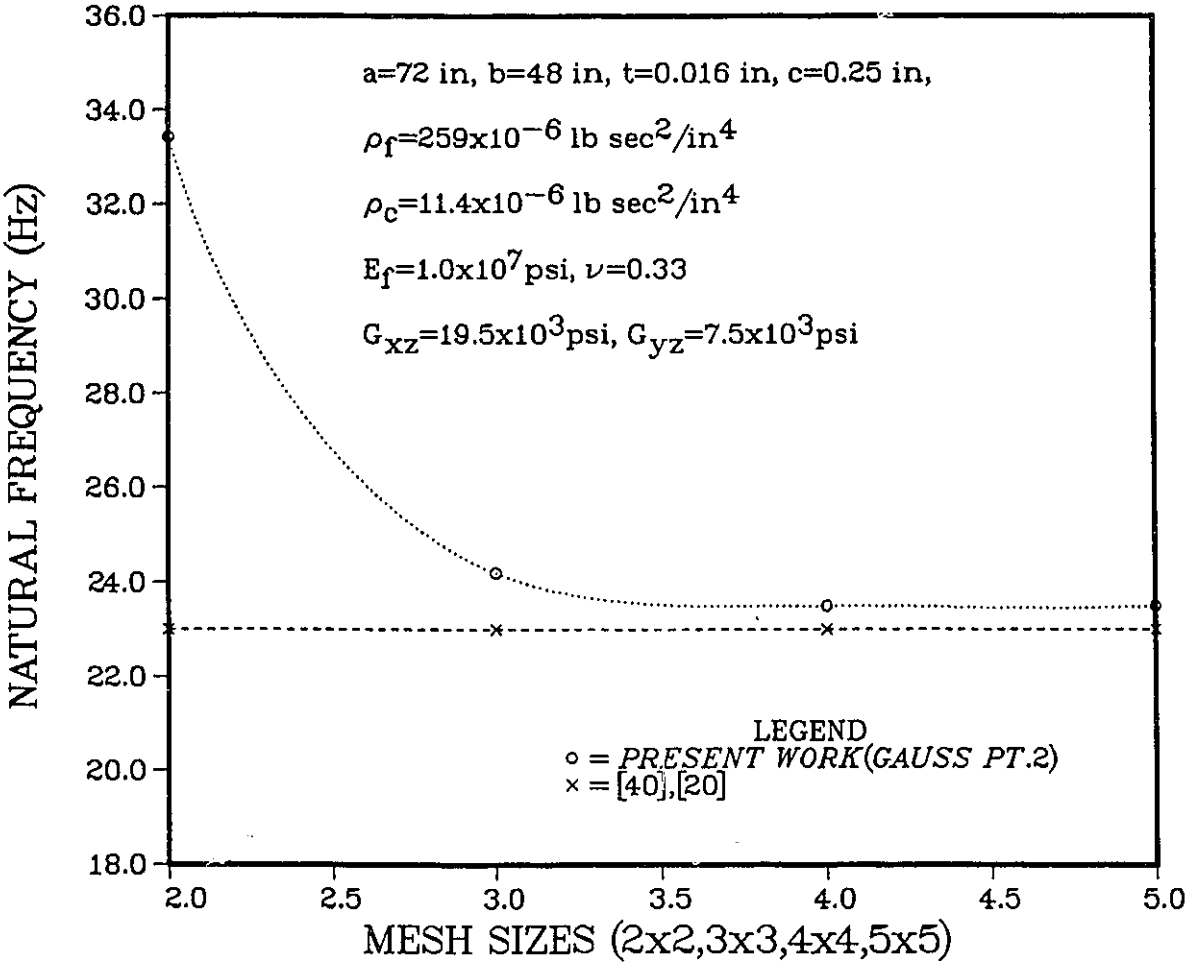

Figure A.30: Comparision and convergence of the natural frequency of a simply supported rectangular sandwich plate with an orthotropic core (Mode 1).

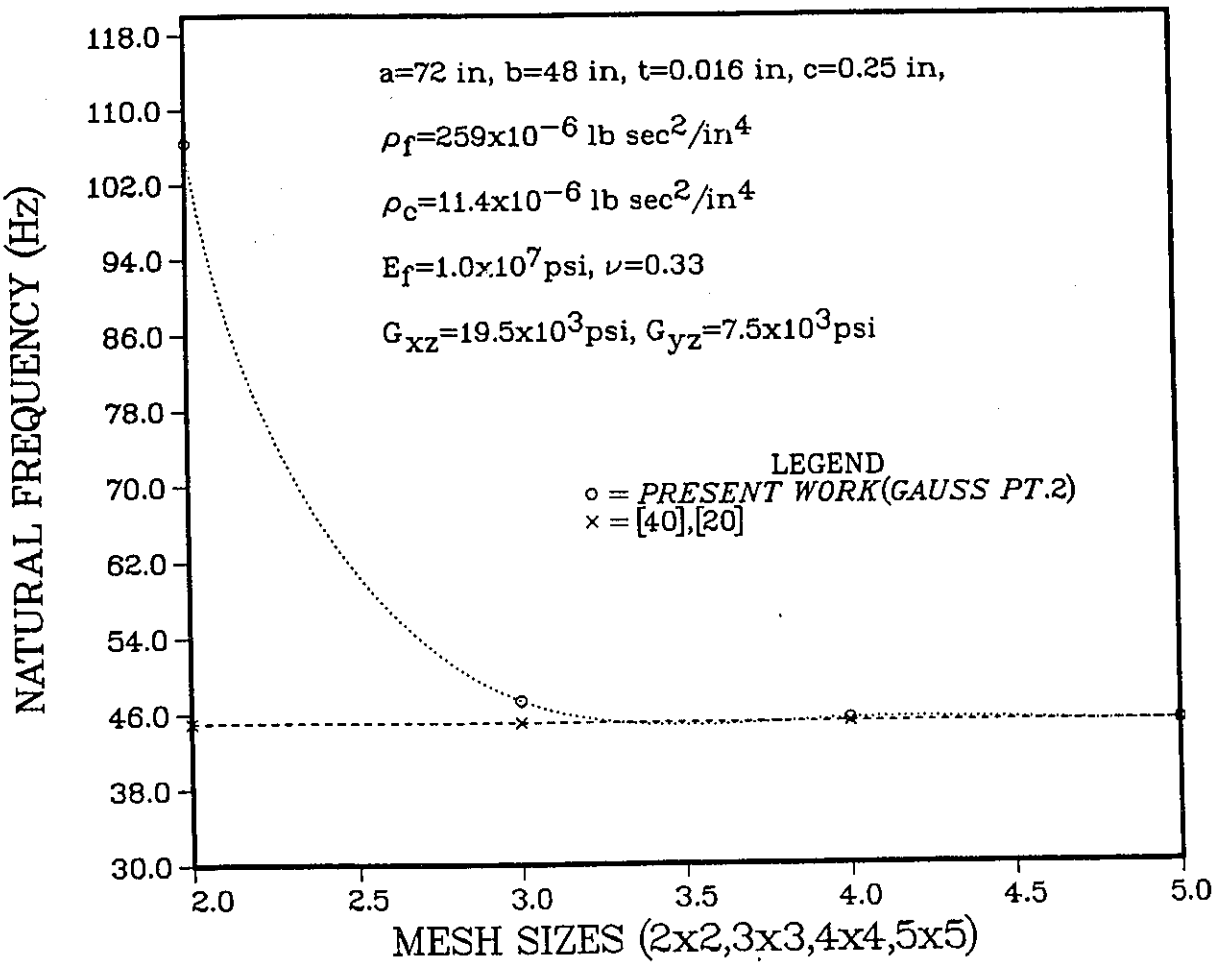

Figure A.31: Comparision and convergence of the natural frequency of a simply supported rectangular sandwich plate with an orthotropic core (Mode 2).

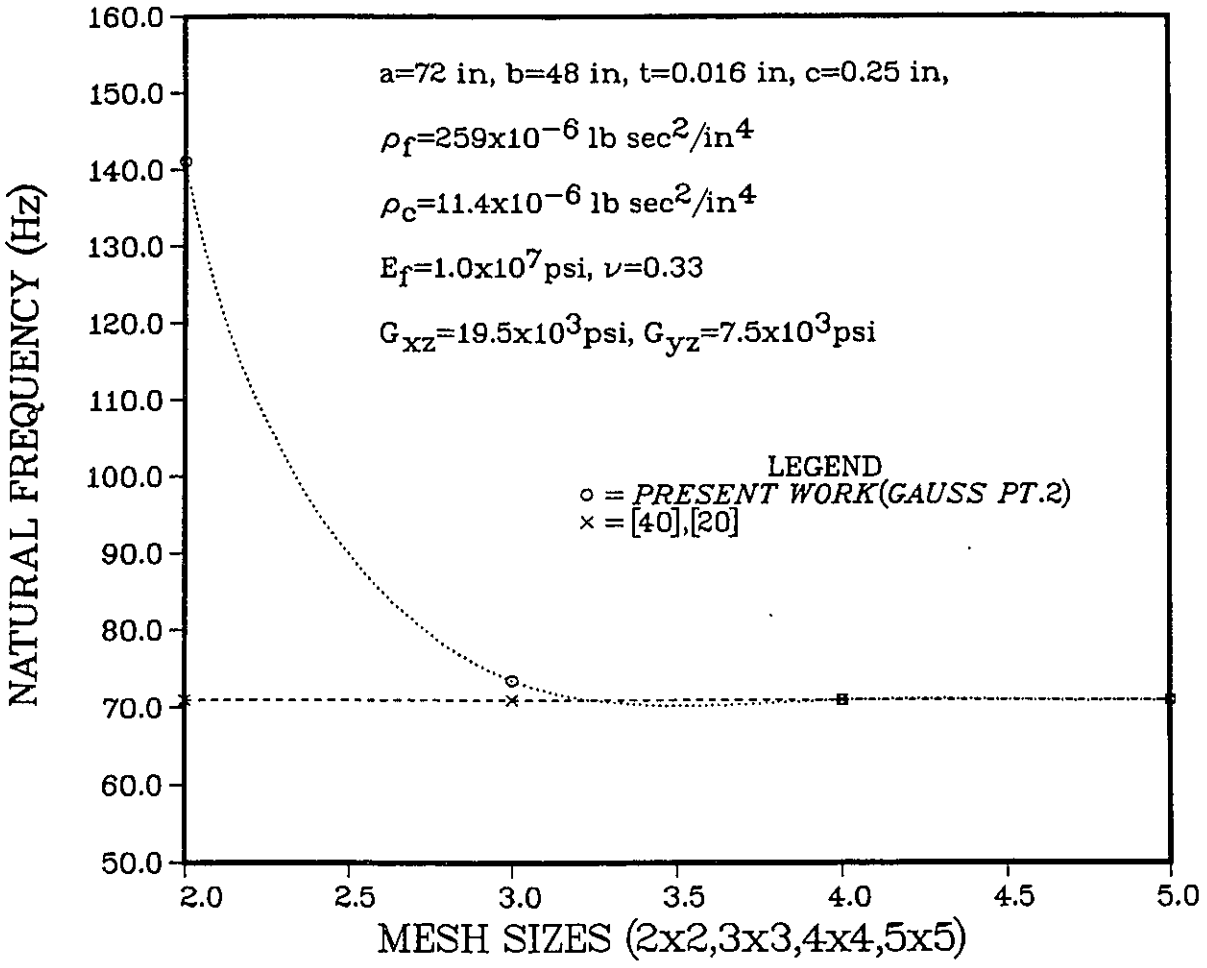

Figure A.32: Comparision and convergence of the natural frequency of a simply supported rectangular sandwich plate with an orthotropic core (Mode 3).

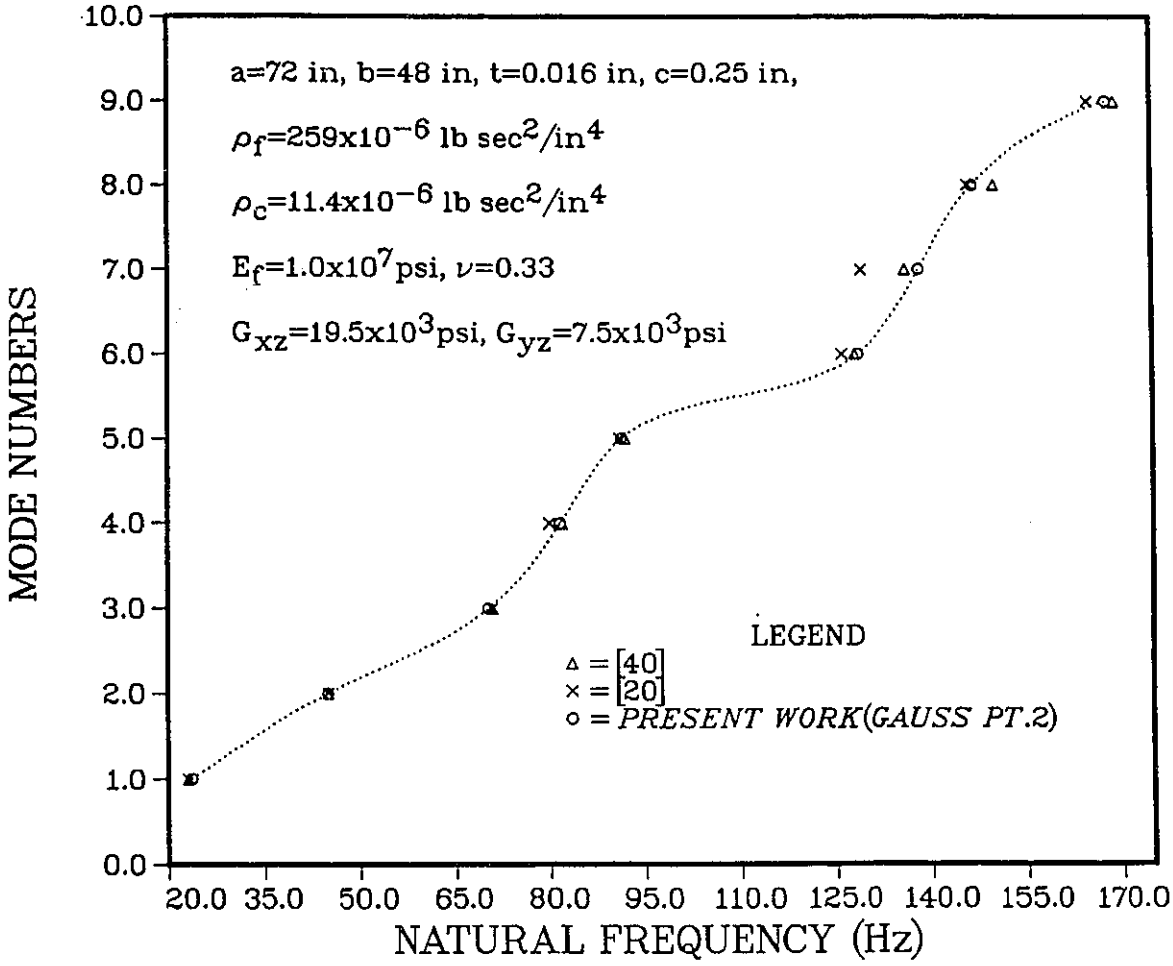

Figure A.33: Comparision of the natural frequencies for a simply supported rectangular sandwich plate with an orthotropic core for various modes determined with a lower order of Gaussian integration (NGAUS=2).

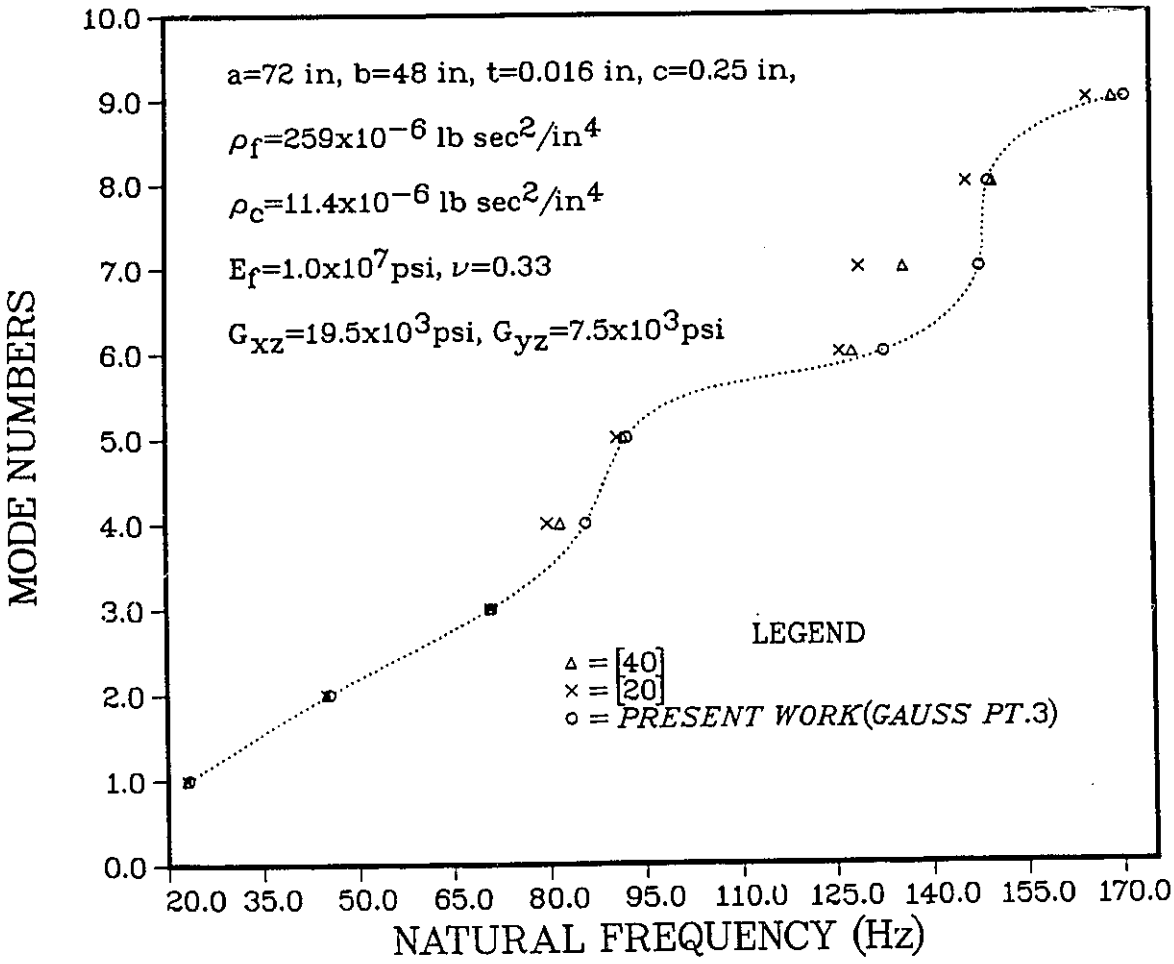

Figure A.34: Comparision of the natural frequencies for a simply supported rectangular sandwich plate with an orthotropic core for various modes determined with a higher order of Gaussian integration (NGAUS=3).

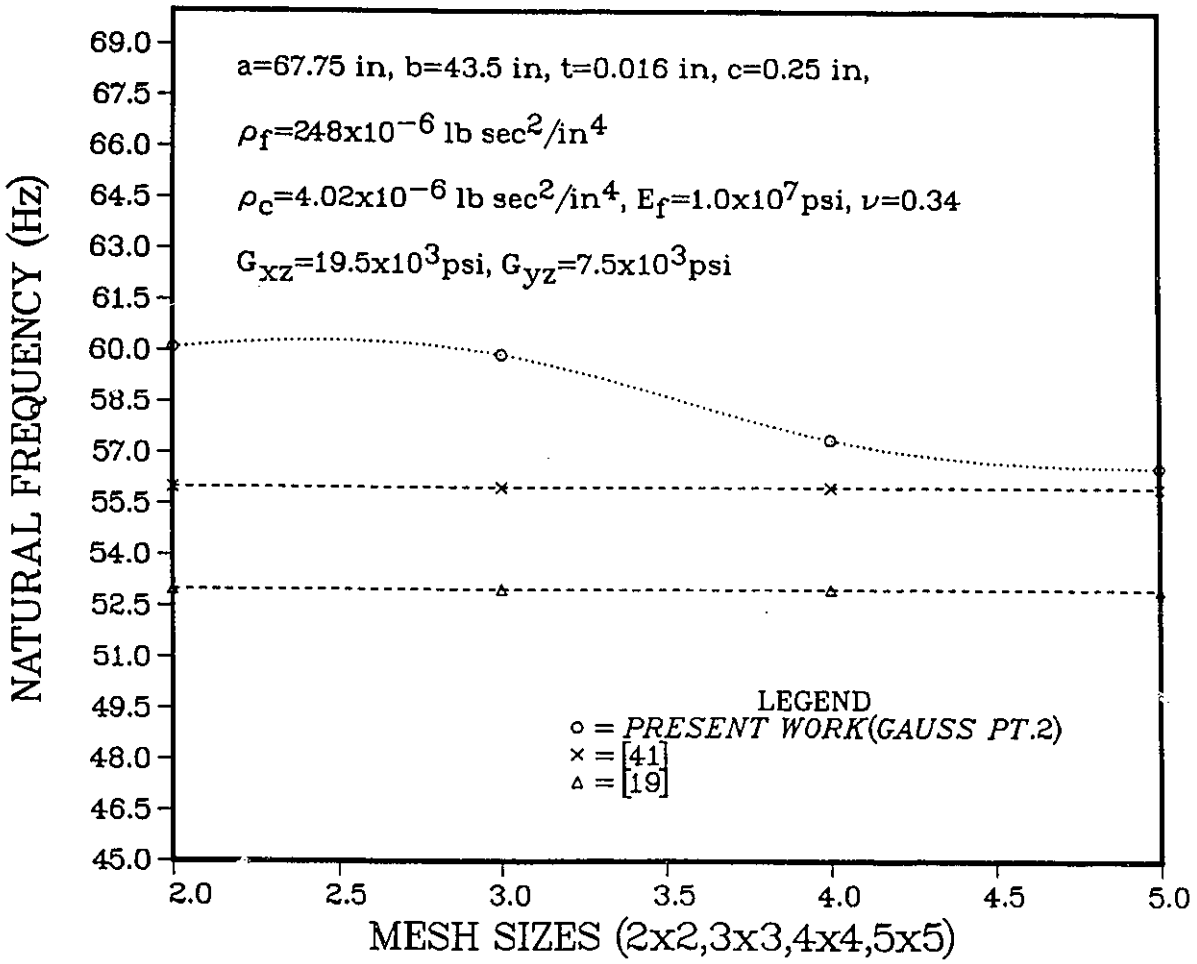

Figure A.35: Comparision and convergence of the natural frequency of a clamped rectangular sandwich plate with an orthotropic core (Mode 1)(Mesh sizes are for the full plate).

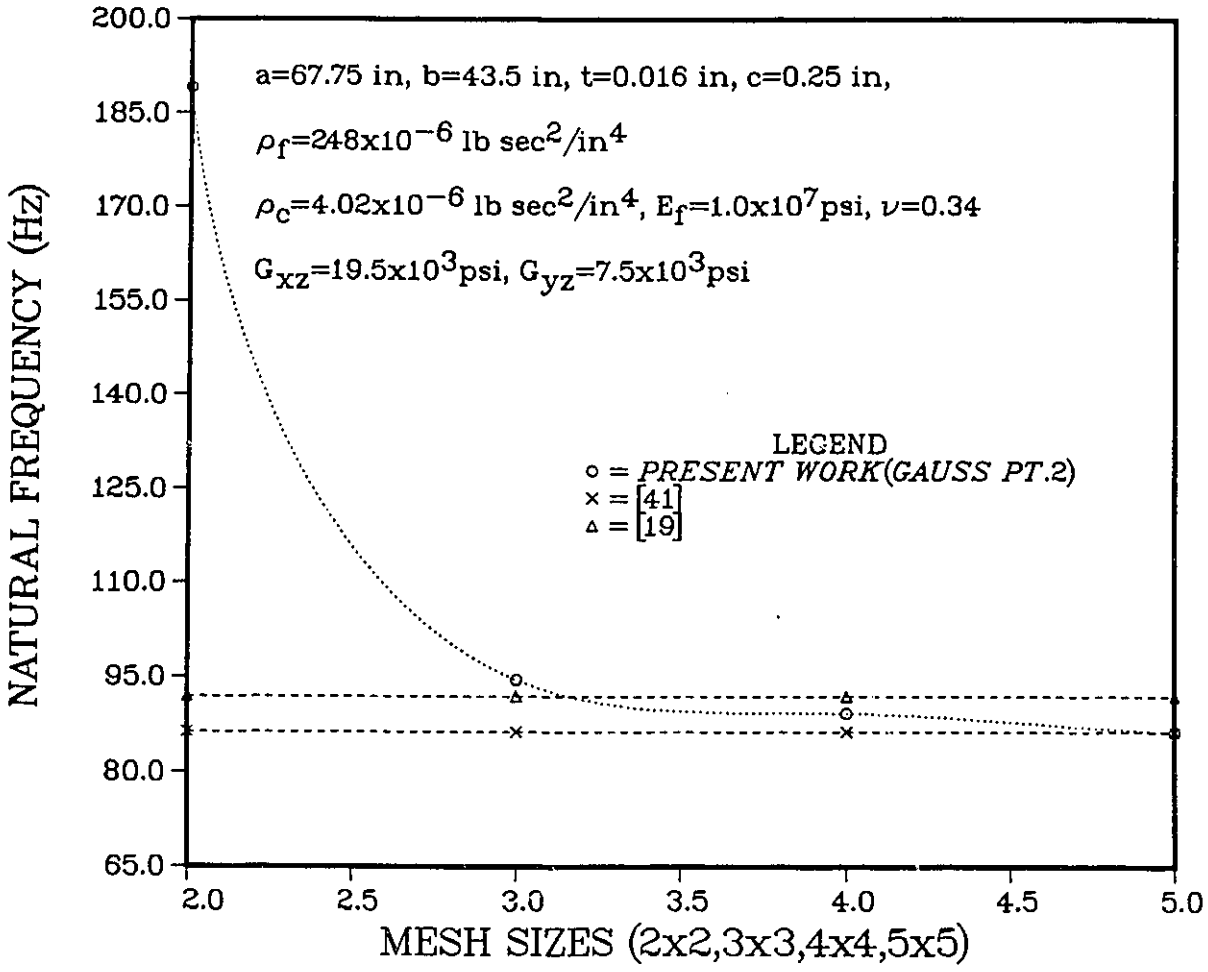

Figure A.36: Comparision and convergence of the natural frequency of a clamped rectangular sandwich plate with an orthotropic core (Mode 2)(Mesh sizes are for the full plate).

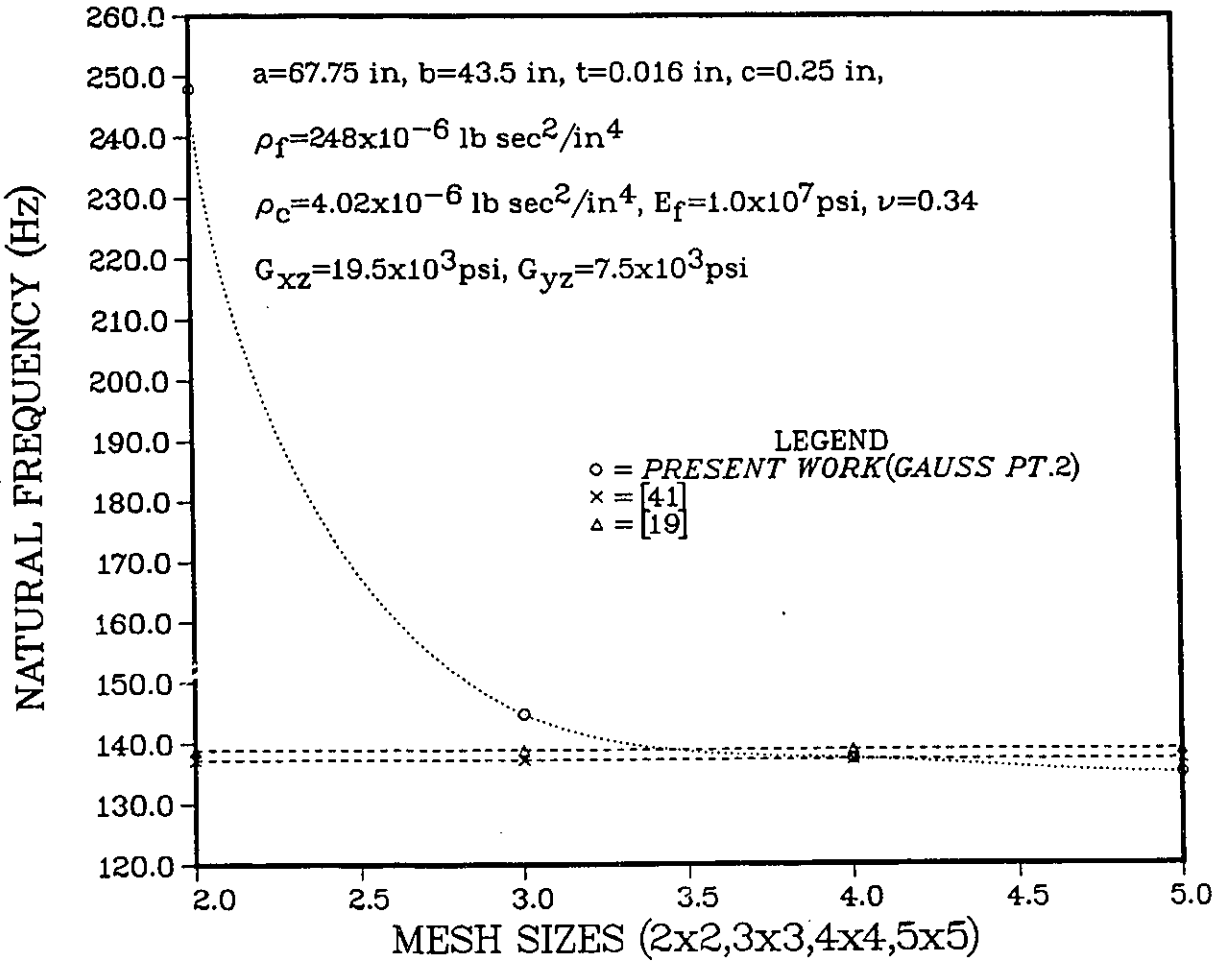

Figure A.37: Comparision and convergence of the natural frequency of a clamped rectangular sandwich plate with an orthotropic core (Mode 3)(Mesh sizes are for the full plate).

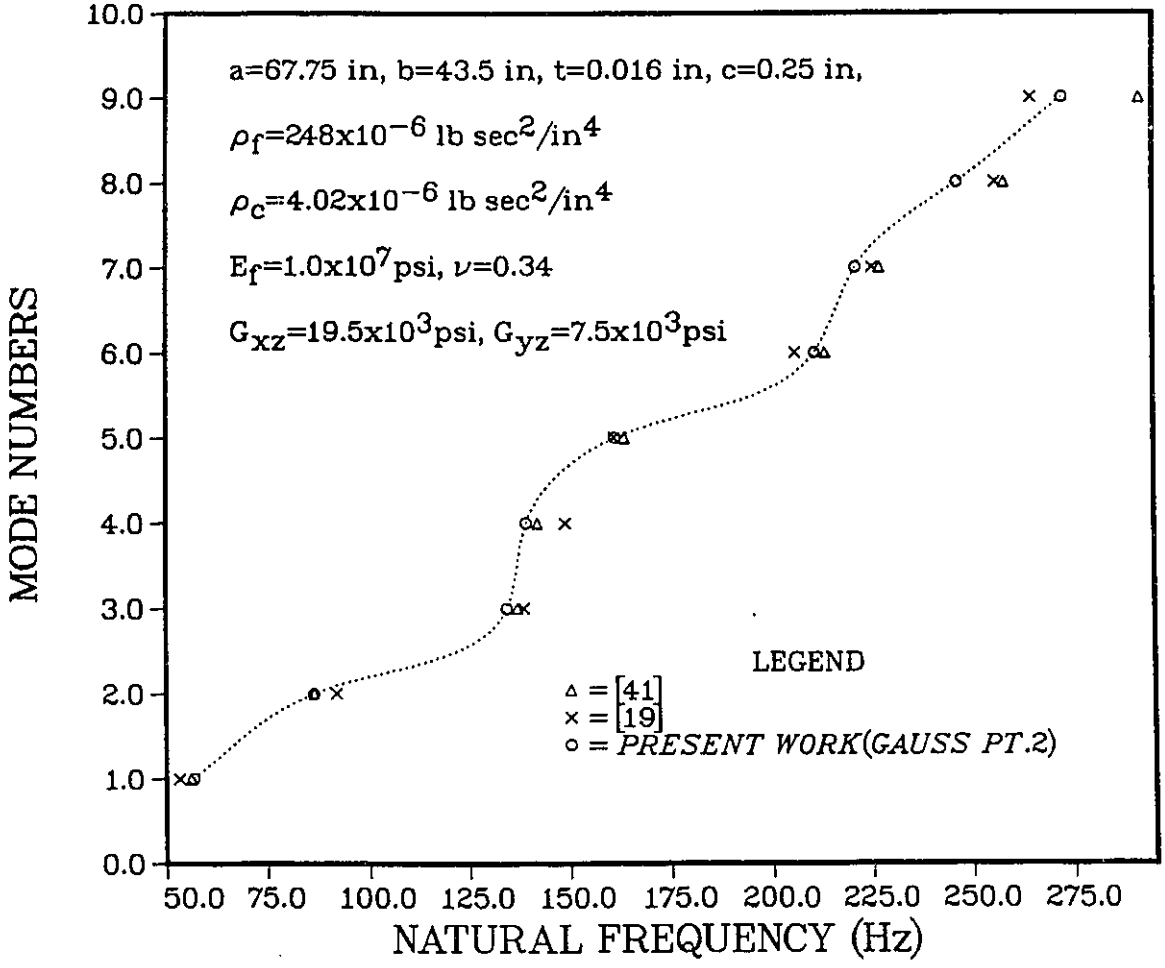

Figure A.38: Comparision of the natural frequencies for a clamped rectangular sandwich plate with an orthotropic core for various modes determined with a lower order of Gaussian integration (NGAUS=2).

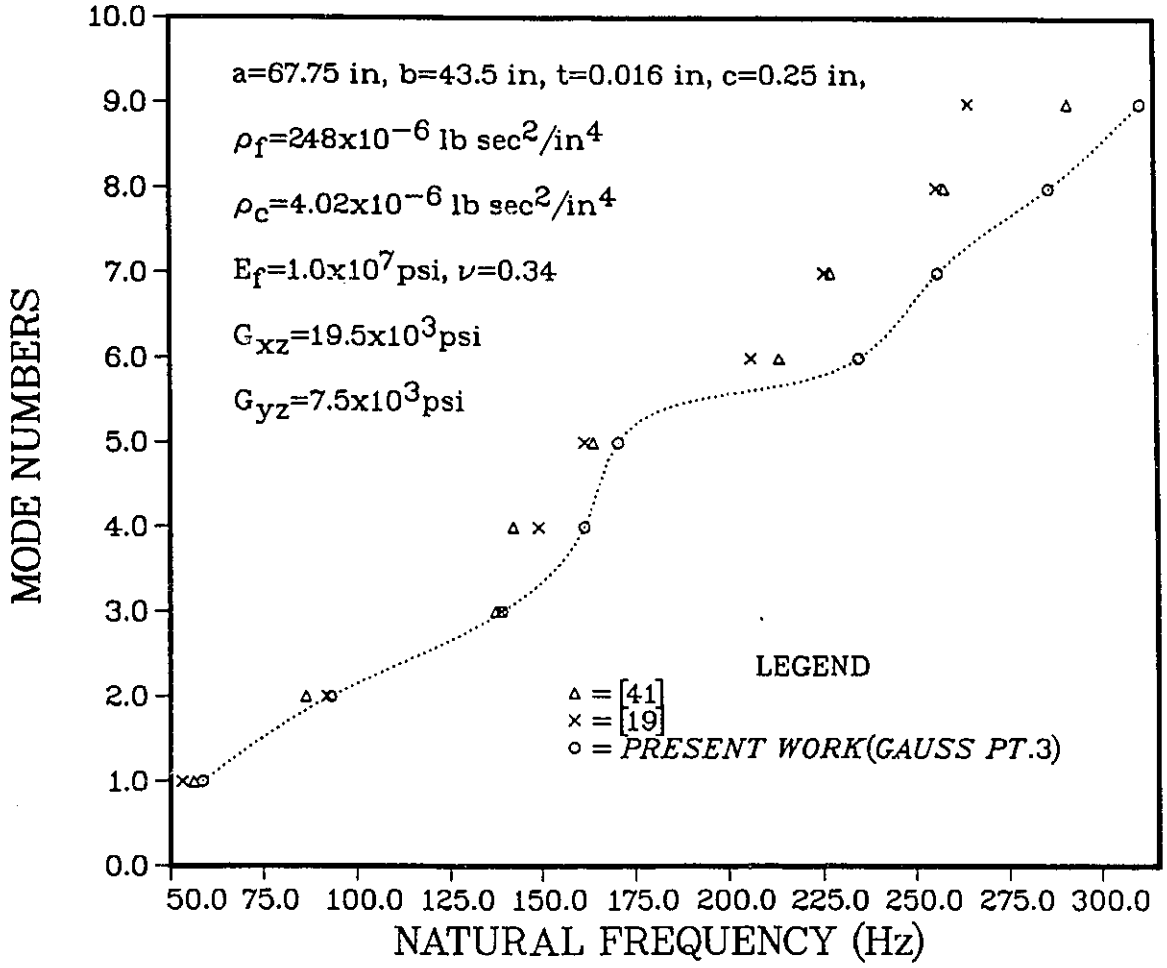

Figure A.39: Comparision of the natural frequencies for a clamped rectangular sandwich plate with an orthotropic core for various modes determined with a higher order of Gaussian integration (NGAUS=3).

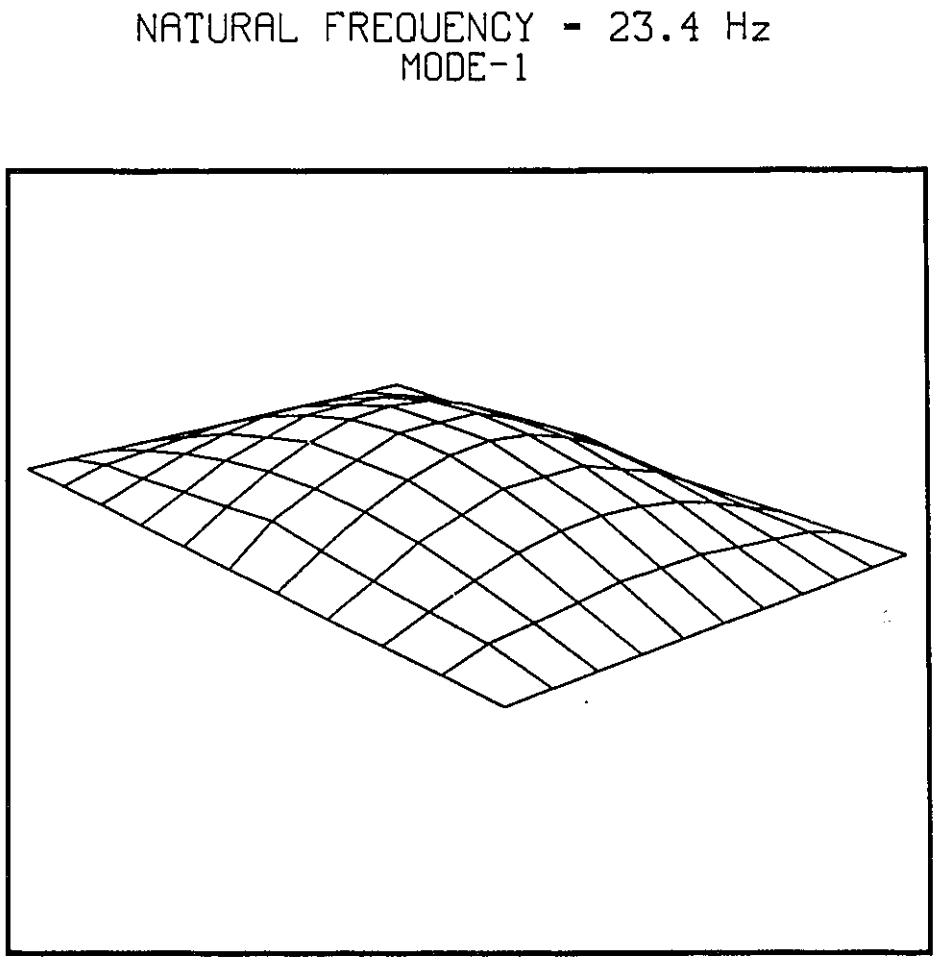

Figure A.40: Mode shape for a simply supported rectangular sandwich plate with an orthotropic core whose natural frequency is 23.4 Hz.

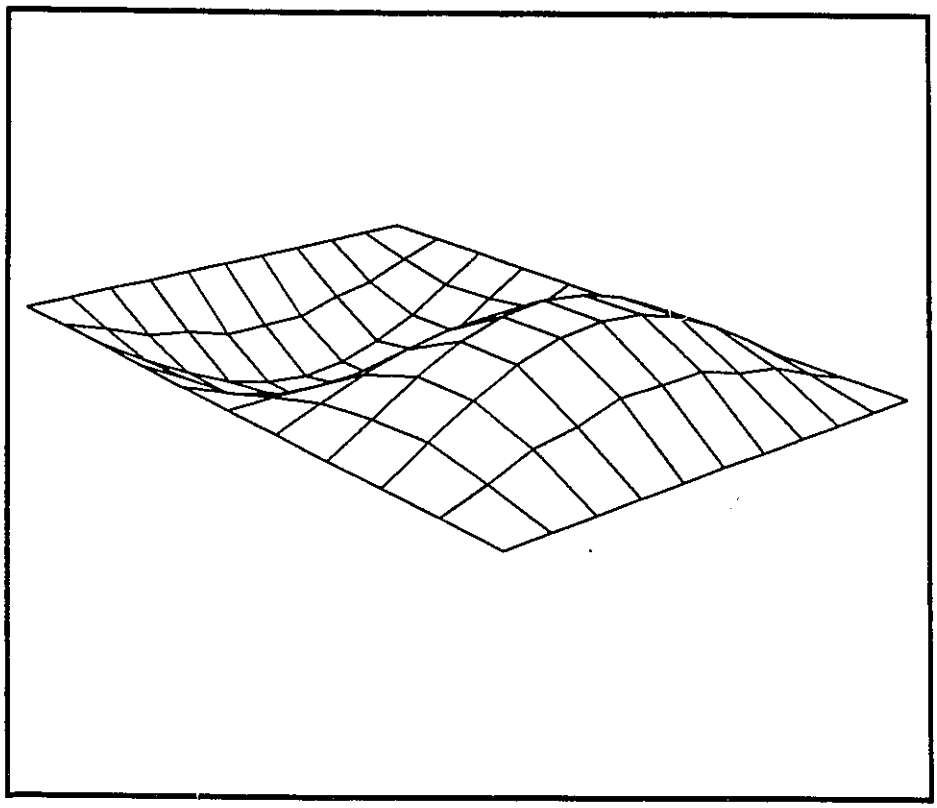

Figure A.41: Mode shape for a simply supported rectangular sandwich plate with an orthotropic core whose natural frequency is 44.9 Hz.

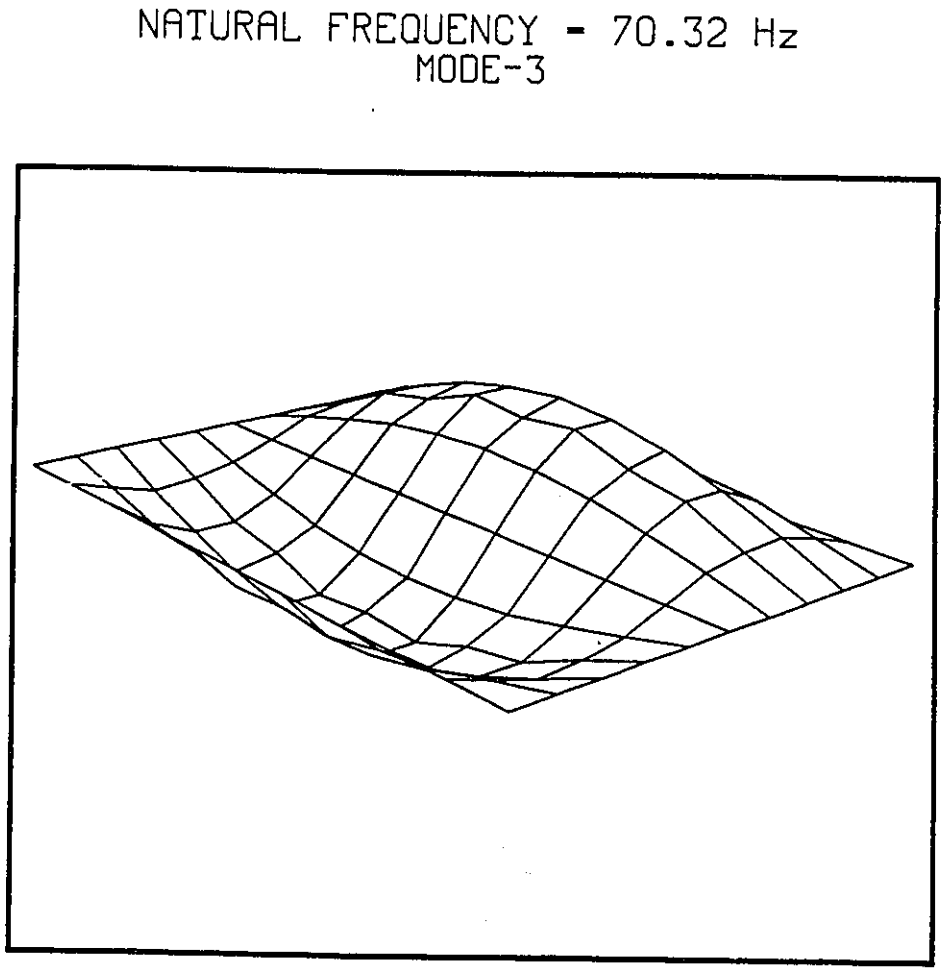

Figure A.42: Mode shape for a simply supported rectangular sandwich plate with an orthotropic core whose natural frequency is 70.32 Hz.

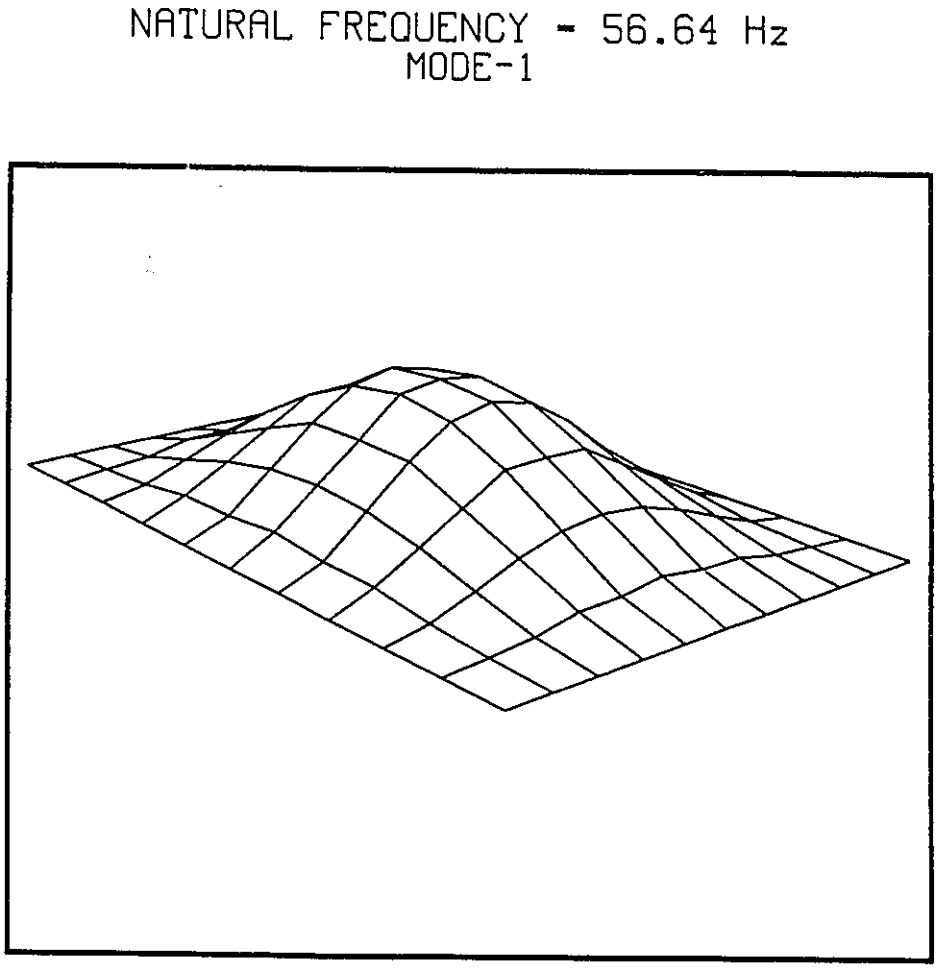

Figure A.43: Mode shape for a clamped rectangular sandwich plate with an orthotropic core whose natural frequency is 56.64 Hz.

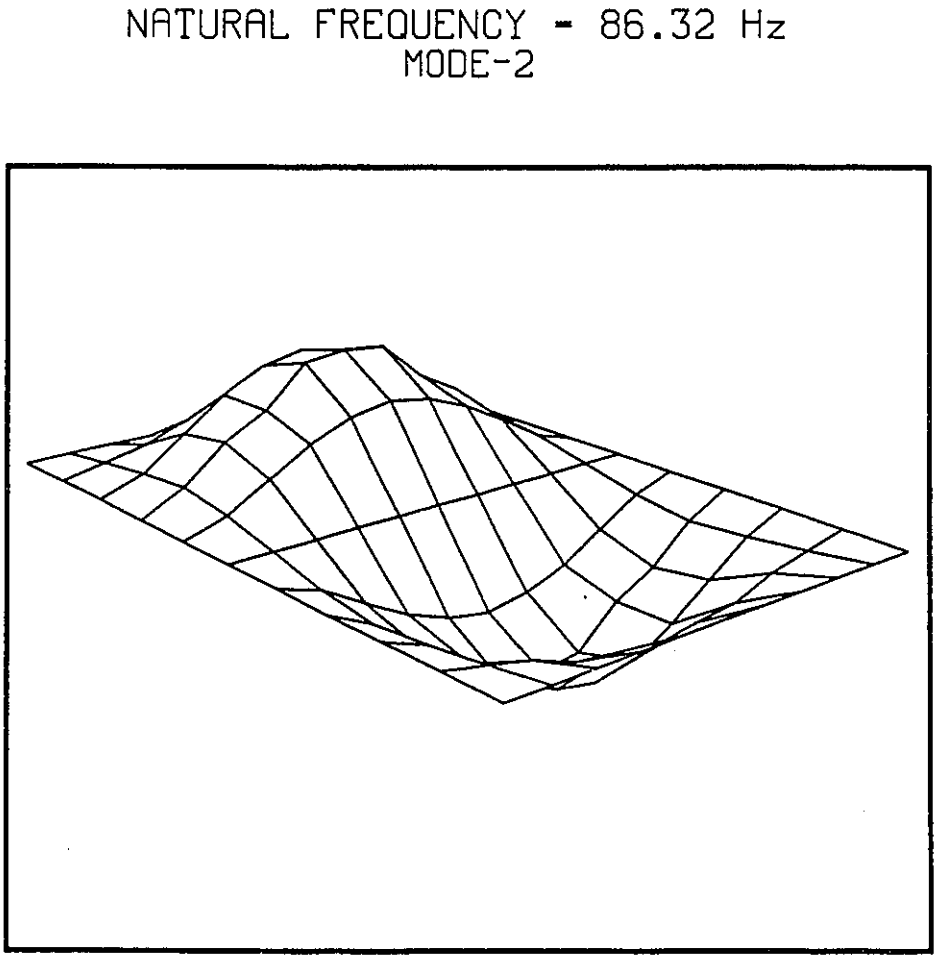

Figure A.44: Mode shape for a clamped rectangular sandwich plate with an orthotropic core whose natural frequency is 86.32 Hz.

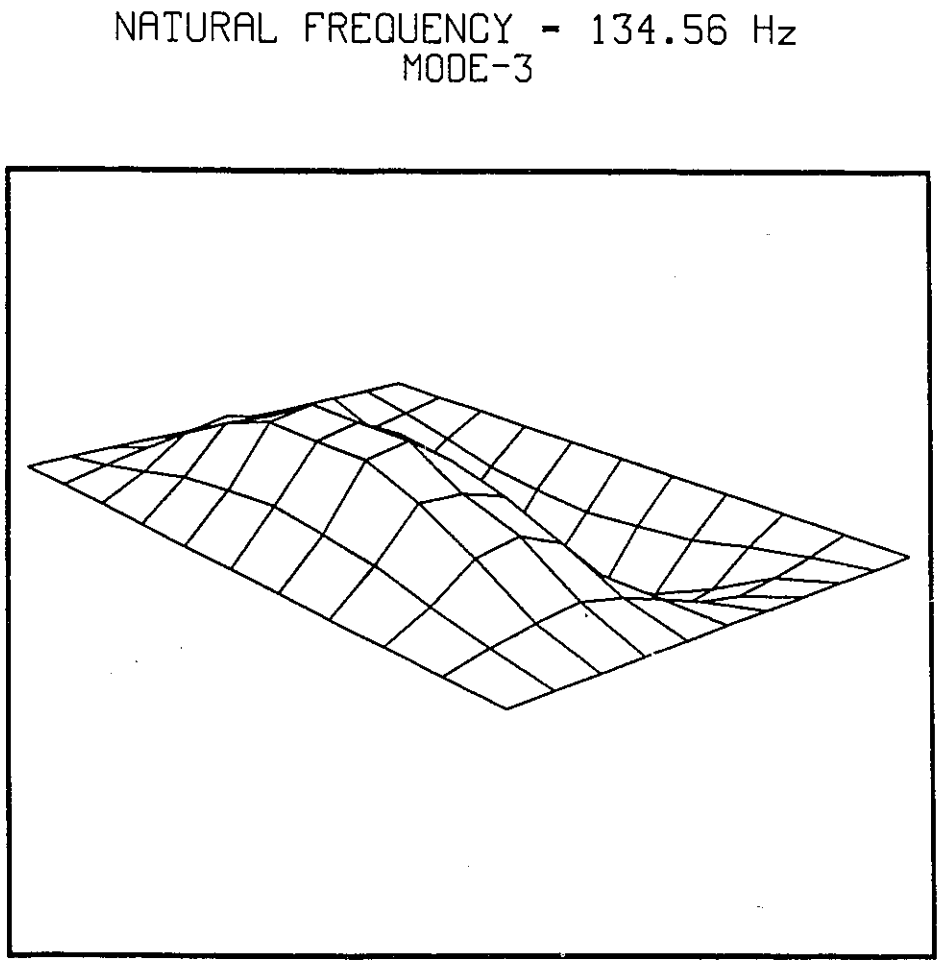

Figure A.45: Mode shape for a clamped rectangular sandwich plate with an orthotropic core whose natural frequency is 134.56 Hz.

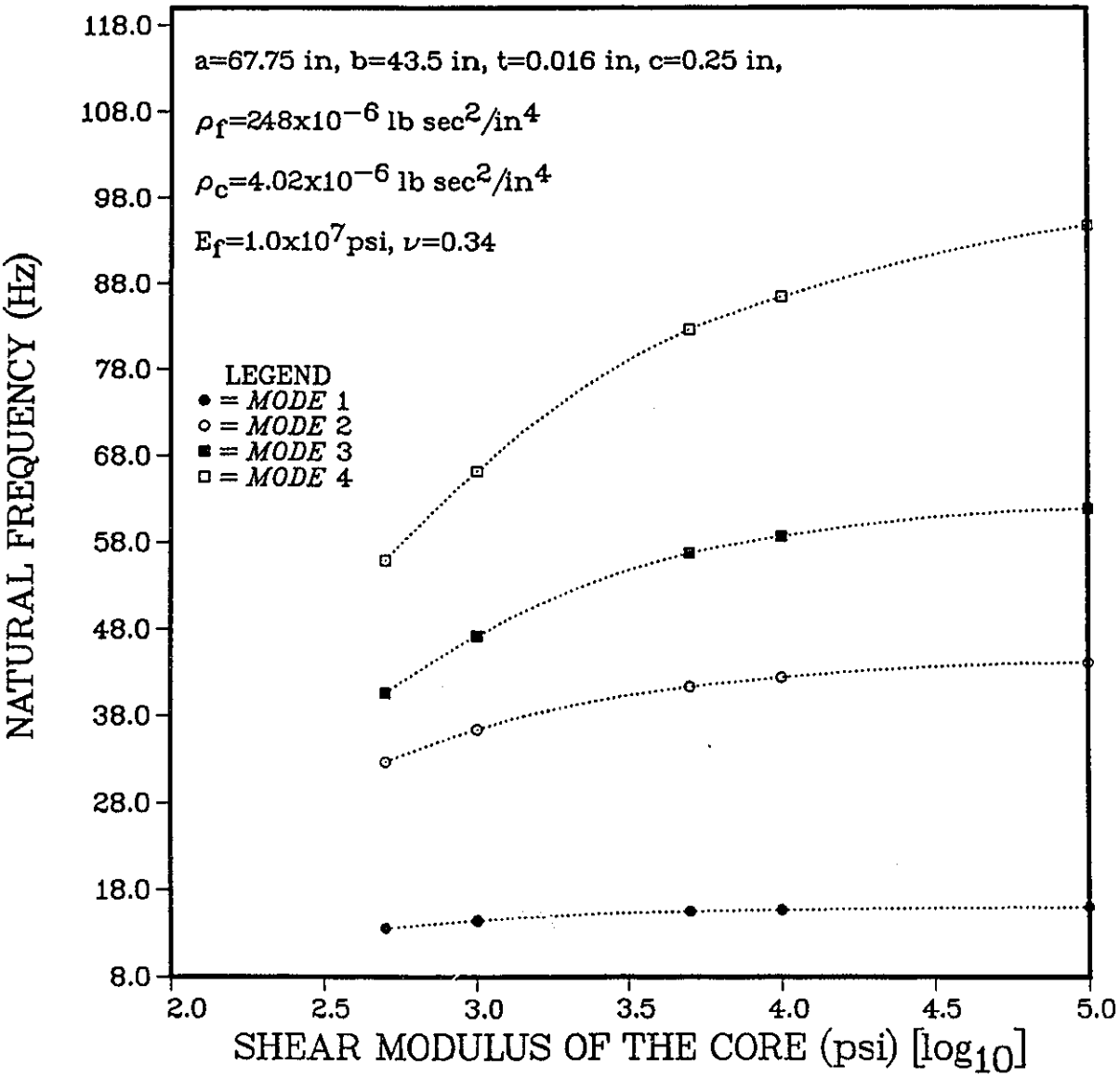

Figure A.46: Variation of the natural frequencies with the shear modulus G_c of the core for a SCSF rectangular sandwich plate with an orthotropic core for the lowest four modes.

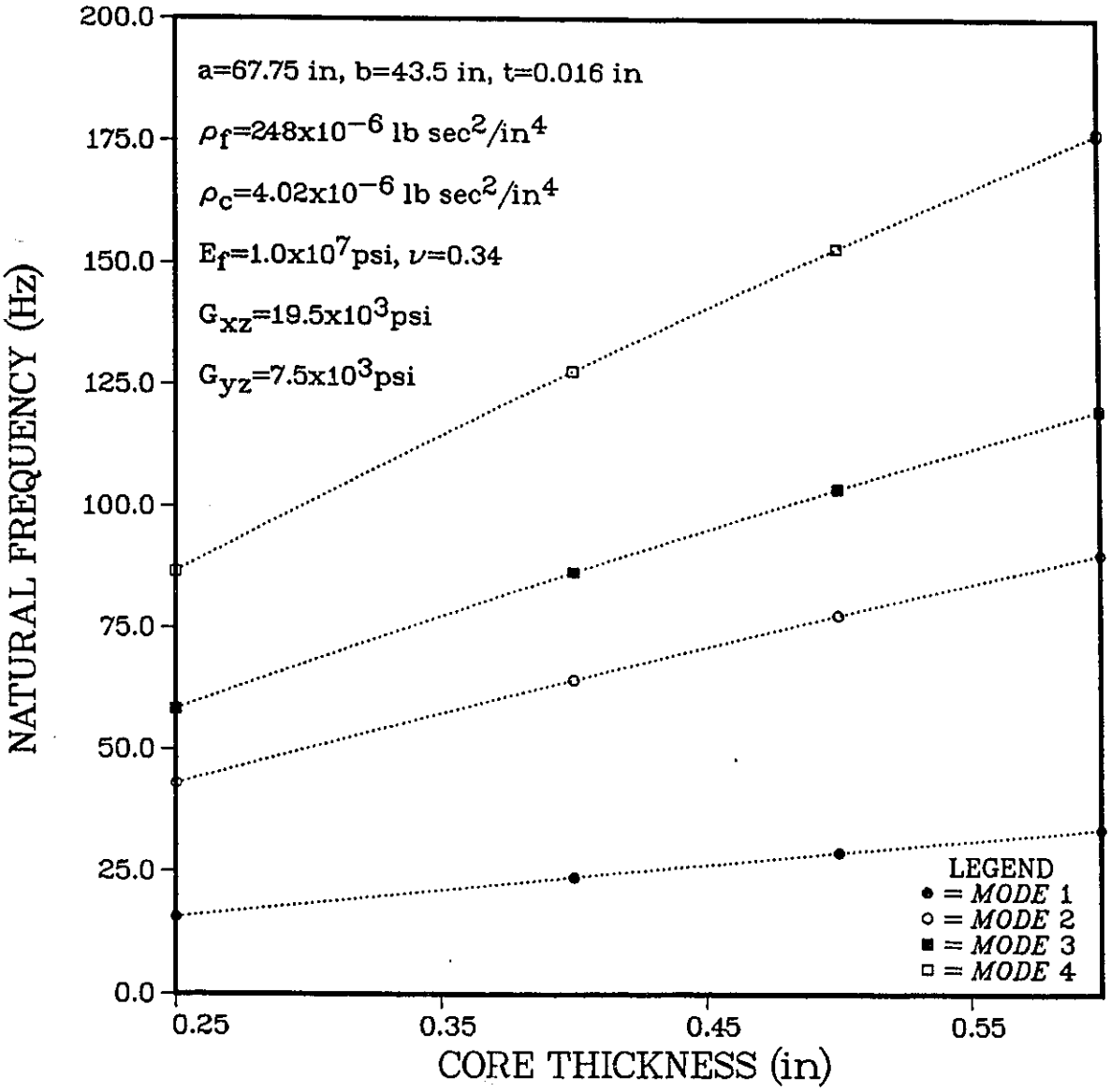

Figure A.47: Variation of the natural frequencies with the thickness of the cor (c) for a SCSF rectangular sandwich plate with an orthotropic core for the lowest four modes.

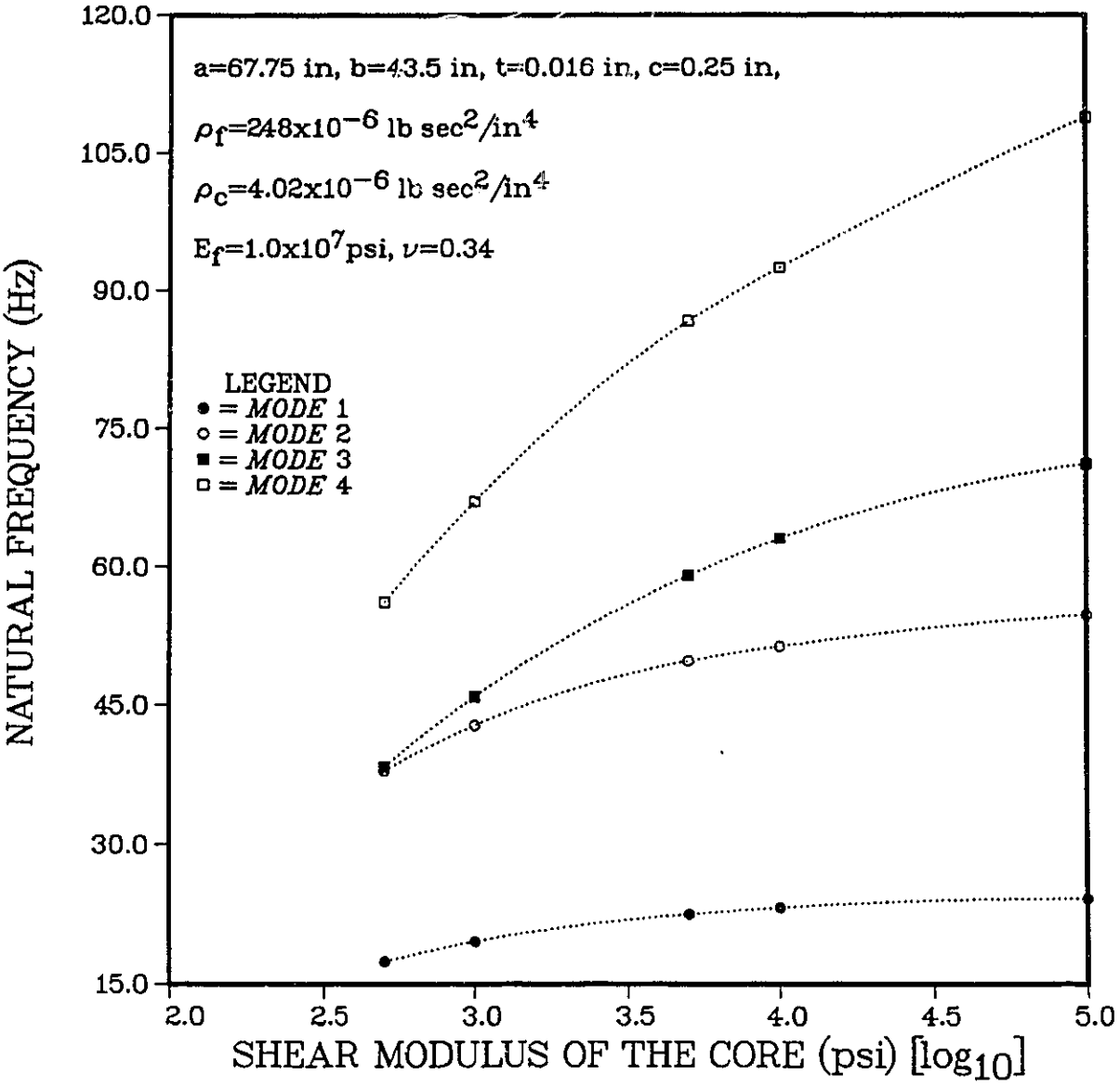

Figure A.48: Variation of the natural frequencies with the shear modulus G_c of the core for a CSCF rectangular sandwich plate with an orthotropic core for the lowest four modes.

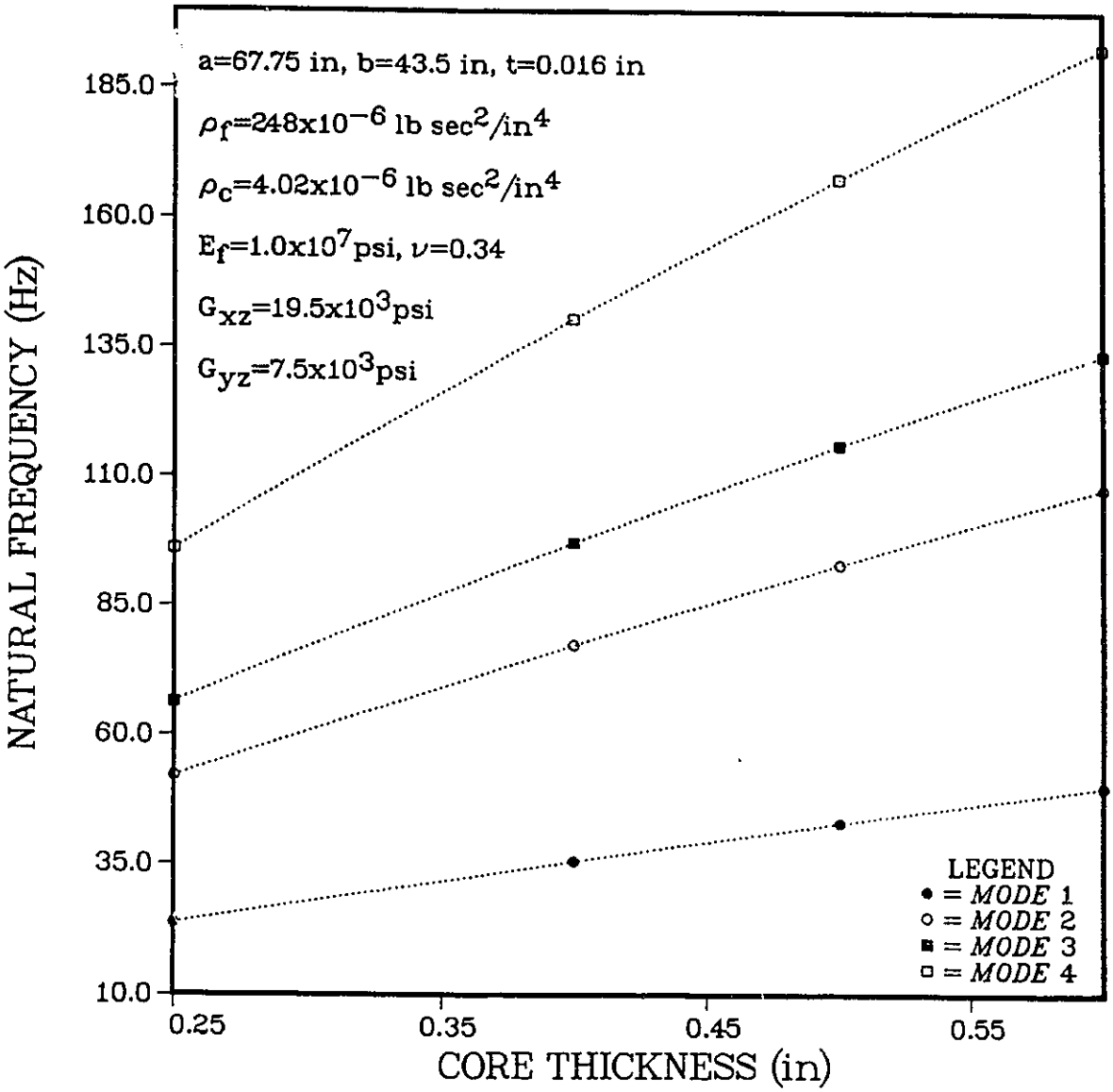

Figure A.49: Variation of the natural frequencies with the thickness of the core (c) for a CSCF rectangular sandwich plate with an orthotropic core for the lowest four modes.

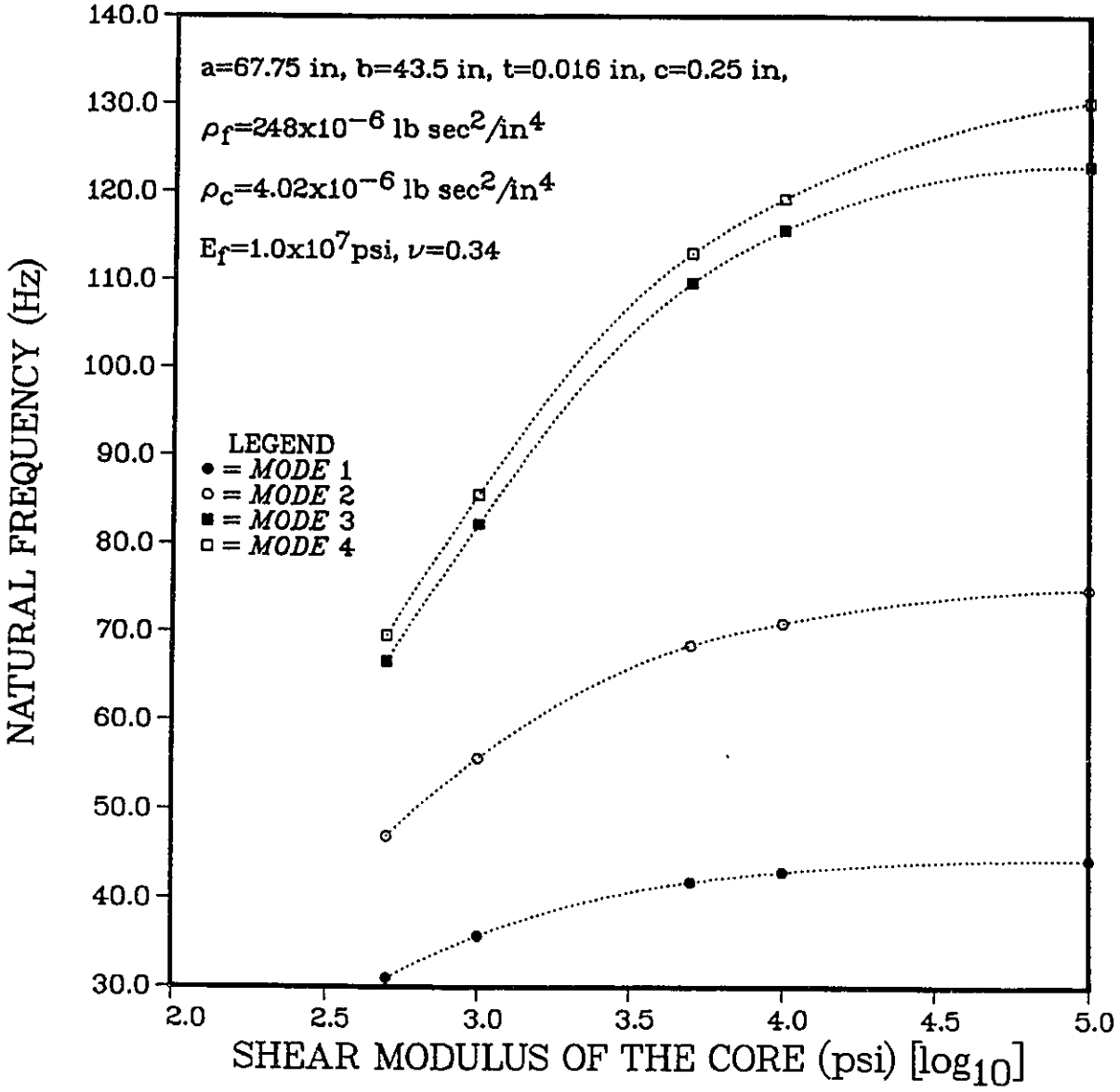

Figure A.50: Variation of the natural frequencies with the shear modulus G_c of the core for a CCSS rectangular sandwich plate with an orthotropic core for the lowest four modes.

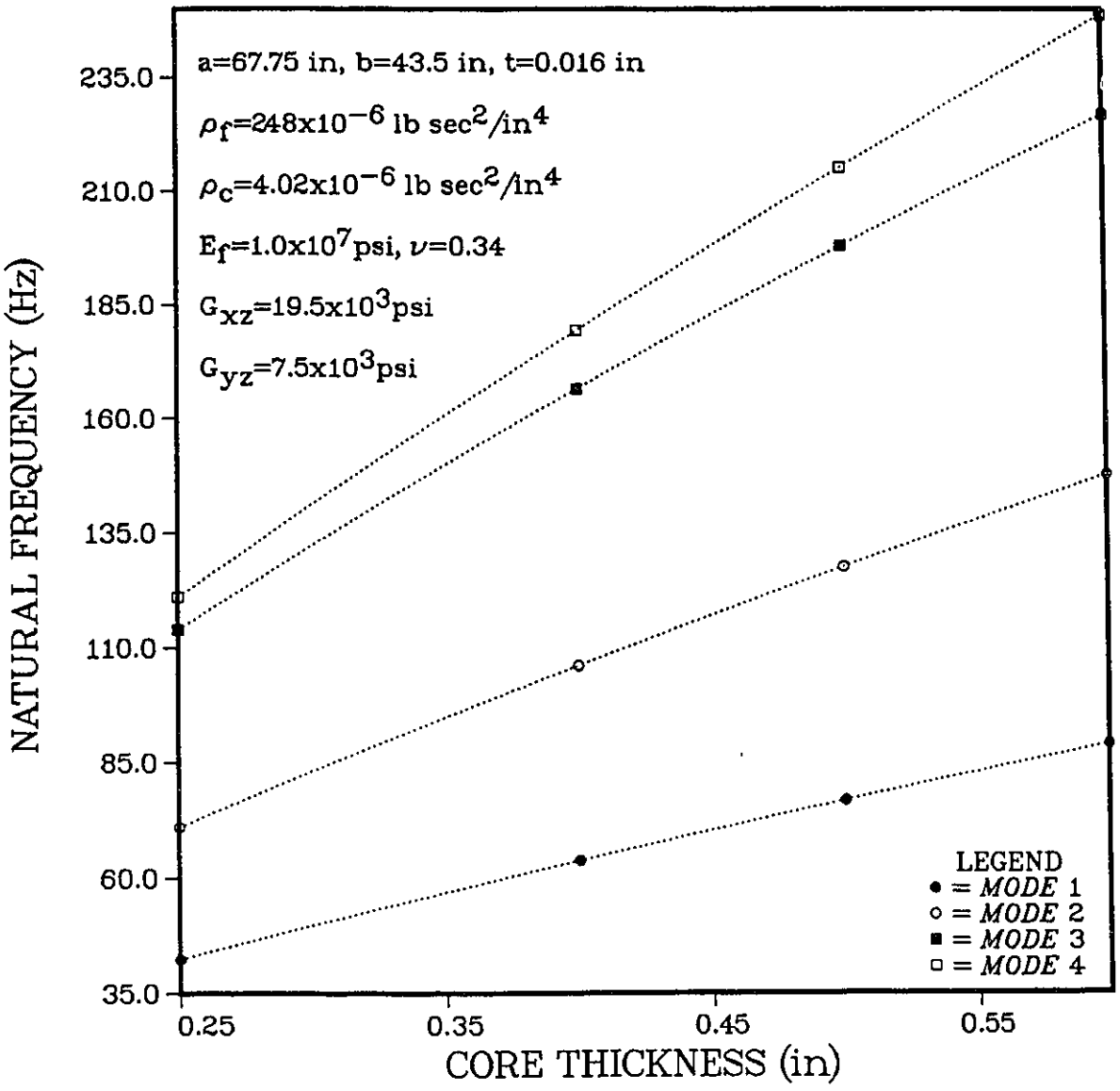

Figure A.51: Variation of the natural frequencies with the thickness of the core (c) for a CCSS rectangular sandwich plate with an orthotropic core for the lowest four modes.

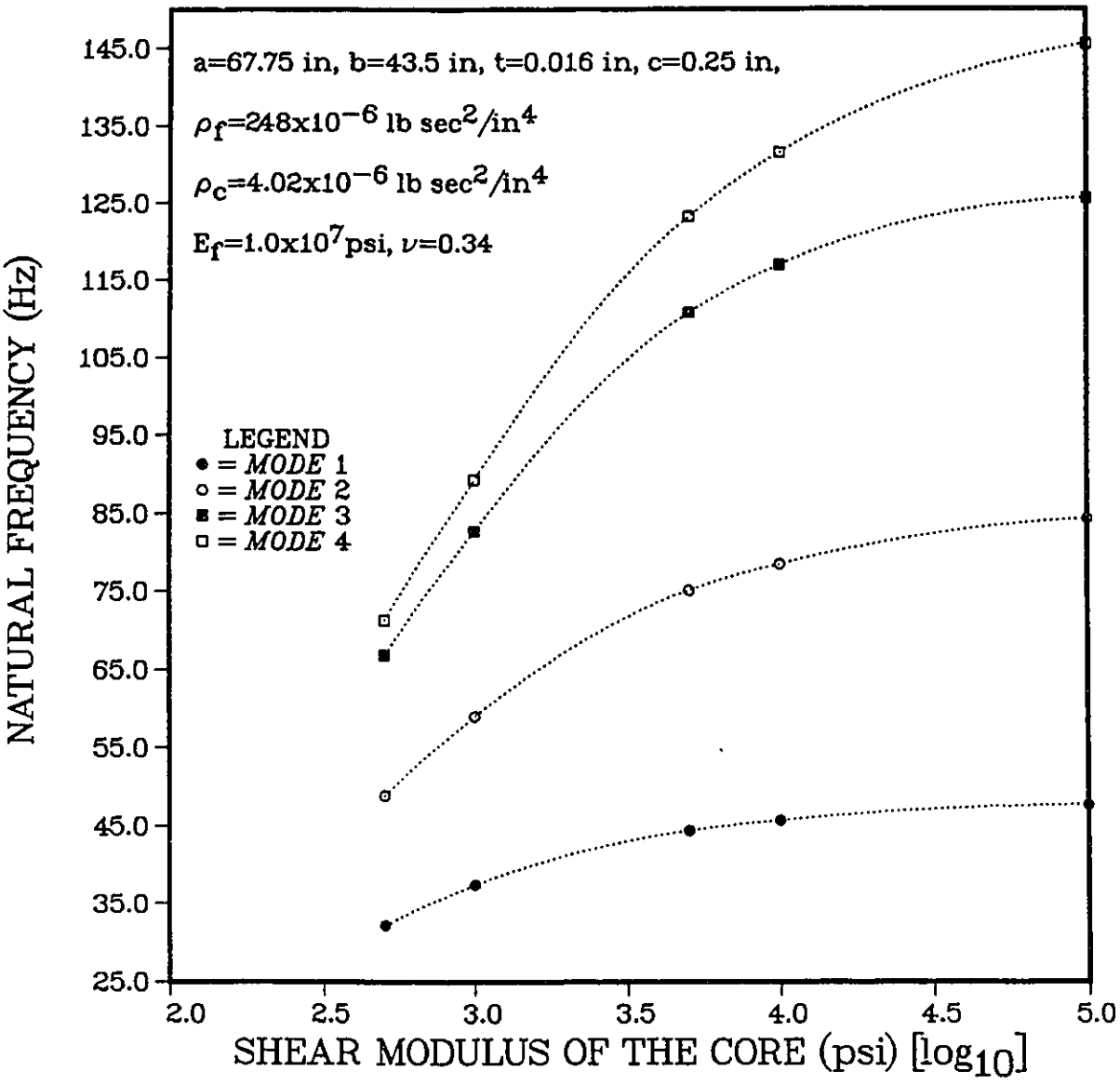

Figure A.52: Variation of the natural frequencies with the shear modulus G_c of the core for a CCCS rectangular sandwich plate with an orthotropic core for the lowest four modes.

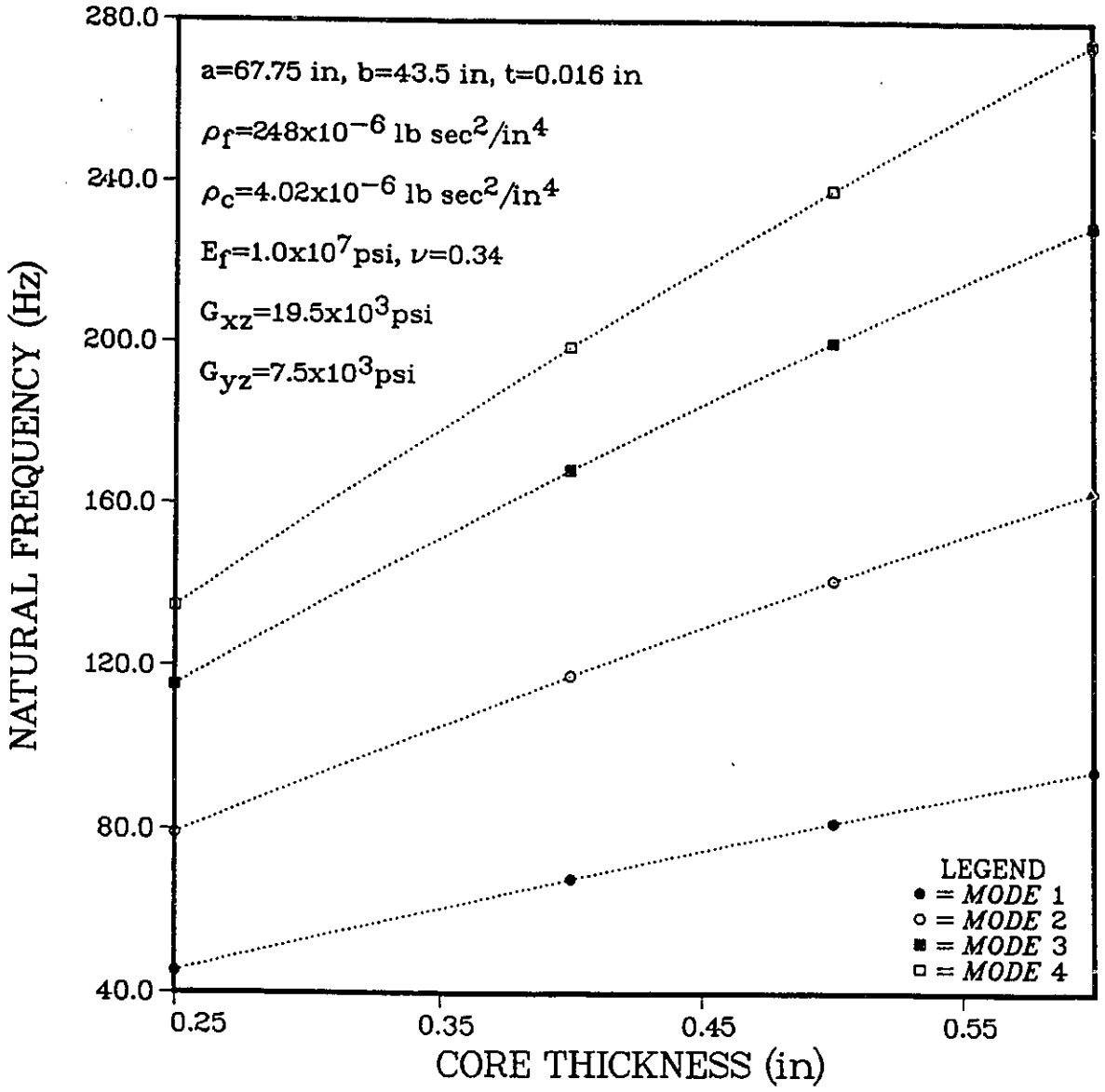

Figure A.53: Variation of the natural frequencies with the thickness of the core (c) for a CCCS rectangular sandwich plate with an orthotropic core for the lowest four modes.

Appendix B

FLOW CHART

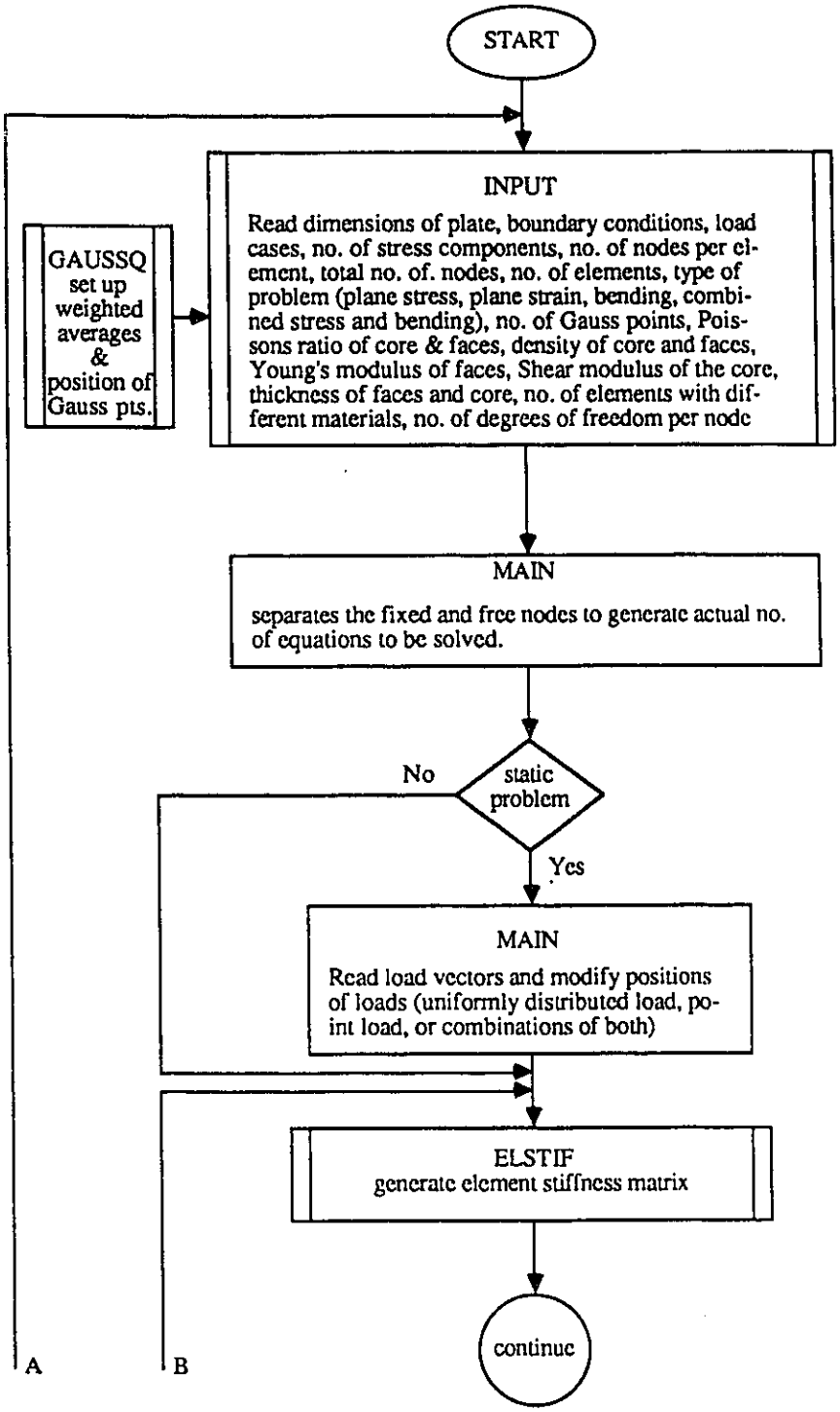
START
INPUT
Read dimensions of plate, boundary conditions, load cases, no. of stress components, no. of nodes per element, total no. of. nodes, no. of elements, type of problem (plane stress, plane strain, bending, combined stress and bending), no. of Gauss points, Poissons ratio of core & faces, density of core and faces, Young's modulus of faces, Shear modulus of the core, thickness of faces and core, no. of elements with different materials, no. of degrees of freedom per node
GAUSSQ set up weighted averages & position of Gauss pts.
MAIN
separates the fixed and free nodes to generate actual no. of equations to be solved.
No
static problem
Yes
MAIN
Read load vectors and modify positions of loads (uniformly distributed load, point load, or combinations of both)
ELSTIF
generate element stiffness matrix
continue
A
B

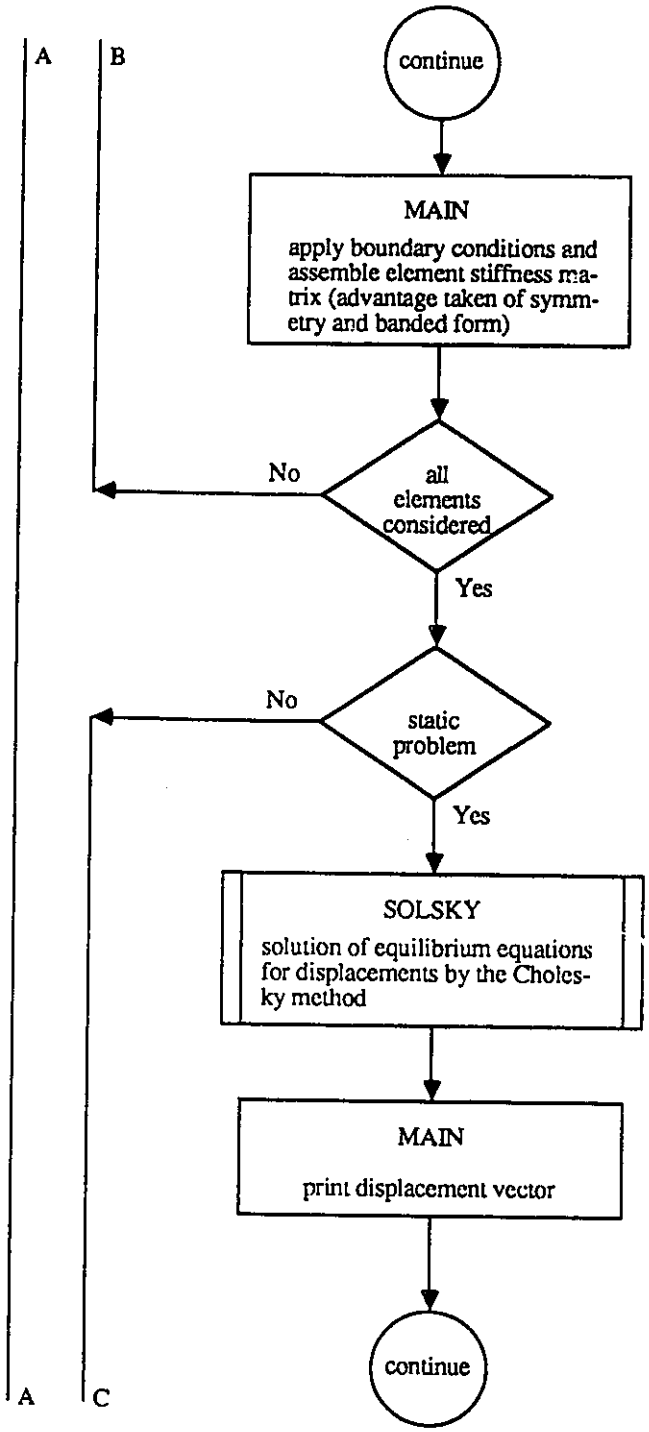
A
B
continue
MAIN
apply boundary conditions and assemble element stiffness matrix (advantage taken of symmetry and banded form)
No
all elements considered
Yes
No
static problem
Yes
SOLSKY
solution of equilibrium equations for displacements by the Choleskky method
MAIN
print displacement vector
continue
A
C

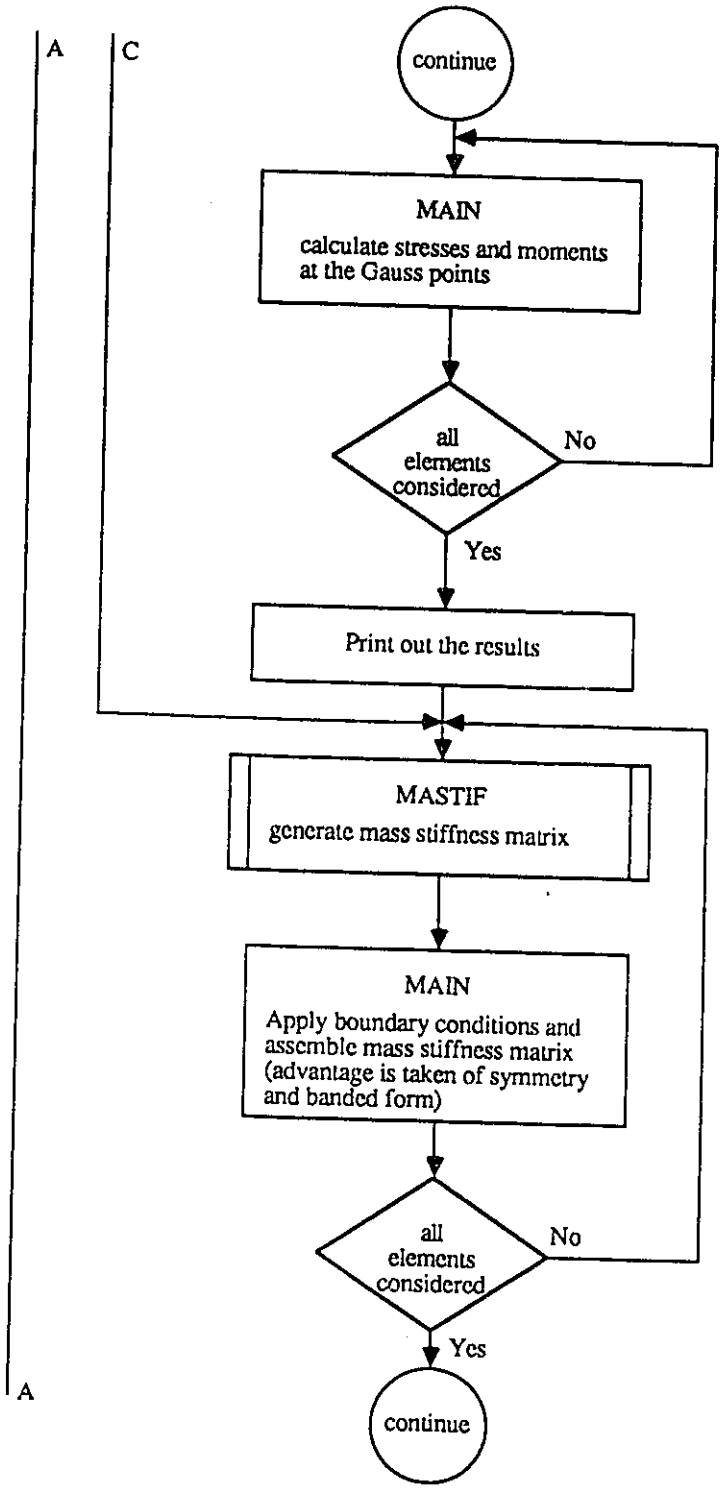
A
C
continue
MAIN
calculate stresses and moments at the Gauss points
all elements considered
No
Yes
Print out the results
MASTIF
generate mass stiffness matrix
MAIN
Apply boundary conditions and assemble mass stiffness matrix (advantage is taken of symmetry and banded form)
all elements considered
No
Yes
continue
A

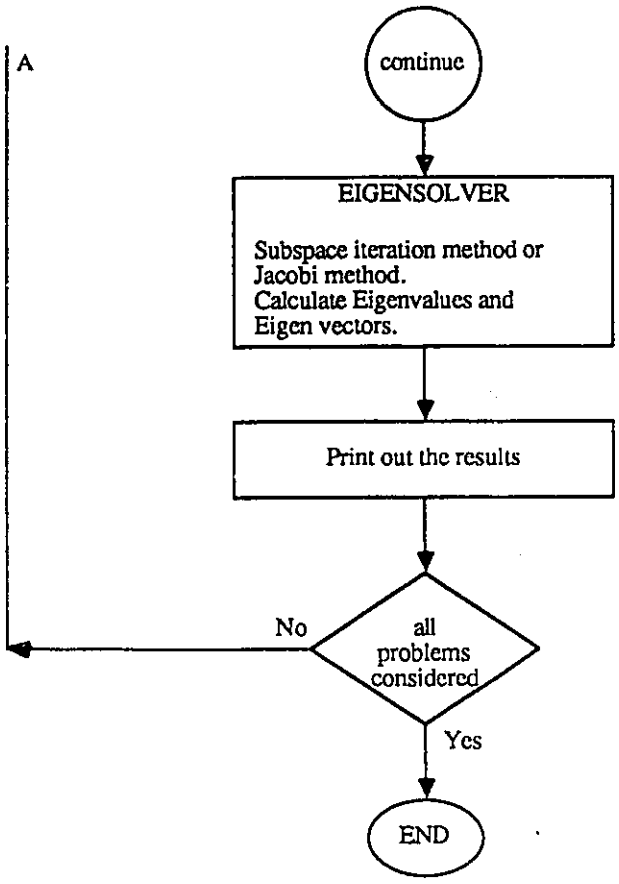
A
continue
EIGENSOLVER
Subspace iteration method or
Jacobi method.
Calculate Eigenvalues and
Eigen vectors.
Print out the results
No
all
problems
considered
Yes
END

FLOW CHART FOR ELSTIF
(Generating the element stiffness matrix)

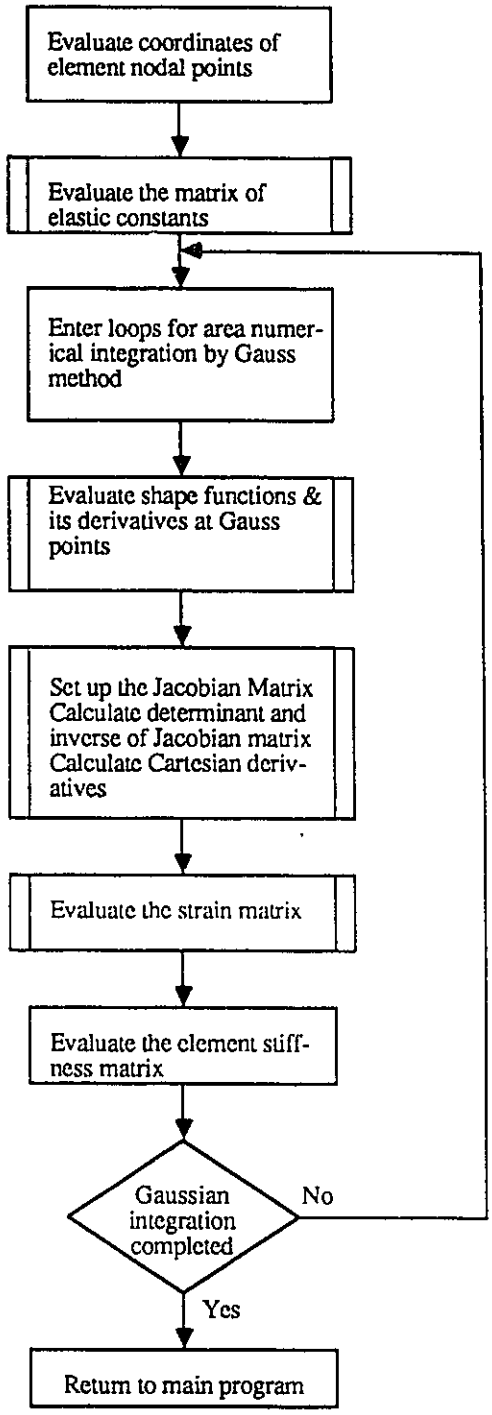

FLOW CHART FOR MASTIF
(Generating the mass stiffness matrix)

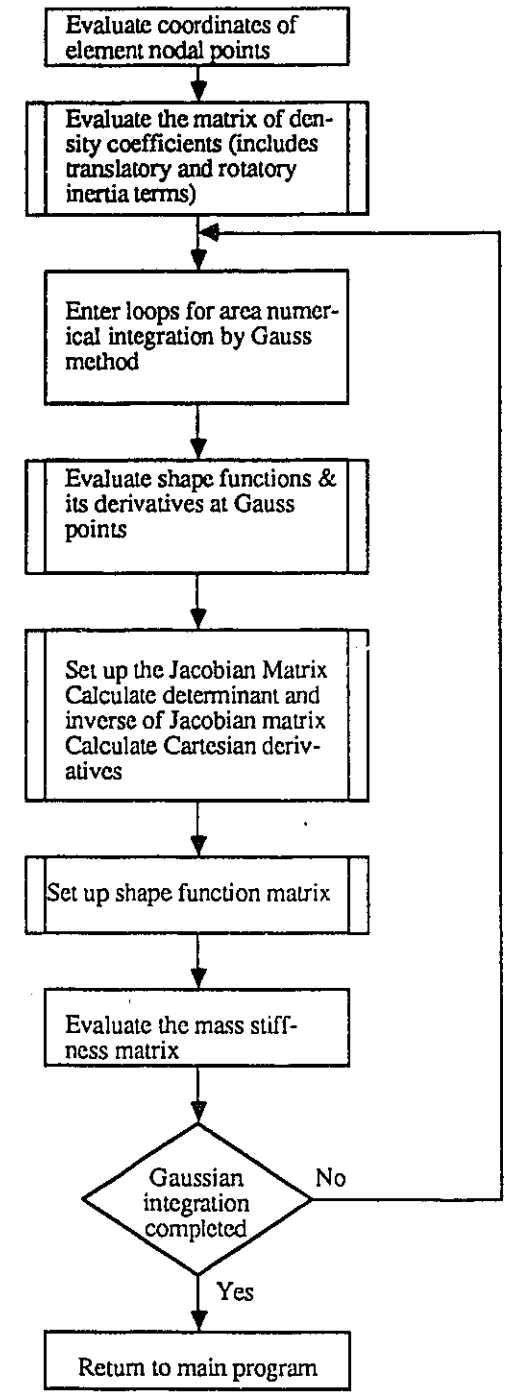

```
SAMPLE INPUT DATA FOR A STATIC PROBLEM FOR SANDWICH PLATE
2 x 2 MESH SIZE FOR A QUARTER PLATE, UNIFORMLY DISTRIBUTED LOAD = 1.0,
NGAUS = 2

1 1 90
2 2 16 3 1 5 2 8
21 4 3 2
17.13 17.13 17.13 17.13
1111 2101 3101 4101 5101 6110
8001 9110 13001 14110 16001 17110
18010 19010 20010 21011
1 8 1 1
1
3.0E06 0.3 0.05 692.31 692.31 0.3 1.0 1.0
1 1
```

```
SAMPLE INPUT DATA FOR A FREE VIBRATION PROBLEM FOR SANDWICH PLATE
3 x 3 MESH SIZE FOR A FULL PLATE, NGAUS = 2

1 1 90
3 3 24 3 1 5 2 8
40 9 3 2
22.58 22.58 22.58 14.5 14.5 14.5
1111 2111 3111 4111 5111 6111 7111 8111
11111 12111 18111 19111 22111 23111 29111 30111
33111 34111 35111 36111 37111 38111 39111 40111
1 9 1 1
1
1.0E07 0.34 0.016 248.0E-06 19.5E03 7.5E03 0.34 0.25 4.02E-06
```

SAMPLE OUTPUT FOR THE STATIC PROBLEM FOR SANDWICH PLATE

PROBLEM NO.: 1

BENDING PROBLEM

NPOIN = 21 NELEM = 4 NNODE = 8
NDOFN = 3 NMATS = 1 NPROP = 8
NGAUS = 2 NVFIX = 16 NSTRE = 5
NDIME = 2 NCASE = 1

ELEMENT NO.	MAT NO.	CONNECTING NODE NUMBERS							
1	1	1	6	9	10	11	7	3	2
2	1	3	7	11	12	13	8	5	4
3	1	9	14	17	18	19	15	11	10
4	1	11	15	19	20	21	16	13	12

NODE NO.	X-COORD	Y-COORD
1	0.00000	0.00000
2	0.00000	8.56500
3	0.00000	17.13000
4	0.00000	25.69500
5	0.00000	34.26000
6	8.56500	0.00000
7	8.56500	17.13000
8	8.56500	34.26000
9	17.13000	0.00000
10	17.13000	8.56500
11	17.13000	17.13000
12	17.13000	25.69500
13	17.13000	34.26000
14	25.69500	0.00000
15	25.69500	17.13000
16	25.69500	34.26000
17	34.26000	0.00000
18	34.26000	8.56500
19	34.26000	17.13000
20	34.26000	25.69500
21	34.26000	34.26000

BOUNDARY CONDITIONS

1111	2101	3101	4101	5101	6110
8001	9110	13001	14110	16001	17110
18010	19010	20010	21011		

LOAD CASE = 1

NODE NO.	DISP-X	DISP-Y	DISP-Z	ROT-X	ROT-Y
1			0.0000E+00	0.0000E+00	0.0000E+00
2			0.0000E+00	0.1936E-01	0.0000E+00
3			0.0000E+00	0.3485E-01	0.0000E+00
4			0.0000E+00	0.4460E-01	0.0000E+00
5			0.0000E+00	0.4762E-01	0.0000E+00
6			0.0000E+00	0.0000E+00	0.1936E-01
7			0.4816E+00	0.3117E-01	0.1226E-01
8			0.6302E+00	0.4291E-01	0.0000E+00
9			0.0000E+00	0.0000E+00	0.3485E-01
10			0.4816E+00	0.1226E-01	0.3117E-01
11			0.8200E+00	0.2222E-01	0.2222E-01
12			0.1034E+01	0.2880E-01	0.1154E-01
13			0.1101E+01	0.3099E-01	0.0000E+00
14			0.0000E+00	0.0000E+00	0.4460E-01
15			0.1034E+01	0.1154E-01	0.2880E-01
16			0.1392E+01	0.1617E-01	0.0000E+00
17			0.0000E+00	0.0000E+00	0.4762E-01
18			0.6302E+00	0.0000E+00	0.4291E-01
19			0.1101E+01	0.0000E+00	0.3099E-01
20			0.1392E+01	0.0000E+00	0.1617E-01
21			0.1484E+01	0.0000E+00	0.0000E+00

SAMPLE OUTPUT OF THE FREE VIBRATION PROBLEM

PROBLEM NO.: 1

PURE BENDING PROBLEM

NPOIN = 40 NELEM = 9 NNODE = 8
NDOFN = 3 NMATS = 1 NPROP = 9
NGAUS = 2 NVFIX = 24 NSTRE = 5
NDIME = 2 NCASE = 1

ELEMENT NO.	MAT NO.	CONNECTING NODE NUMBERS							
1	1	1	8	12	13	14	9	3	2
2	1	3	9	14	15	16	10	5	4
3	1	5	10	16	17	18	11	7	6
4	1	12	19	23	24	25	20	14	13
5	1	14	20	25	26	27	21	16	15
6	1	16	21	27	28	29	22	18	17
7	1	23	30	34	35	36	31	25	24
8	1	25	31	36	37	38	32	27	26
9	1	27	32	38	39	40	33	29	28

NODE NO.	X-COORD	Y-COORD
1	0.00000	0.00000
2	0.00000	7.25000
3	0.00000	14.50000
4	0.00000	21.75000
5	0.00000	29.00000
6	0.00000	36.25000
7	0.00000	43.50000
8	11.29000	0.00000
9	11.29000	14.50000
10	11.29000	29.00000
11	11.29000	43.50000
12	22.58000	0.00000
13	22.58000	7.25000
14	22.58000	14.50000
15	22.58000	21.75000
16	22.58000	29.00000
17	22.58000	36.25000
18	22.58000	43.50000
19	33.87000	0.00000
20	33.87000	14.50000

21	33.87000	29.00000
22	33.87000	43.50000
23	45.16000	0.00000
24	45.16000	7.25000
25	45.16000	14.50000
26	45.16000	21.75000
27	45.16000	29.00000
28	45.16000	36.25000
29	45.16000	43.50000
30	56.45000	0.00000
31	56.45000	14.50000
32	56.45000	29.00000
33	56.45000	43.50000
34	67.74000	0.00000
35	67.74000	7.25000
36	67.74000	14.50000
37	67.74000	21.75000
38	67.74000	29.00000
39	67.74000	36.25000
40	67.74000	43.50000

BOUNDARY CONDITIONS

1111	2111	3111	4111	5111	6111
7111	8111	11111	12111	18111	19111
22111	23111	29111	30111	33111	34111
35111	36111	37111	38111	39111	40111

EIGENVALUES ARE AS FOLLOWS

59.9257085982490700	94.3046021910168122	144.678921132360582
177.510063082181791	197.065469893155409	320.342266230027406
376.496544776005123	425.690010106412331	459.983688516036977
534.889089049083339		

EIGENVECTORS ARE AS FOLLOWS

0.420276576994D+01	0.583706833704D+00	0.262176448187D+00
0.420312146002D+01	0.583483304515D+00	-0.262466946711D+00
0.406262884402D+01	0.114875056959D+00	0.773268298141D+00
0.100323278782D+02	0.276712030522D+00	0.558217670703D+00
0.123629708620D+02	0.394389486773D+00	0.339459352090D-03
0.100301269205D+02	0.276820919870D+00	-0.558528280007D+00
0.406145324993D+01	0.114993665134D+00	-0.772893678116D+00
0.118060456249D+02	-0.280978978893D-04	0.707864784671D+00
0.118071269709D+02	0.439801718583D-04	-0.708724515562D+00
0.406233238289D+01	-0.114702760979D+00	0.773328213826D+00
0.100318484821D+02	-0.276371534815D+00	0.558093544918D+00
0.123630243864D+02	-0.394364591010D+00	0.405838785762D-03
0.100305935501D+02	-0.276452746904D+00	-0.558286191159D+00
0.406177871211D+01	-0.114812558320D+00	-0.772924915475D+00
0.420248287316D+01	-0.583638251016D+00	0.262095130719D+00
0.420341610127D+01	-0.583538499373D+00	-0.262407373140D+00

0.793990246421D+01	0.965037393649D+00	0.351729020872D+00
0.794068936326D+01	0.964904348591D+00	-0.352035884319D+00
0.590355238286D+01	-0.247919835458D+00	0.997126343347D+00
0.125908060451D+02	-0.490378112317D+00	0.425384158429D+00
0.143913219344D+02	-0.555150446386D+00	0.280716244702D-04

```
 0.125902510216D+02 -0.489839412324D+00 -0.425664626498D+00
 0.590323523877D+01 -0.247839775249D+00 -0.996937645237D+00
 0.193580835243D-02 -0.141396500540D+01  0.118852272663D-03
 0.102615421395D-03 -0.141429364805D+01  0.412288131096D-04
-0.590466792243D+01 -0.248202483008D+00 -0.996880411914D+00
-0.125896210704D+02 -0.491066591664D+00 -0.425166961548D+00
-0.143927333621D+02 -0.555566004237D+00 -0.290694507828D-04
-0.125882784188D+02 -0.489896310214D+00  0.425511188628D+00
-0.590376816501D+01 -0.247577239243D+00  0.996710137576D+00
-0.794021248935D+01  0.965352667358D+00 -0.352627463916D+00
-0.793826687995D+01  0.964908425603D+00  0.352655877736D+00
     ----------------------
-0.601880856086D+01 -0.789288042310D+00  0.373689538266D+00
 0.601976311598D+01  0.789650724424D+00  0.373422640964D+00
-0.846717936168D+01 -0.157365508377D+00 -0.116184416004D+01
-0.125019633396D+02 -0.826000271634D-01  0.709690275462D+00
-0.533258468037D-03 -0.410932642005D-03  0.191924363093D+01
 0.125057240829D+02  0.821456562135D-01  0.711276354461D+00
 0.846732001561D+01  0.157089062989D+00 -0.116124132886D+01
-0.133702218391D+02  0.108352967831D-02  0.792030692496D+00
 0.133697055950D+02 -0.124402868216D-02  0.792804247079D+00
-0.846076393151D+01  0.156180909402D+00 -0.116191127828D+01
-0.124950183339D+02  0.809817309798D-01  0.710551608236D+00
 0.114168126568D-02  0.185487241763D-03  0.191730255000D+01
 0.124937527384D+02 -0.805264773538D-01  0.710611105009D+00
 0.846252502849D+01 -0.156151035809D+00 -0.116143240836D+01
-0.602160211080D+01  0.789457790810D+00  0.373156409135D+00
 0.602004660106D+01 -0.789321755220D+00  0.373587234819D+00
     ----------------------
```

Appendix C

Element	Usually Best Integration Order	Maximum Integration Order
4-node rectangle 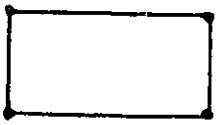	2 by 2	2 by 2
4-node distorted 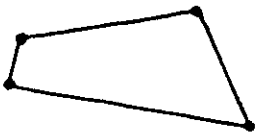	2 by 2	3 by 3
8-node rectangle 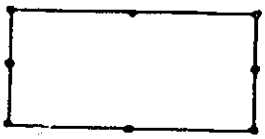	2 by 2	3 by 3
8-node distorted 	3 by 3	4 by 4

RECOMMENDED ORDER OF GAUSS NUMERICAL INTEGRATION FOR TWO-DIMENSIONAL ISOPARAMETRIC ELEMENTS